Theoretical aspects of relaxation phenomena accompanying photoionization of core and valence electrons

Jiri Miller

UNIVERSITY OF DURHAM

A thesis entitled

THEORETICAL ASPECTS OF RELAXATION PHENOMENA ACCOMPANYING PHOTOIONIZATION OF CORE AND VALENCE ELECTRONS

Submitted by

Jiri Müller, B.Sc.

(Hatfield College)

A candidate for the Degree of Doctor of Philosophy

1976

TO MY PARENTS

ACKNOWLEDGEMENTS

The work described in this thesis was carried out under the supervision of Dr. D.T. Clark to whom I wish to express my sincere gratitude for his unfailing help and enthusiasm. Thanks are also due to my colleagues Drs. I.W. Scanlan and D.B. Adams for many helpful discussions. Further I would like to thank the staff of the Atlas Computer Laboratory (in particular Dr. M. Guest) for their help in the implementation of the ab initio molecular programs employed in this work.

Gratitude is also expressed to the Science Research Council for the provision of computing facilities (through the Atlas Laboratory) and financial support which has been extended to sponsor my participation in the International Summer Institute in Quantum Chemistry and Solid-State Physics organized by the University of Uppsala.

Finally I would like to thank Mrs. Eileen Duddy for her great patience and secretarial skill in typing this manuscript.

SUMMARY

A brief summary of some fundamental concepts and relationships needed for the theory of electronic structure of many electron systems with an emphasis on Molecular Orbital theory is presented. Basic concepts behind core and valence electron ionizations in particular their experimental and theoretical aspects are briefly discussed.

Binding and relaxation energies have been computed by ab initio methods with modest basis sets for series of small molecules and their shifts studied as a function of electronic environment. A comparison has been drawn with the available experimental data (ESCA). The empirical correction of Koopmans' theorem for differences in relaxation energies at different sites within a molecule has been studied for large systems.

Ab initio calculations have been carried out on N_2, CO, CO_2 and the relevant core and valence hole states to investigate differences in geometries and force constants. From these calculations vibrational band profiles of photoelectron spectra (ESCA and UPS) for these molecules have been computed and compared with the available high resolution experimental data. The differences between CO and CO_2 with particular emphasis on the band shapes of their ESCA spectra are investigated. Binding and relaxation energies pertaining to the core and valence levels of these three molecules have been computed with various models at different basis set levels and their trends studied. Relaxation energies have been compared with the localization characteristics of the appropriate molecular orbitals. Calculations indicate that the O_{2s} hole state is localized.

MEMORANDUM

The work described in this thesis was carried out in the University of Durham between October 1973 and September 1976. Except where acknowledged by reference it is the original work of the author and has not been submitted in whole or in part for any other degree.

Part of the work in this thesis has formed the subject matter of the following publications:

(1) Non-Empirical LCAO SCF MO Investigations of Electronic Reorganizations Accompanying Core Ionizations. D.T. Clark, I.W. Scanlan and J. Müller, Theoret. Chim. Acta, 35, 341 (1974). (In part presented at S.R.C. Atlas Symposium, No. 4, St. Catherine's College, Oxford, April 1974).

(2) A Non-Empirical LCAO MO SCF Investigation of Electronic Relaxations Accompanying Core Ionizations in the Series X_2 and HX (X = F, Cl and Br). D.T. Clark and J. Müller, Chem. Phys. Letters, 30, 394 (1975).

(3) Some Theoretical Aspects of Vibrational Fine Structure Accompanying Core Ionizations in N_2 and CO. D.T. Clark and J. Müller, Theoret. Chim. Acta, 41, 193 (1976).

(4) A Non-Empirical LCAO MO SCF Investigation of the Valence Ionized States of N_2 and CO. D.T. Clark and J. Müller, Theoret. Chim. Acta, (submitted for publication).

(5) Theoretical Aspects of the Core and Valence Ionized States of CO_2. D.T. Clark and J. Müller, Chem. Phys. Letters, (submitted for publication).

ABBREVIATIONS

AO	Atomic Orbital
A.U.	Atomic Unit
BE	Binding Energy
CI	Configuration Interaction
CNDO	Complete Neglect of Differential Orbital
DOMO	Doubly Occupied Molecular Orbital
EBS	Extended Basis Set
ESCA	Electron Spectroscopy for Chemical Analysis
eV	Electron volt
GPM	Ground State Potential Model
GTO	Gaussian Type Orbital
h	Planck's constant
HF	Hartree-Fock
IP	Ionization Potential
KE	Kinetic Energy
LCAO	Linear Combination of Atomic Orbitals
MC	Multiconfiguration Interaction
MO	Molecular Orbital
PE	Potential Energy
PES	Potential Energy Surface
RE	Relaxation (Reorganization) Energy
RHF	Restricted Hartree-Fock
RPM	Relaxation Potential Model
SCF	Self Consistent Field
SOMO	Singly Occupied Molecular Orbital
STO	Slater Type Orbital
TPM	Transition Potential Model
UHF	Unrestricted Hartree-Fock
UPS	Ultraviolet Photoelectron Spectroscopy
VB	Valence Bond
X^* or $\underline{X}$	indicate that a core hole has been created on the atom X

$< \ldots | \ldots > \equiv \int \ldots\ldots d\tau$

$< \ldots | M | \ldots > \equiv \ldots M \ldots d\tau$ where M is an operator

A matrix with a general element M_{ij} is denoted using the fat symbol formalism as $\mathbb{M}$. The same applies for vectors.

C O N T E N T S

CHAPTER I

MANY ELECTRON THEORY

Abstract.

This chapter contains a brief survey of some fundamental concepts and relationships needed for the theory of electronic structure of many electron systems with special emphasis on Molecular Orbital (MO) theory.

Firstly we state the problem: we need to solve the electronic Schrödinger equation for many electron systems. For this we need the appropriate Hamiltonian and a proper form of the wave functions. Having determined these, we solve the Schrödinger equation to a first approximation by the Hartree-Fock method. We find that the concept of density matrices and Slater's rules for evaluation of complicated integrals are valuable tools not only in the Hartree-Fock approximation but generally in MO theory. The LCAO method is introduced to solve the Hartree-Fock equations and to analyse the resulting wave function. The main deficiency of the Hartree-Fock theory - the correlation error is pointed out, and various schemes for overcoming it are briefly discussed. Finally a brief description of the computer program ATMOL 2 used for non-empirical LCAO MO calculations is given.

1.1. Schrödinger Equations.

a. Molecular Schrödinger Equation.

With any state of a molecule is associated a wave function Ξ_T which depends on the nuclear and electronic coordinates and on time, t. The time evolution of the wave function is governed by the time dependent Schrödinger equation

$$\mathcal{H}_T \Xi_T = ih \frac{\delta \Xi_T}{\delta_t} \qquad \ldots (1.1)$$

where $\mathcal{H}_T$ is the total Hamiltonian (energy) operator to be specified below.

The stationary states of the molecule, i.e. those states for which energy E_T is well defined, are described by the wave function of the form

$$\Xi_T = \Psi_T \exp(-iE_T t/\hbar) \qquad \ldots (1.2)$$

where Ψ_T is independent of time, and a solution of the time independent eigen-value equation

$$\mathcal{H}_T \Psi_T = E_T \Psi_T \qquad \ldots (1.3)$$

which is called the Molecular Schrödinger equation. We shall consider time independent molecular stationary states exclusively in what follows. (Although in theory this may not be justified a priori for the discussion of photo-ionization phenomena, it will become clear later on that our discussions based on the time independent Molecular Schrödinger equation are entirely adequate.)

b. The Electronic Schrödinger Equation.

The Hamiltonian operator ($\mathcal{H}_T$) for a system of N nuclei (g,h, ...) of coordinates X and n electrons (i,j, ...) of coordinates x has the form

$$\mathcal{H}_T \equiv \mathcal{H}(x,X) = -\sum_{g=1}^{N} \frac{h^2}{8\pi^2 M_g} \nabla_g^2 - \sum_{i=1}^{n} \frac{h^2}{8\pi^2 m} \nabla_i^2 + V_{ne}(x,X)$$

$$+ V_{ee}(x) + V_{nn}(X) \qquad \ldots (1.4)$$

with all relativistic and spin effects neglected, where

$$V_{ne}(x,X) = -\sum_{g=1}^{N} \sum_{i=1}^{n} \frac{Z_g e^2}{r_{ig}}$$

$$V_{ee}(x) = \frac{1}{2} \sum_{i=1}^{n} \sum_{j=1}^{n\,\prime} \frac{e^2}{r_{ij}}$$

$$V_{nn}(X) = \frac{1}{2} \sum_{g=1}^{N} \sum_{h=1}^{N\,\prime} \frac{Z_g Z_h e^2}{R_{gh}} \qquad \ldots (1.5)$$

(Prime ' indicates that terms for which two indices become equal are to be omitted in a double sum, and subscripts n and e stand for nucleus and electron respectively.)

In order to find a wave function describing electronic motion for fixed nuclear coordinates we have to invoke the Born-Oppenheimer approximation,[1] which amounts to separating the nuclear kinetic energy term from $\mathcal{H}(x,X)$ and considering only the part of the Hamiltonian which depends on the position but not the momenta of the nuclei, ($\mathcal{H}_e$). Mathematically this amounts to:

$$\mathcal{H}_n(X) = - \sum_{g=1}^{N} \frac{h^2}{8\pi^2 M_g} \nabla_g^2 \qquad \ldots (1.6)$$

$$\mathcal{H}(x,X) - \mathcal{H}_n(X) = \mathcal{H}_e(x,X) \qquad \ldots (1.7)$$

We assume that Ψ_T can be written as a product of electronic and nuclear wave functions

$$\Psi_T = \Psi_e(x,X)\, \chi_{ne}(X) \qquad \ldots (1.8)$$

where the electronic wave function is defined in the Electronic Schrödinger equation

$$\mathcal{H}_e(x,X)\ \Psi_e(x,X) = E_e(X)\ \Psi_e(x,X) \qquad \ldots (1.9)$$

and the nuclear function is given by

$$[\mathcal{H}_n(X) + E_e(X)]\chi_{ne}(X) = E\chi_{ne}(X) \qquad \ldots (1.10)$$

Thus using the Born-Oppenheimer approximation we have separated the total wave function into an electronic and a nuclear part. The electronic wave function is obtained for various fixed positions of nuclei by solving (1.9). This gives an electronic energy E_e which if plotted as a function of X

gives rise to so-called potential energy curves which we shall discuss in more detail in later chapters. This electronic energy E_e is referred to as a potential energy, determining the motion of the nuclei (hence the term potential energy curve) so that the Schrödinger equation for the nuclei has the form (1.10). However we shall only be concerned with solving the Electronic Schrödinger equation (1.9). (The range of validity of the Born-Oppenheimer approximation is described e.g. in reference 2.)

Now we shall direct our attention towards determining the form of the electronic wave function Ψ_e.

1.2. Determinantal Wave Functions.

a. Pauli Principle and Antisymmetric Wave Functions.

The wave function for an electron system $\Psi_e(x,X)$, which we shall now simply write as $\Psi \equiv \Psi(x_1, x_2, \ldots, x_n)$ depends on n electronic coordinates $x_i = (r_i, \xi_i)$, each consisting of a space coordinate r_i and a spin coordinate ξ_i. In order to fulfil the Pauli principle we require that the wave function Ψ should be antisymmetric under the permutation P of the coordinates

$$P\Psi(x_1, x_2, \ldots, x_n) = (-1)^p \Psi(x_1, x_2, \ldots, x_n) \qquad \ldots (1.11)$$

where p is the parity of P, i.e. the number of transpositions in which P can be factorized.

Consider now an arbitrary trial function $f(x_1, x_2, \ldots, x_n)$ without symmetry properties. By means of the antisymmetrization operator

$$\mathcal{A} = (n!)^{-\frac{1}{2}} \sum_P (-1)^p P \qquad \ldots (1.12)$$

where the sum is taken over all n! permutations, we may construct a wave function

$$\Psi = \mathcal{A}f = (n!)^{-\frac{1}{2}} \sum_P (-1)^p Pf(x_1, x_2, \ldots, x_n) \qquad \ldots (1.13)$$

which can readily be shown to possess the requisite anti-symmetry property (1.11). The arbitrary function f may be constructed as the sum of components of different symmetry types, and by means of the operator (1.12) we have simply selected the anti-symmetric component and multiplied by $(n!)^{\frac{1}{2}}$. This follows from the fact that the operator $(n!)^{-\frac{1}{2}}\mathcal{A}$ can be shown straightforwardly to be a projection operator fulfilling the characteristic relation $O^2 = O$, and by means of such an operator we can always select a component of any desired symmetry type. If the operation is repeated we shall be left with the same component, hence the relation $O^2 = O$.

b. Spin Orbitals.

Although we are interested in many electron functions it is reasonable, both from a physical and a mathematical view point to construct them from one electron functions, so-called spin orbitals.

A spin orbital is a function of coordinates of one electron and is usually written in the form

$$\psi(x) = \begin{cases} \phi(r)\,\alpha(\xi) \\ \quad \text{or} \\ \phi(r)\,\beta(\xi) \end{cases}$$

where $\phi(r)$ represents the spatial part and α and β are two spin functions which are needed to span the spin function space of a particle with spin $\frac{1}{2}$.

It is important to distinguish between spin coordinates and spin functions, α and β. The functions are defined only for two values of their arguments which are conventionally chosen to be $\pm\frac{1}{2}$.

$$\alpha(\tfrac{1}{2}) = 1 \qquad \beta(\tfrac{1}{2}) = 0$$

$$\alpha(-\tfrac{1}{2}) = 0 \qquad \beta(-\tfrac{1}{2}) = 1 \qquad \ldots (1.14a)$$

From 1.14a it follows that α and β form an orthonormal set.

$$\int \alpha(\xi)\alpha(\xi)\,d\xi = \sum_{\xi} |\alpha(\xi)|^2 = 1.1 + 0.0 = 1,$$
$$\int \beta(\xi)\beta(\xi)\,d\xi = \sum_{\xi} |\beta(\xi)|^2 = 1.1 + 0.0 = 1,$$
$$\int \alpha(\xi)\beta(\xi)\,d\xi = \sum_{\xi} \alpha(\xi)\beta(\xi) = 1.0 + 0.1 = 0. \qquad \ldots (1.14b)$$

c. Expansion Theorem.

Let us introduce a certain orthonormal and complete set of spin orbitals $\{\psi_k(x)\}$ as a basis such that

$$\langle i|j\rangle = \int \psi_i(x)\psi_j(x)\,dx = \delta_{ij} \qquad \ldots (1.15)$$

where δ_{ij} is the Kronecker delta, and further let us assume that every normalizable function $\psi(x)$ of a single electronic coordinate $x = (r, \xi)$ may be expanded in this set:

$$\psi(x) = \sum_{k=1}^{\infty} c_k \psi_k(x) \qquad \ldots (1.16)$$

(The validity of such an expansion theorem has been carefully studied in mathematics, and hence requires no proof in the context of this work.)

If we instead have a normalizable function $\Psi(x_1, x_2)$ of two electronic coordinates we can first consider x_2 as a fixed parameter and expand it according to (1.16) with respect to x_1. The coefficients $c_k \equiv c_k(x_2)$ are normalizable functions of x_2 and by expanding once more with respect to x_2 we obtain

$$\Psi(x_1, x_2) = \sum_{k=1}^{\infty} c_k(x_2)\psi_k(x_1) = \sum_{k,\ell=1}^{\infty} c_{k\ell}\psi_k(x_1)\psi_\ell(x_2) \qquad \ldots (1.17)$$

For a normalizable function $\Psi(x_1, x_2, \ldots, x_n)$ of n electronic coordinates we have similarly

$$\Psi(x_1, x_2, \ldots, x_n) = \sum_{k_1, k_2, \ldots, k_n=1}^{\infty} c(k_1 k_2 \ldots k_n)\psi_{k_1}(x_1)\psi_{k_2}(x_2)\ldots\psi_{k_n}(x_n) \qquad \ldots (1.18)$$

Projecting the anti-symmetric component of (1.18) by the operator $(n!)^{-\frac{1}{2}}\mathcal{A}$ defined by the equation (1.12) we obtain directly a normalized and anti-symmetric wave function satisfying the relation (1.11).

$$\Psi(x_1,x_2,\ldots,x_n) =$$

$$(n!)^{-\frac{1}{2}} \mathcal{A} \sum_{k_1,k_2,\ldots,k_n=1} c(k_1 k_2 \ldots k_n)\psi_{k_1}(x_1)\psi_{k_2}(x_2)\ldots\psi_{k_n}(x_n)$$

$$= (n!)^{-1} \sum_{k_1,k_2,\ldots k_n=1} c(k_1 k_2 \ldots k_n)\Sigma_P (-1)^p P\psi_{k_1}(x_1)\psi_{k_2}(x_2)\ldots\psi_{k_n}(x_n)$$

$$= (n!)^{-1}\sum_{k_1,k_2,\ldots,k_n=1} c(k_1 k_2 \ldots k_n)\det[\psi_{k_1}(x_1),\psi_{k_2}(x_2),\ldots,\psi_{k_n}(x_n)]$$

$$= \sum_{k_1<k_2<\ldots<k_n} c(k_1 k_2 \ldots k_n)\det[\psi_{k_1}(x_1)\ \psi_{k_2}(x_2),\ldots,\psi_{k_n}(x_n)] \qquad \ldots (1.19)$$

where the operator P permutes coordinates of electrons (not the suffixes of the spin orbitals).

Every selection of n one electron indices $k_1 < k_2 < \ldots < k_n$ is called an ordered configuration K and the function

$$\Psi_K(x_1,x_2,\ldots,x_n) = (n!)^{-\frac{1}{2}}\det[\psi_{k_1}(x_1),\psi_{k_2}(x_2),\ldots,\psi_{k_n}(x_n)]$$

$$= \frac{1}{(n!)^{-\frac{1}{2}}} \begin{vmatrix} \psi_{k_1}(x_1) & \psi_{k_1}(x_2) & \ldots & \psi_{k_1}(x_n) \\ \psi_{k_2}(x_1) & \psi_{k_2}(x_2) & \ldots & \psi_{k_2}(x_n) \\ \vdots & \vdots & & \\ \psi_{k_n}(x_1) & \psi_{k_n}(x_2) & \ldots & \psi_{k_n}(x_n) \end{vmatrix} \qquad \ldots (1.20)$$

is the normalized Slater determinant belonging to this configuration. In $(x_1,x_2,\ldots,x_n)$ space the functions Ψ_K taken for all ordered configurations form an orthonormal set. Taking $C_K = (n!)^{\frac{1}{2}} c(k_1 k_2 \ldots k_n)$ we can write (1.19) in the form

$$\Psi(x_1,x_2,\ldots,x_n) = \sum_K C_K \Psi_K(x_1,x_2,\ldots,x_n)$$

$$= \sum_K C_K D_K \qquad \ldots (1.21)$$

Thus every normalizable anti-symmetric wave function can be expressed as the sum of a series of Slater determinants built up from a complete basic set of one electron functions. This statement is in fact a basic theorem in the method of configuration interaction which will be discussed in the latter part of this chapter.

c. Slater's Rules for Calculation of Matrix Elements.

As we have seen the Slater determinants are natural building blocks in constructing many electron functions. It is therefore essential to be able to manipulate such quantities. In particular the need often arises for calculating matrix elements of various kinds of operators with respect to Slater determinants. Such rules were derived by Slater[3] for the case of orthonormal spin orbitals. (The general case without the orthonormality constraint has been treated by Löwdin[4] whose rules form a basic procedure for the Valence Bond method which will be briefly discussed at the end of this chapter).

A Slater determinant, if written out explicitly as a sum of products, is a very complicated function. The determinants are most easily handled by means of the anti-symmetrizer (1.12), and it should be recalled that a Slater determinant is the anti-symmetric component of a product of spin orbitals

$$D(x_1, x_2 \ldots, x_n) = \mathcal{A}[\psi_1(x_1)\ \psi_2(x_2)\ \ldots\ \psi_n(x_n)]$$

$$= \mathcal{A}\Phi(x_1, x_2, \ldots, x_n) \qquad \ldots (1.22)$$

We shall derive one of Slater's rules explicitly and then state the rest. Consider the case in which we want to calculate a matrix element $\langle D|\Omega|D\rangle$ where the operator Ω is a sum of equivalent one electron operators

$$\Omega = \sum_{i=1}^{n} \Omega_i \qquad \ldots (1.23)$$

The index i in Ω_i means that Ω_i operates on function x_i and since Ω is symmetrical in the indices i, we have for any permutation P a commutator relationship

$$[P,\Omega] = 0 \qquad \ldots (1.24)$$

which implies

$$[\mathcal{A},\Omega] = 0 \qquad \ldots (1.25)$$

Knowing that the anti-symmetrizer is a self-adjoint operator ($\mathcal{A}^+ = \mathcal{A}$) satisfying the relation $\mathcal{A}^2 = (n!)^{-\frac{1}{2}}\mathcal{A}$ we obtain by means of the 'turn-over'* rule the following result:

$$< D|\Omega|\ D > = <\mathcal{A}\Phi|\ \Omega|\mathcal{A}\Phi\ > =$$

$$<\Phi|\mathcal{A}^+\Omega|\ \mathcal{A}\Phi\ > = <\Phi|\Omega\ \mathcal{A}^+\mathcal{A}\ |\ \Phi> =$$

$$(n!)^{-\frac{1}{2}} <\Phi|\ \Omega\ \mathcal{A}\qquad |\Phi> = \sum_P (-1)^P <\Phi\ |\ \Omega|P\Phi\ > \qquad \ldots (1.27)$$

Let us consider the terms in Ω one by one starting with i = 1, i.e. Ω_1. We need to evaluate

$$\sum_P (-1)^P <\Phi\ |\ \Omega_1\ |\ P\Phi\ > = <\Phi\ |\ \Omega_1\ |\ \Phi\ > +$$

$$(-1)^{P_2} <\Phi\ |\ \Omega_1 P_2|\Phi\ > + \ldots \qquad \ldots (1.28)$$

where P_1 is an identity operator. The first term in (1.28) becomes

$$< 1|\Omega_1|1\ >\ <\ 2|2\ >\ <\ 3|3\ > \ldots <\ k|k\ > \ldots <\ n|n\ > =$$

$$< 1|\Omega_1|1\ > \qquad \ldots (1.29)$$

where the general term

---

*If an arbitrary operator T has a domain D_T, then for any two functions Ψ_1 and Ψ_2 belonging to D_T we have

$$< T\Psi_1|\Psi_2> \quad = <\Psi_1|T^+|\Psi_2> \qquad \ldots (1.26)$$

$$< k|k > = \int \psi_k^*(x_k)\psi_k(x_k)dx_k = \int \psi_k^*(x_1)\psi_k(x_1)dx_1 = \delta_{kk} \quad \ldots (1.30)$$

since electrons are indistinguishable and

$$< 1 | \Omega_1 | 1 > = \int \psi_1^*(x_1)\Omega_1\psi_1(x_1)dx_1 \quad \ldots (1.31)$$

The second and higher terms in (1.28) involve terms

$$< k|j > = \int \psi_k(x)\psi_j(x)dx \quad \ldots (1.32)$$

which are according to the orthonormality constraint (1.15) equal to zero, hence they vanish. The contribution to (1.27) from the integrals involving Ω_2 is obtained in exactly the same way and amounts to

$$< 2|\Omega_2|2 > = \int \psi_2^*(x_2)\Omega_2\psi_2(x_2)dx_2$$

$$= \int \psi_2^*(x_1)\Omega_1\psi_2(x_1)dx_1 \quad \ldots (1.33)$$

due to the indistinguishability of electrons.

Therefore

$$< D | \Omega | D > = \sum_{k=1}^{n} < k | \Omega_1 | k > =$$

$$\sum_{k=1}^{n} \int \psi_k^*(x_1)\Omega_1\psi_k^*(x_1)dx_1 \quad \ldots (1.34)$$

All of Slater's rules can be obtained in a similar way and are summarised below.

1) Overlap integral:

$$< D_1 | D_2 > = \pm \delta_{k_1\ell_1}\delta_{k_2\ell_2} \ldots \delta_{k_n\ell_n} \quad \ldots (1.35)$$

where $\delta_{k_j\ell_j} = \int \psi^*_{k_j}(x)\psi_{\ell_j}(x)dx \quad \ldots (1.36)$

2) One electron operators:

i) Diagonal elements:

$$< D | \sum_i \Omega_i | D > = \sum_{k=1}^{n} < k | \Omega_1 | k > \quad \ldots (1.37)$$

ii) The case $\psi_j \to \psi_u$ (i.e. two determinants differ in one spin orbital only, where we replaced ψ_j orbital by ψ_u):

$$< D | \sum_i \Omega_i | D_j^u > = < j | \Omega_1 | u > \quad \ldots (1.38)$$

iii) Zero in all other cases. ... (1.39)

3. Two electron operators:

i) Diagonal elements:

$$< D| \sum_{i>j} \Omega_{ij} |D > = \sum_{k<\ell} k\ell|\Omega_{12}(1-P_{12})|k\ell > \quad \ldots (1.40)$$

ii) The case $\psi_\ell \rightarrow \psi_\upsilon$:

$$< D| \sum_{i>j} \Omega_{ij} |D_\ell^\upsilon > = \sum_{k} < k\ell|\Omega_{12}(1-P_{12})|k\upsilon > \quad \ldots (1.41)$$

iii) The case $\psi_k \rightarrow \psi_\mu$; $\psi_\ell \rightarrow \psi_\upsilon$:

$$< D| \sum_{i>j} \Omega_{ij} | D_{k\ell}^{\mu\upsilon} > = < k\ell|\Omega_{12}(1-P_{12})|\mu\upsilon > \quad \ldots (1.42)$$

iv) Zero in all other cases.

The notation in (1.40) means

$$< k\ell |\Omega_{12}(1-P_{12})|\mu\upsilon> =$$

$$\int \psi_k^*(x_1)\psi_\ell^*(x_2)\Omega_{12}(1-P_{12})\psi_\mu(x_1)\psi_\upsilon(x_2)dx_1dx_2 =$$

$$\int \psi_k^*(x_1)\psi_\ell^*(x_2)\Omega_{12}\psi_\mu(x_1)\psi_\upsilon(x_2) -$$

$$\int \psi_k^*(x_1)\psi_\ell^*(x_2)\Omega_{12}\psi_\upsilon(x_1)\psi_\mu(x_2)dx_1dx_2 =$$

$$< k\ell|\Omega_{12}|\mu\upsilon > - < k\ell|\Omega_{12}|\upsilon\mu > \quad \ldots (1.43)$$

For the special case when $\Omega_{12} = \frac{1}{r_{12}}$ (the electron repulsion operator) one often uses the Mulliken notation which visualizes the interacting electron densities:

$$< k\ell\left|\frac{1}{r_{12}}\right|\mu\upsilon > = \int \frac{\psi_k^*(x_1)\psi_\mu(x_1)\psi_\ell^*(x_2)\psi_\upsilon(x_2)dx_1dx_2}{r_{12}} = (k\mu|\ell\upsilon) \quad \ldots (1.44)$$

1.3. Density Matrices.

a. Definitions and Properties of Density Matrices.

In this section only an outline of the important definitions and properties associated with these quantities is given. Further details are available in standard references.[4-7]

We define a series of density matrices of various orders (first, second, ... , p-th, ... n-th)

$$\Gamma^1(x_1'|x_1) = n\int \Psi^*(x_1', x_2, \ldots, x_n)\Psi(x_1, x_2, \ldots, x_n)dx_2dx_3 \ldots dx_n \quad \ldots (1.45)$$

$$\Gamma^2(x_1'x_2'|x_1x_2) = \binom{n}{2}\int \Psi^*(x_1', x_2', x_3, \ldots, x_n)\Psi(x_1, x_2, x_3, \ldots, x_n)dx_3 \ldots dx_n \quad (1.46)$$

$$\Gamma^p(x_1'x_2' \ldots x_p'|x_1x_2 \ldots x_p) = \binom{n}{p}\int \Psi^*(x_1', x_2', \ldots, x_p', x_{p+1}, \ldots, x_n)$$

$$\Psi^*(x_1, x_2, \ldots, x_p, x_{p+1}, \ldots, x_n)dx_{p+1} \ldots dx_n \quad \ldots (1.47)$$

$$\Gamma^n(x_1'x_2' \ldots x_n'|x_1x_2 \ldots x_n) = \Psi^*(x_1', x_2', \ldots, x_n')\Psi(x_1, x_2, \ldots, x_n) \quad \ldots (1.48)$$

where $\Psi(x_1, x_2, \ldots, x_n)$ is a normalised wave function fulfilling the anti-symmetry condition (1.11) and $\binom{n}{p} = \frac{n!}{p!(n-p)!}$. The meaning of the primed co-ordinates will be explained below.

We shall now calculate the expectation value of the one electron operator $M = \sum_{i=1}^{n} M_i$ to illustrate the use of density matrices.

$$\langle M \rangle = \int \Psi^*(x_1, x_2, \ldots, x_n) \sum_{i=1}^{n} M_i \Psi(x_1, x_2, \ldots, x_n)dx_1dx_2 \ldots dx_n \quad \ldots (1.49)$$

A typical term in the sum (1.49) can be written as

$$\int \Psi^*(x_1, x_2, \ldots, x_i, \ldots, x_n)M_i\Psi(x_1, x_2, \ldots, x_i, \ldots, x_n)dx_1dx_2 \ldots dx_n \quad \ldots (1.50a)$$

The condition (1.11) allows us to write (1.50a) as

$$(-1)^{p_{i+}p_i}\int \Psi^*(x_i, x_2, \ldots, x_1, \ldots, x_n)M_i\Psi(x_i, x_2, \ldots, x_1, \ldots x_n)dx_1dx_2 \ldots dx_i \ldots dx_n$$

$$\ldots (1.50b)$$

Because i and 1 are dummy indices, we can write (1.50b) as

$$\int \Psi^*(x_1,x_2,\ldots, x_i,\ldots, x_n) M_1 \Psi(x_1,x_2,\ldots, x_i,\ldots,x_n) dx_1 dx_2 \ldots dx_i \ldots dx_n \quad (1.50c)$$

Consequently collecting all n terms we get

$$< M > = n \int \Psi^*(x_1,x_2,\ldots, x_n) M_1 \Psi(x_1,x_2,\ldots, x_n) dx_1 dx_2 \ldots dx_n \quad \ldots(1.51)$$

(1.51) can be conveniently written as

$$< M > = n \int [M_1 \Psi^*(x_1',x_2,\ldots, x_n) \Psi(x_1,x_2,\ldots, x_n)]_{x_1'=x_1} dx_1 dx_2 \ldots dx_n \quad \ldots(1.52)$$

Using (1.45) we get

$$< M > = n \int [M_1 \Gamma^1(x_1'|x_1)]_{x_1'=x_1} dx_1 \quad \ldots(1.53)$$

Here we have introduced the convention that in the integrands (1.53) and (1.52) the operator M_1 shall work only on the unprimed coordinate x_1 and that after this operation has been carried out we put $x_1' = x_1$ before the actual integration.

Generally for an operator

$$\Omega = \Omega_o + \sum_{i=1}^{n} \Omega_i + \frac{1}{2!} \sum_{i,j=1}^{n}{}' \Omega_{ij} + \frac{1}{3!} \sum_{i,j,k=1}^{n}{}' \Omega_{ijk} + \ldots \quad \ldots(1.54)$$

we obtain in a similar way

$$< \Omega > = < \Psi | \Omega | \Psi > =$$

$$\Omega_o + \int \Omega_1 \Gamma^1(x_1'|x_1) dx_1 + \int \Omega_{12} \Gamma^2(x_1'x_2'|x_1x_2) dx_1 dx_2$$

$$+ \Omega_{123} \Gamma^3(x_1'x_2'x_3'|x_1x_2x_3) dx_1 dx_2 dx_3 + \ldots \quad \ldots (1.55)$$

where the meaning of the primed indices again indicates which coordinates the operators operate upon before the integration.

We shall show in the next sections how density matrices can be useful in MO theory.

1.4. The Hartree-Fock Method.

a. Introduction.

There are many ways of looking at this fundamental approximation. From the point of view of the expansion (1.21) the Hartree-Fock (HF) approximation means that this expansion is truncated to one single term. The ingredients in this single determinant - the spin orbitals - are allowed to vary so as to minimize the expectation value of the total Hamiltonian with respect to the determinant. The resulting Hartree-Fock equations are effective one electron equations for these spin orbitals.

In the literature one encounters a whole series of abbreviations like RHF, VHF, SUHF, SEHF, SOHF etc. These refer to the specification of certain conditions imposed on the basic Hartree-Fock approximation and some will be briefly discussed in a later part of this chapter.

For many atoms and molecules in certain states, e.g. 'shake-up' states and for many open shell systems it is however not possible to restrict the treatment to one determinant and the method of configuration interaction (which we shall also mention later on) has to be used. The following discussion refers primarily to closed shell cases, but may readily be extended to some open shell systems.

b. Invariance Properties of Determinants.

We shall be working primarily with an orthonormal set of linearly independent spin orbitals satisfying the relation (1.15) in order to make use of Slater's rules. Justification for this restriction stems from a well known relationship in mathematics.

$$D' = D \cdot \det\{\mathcal{U}\} \qquad \ldots (1.56)$$

where

$$D = \mathcal{A}[\psi_1(x_1)\ \psi_2(x_2)\ \ldots\ \psi_n(x_n)] \qquad \ldots (1.57)$$

$$D' = \mathcal{A}[\psi'_1(x_1)\ \psi'_2(x_2)\ \ldots\ \psi'_n(x_n)] \qquad \ldots (1.58)$$

and $\mathcal{A}$ is a non-singular nxn matrix transforming one set of spin orbitals

$$\Psi = [\psi_1 \psi_2 \ldots\ \psi_n] \qquad \ldots (1.59)$$

to another set

$$\Psi' = [\psi'_1 \psi'_2 \ldots\ \psi'_n] \qquad \ldots (1.60)$$

by means of a linear transformation

$$\Psi' = \Psi \mathcal{A} \qquad \ldots (1.61)$$

From the equation (1.56) it is obvious that D' represents the same physical situation as D. Since we work with a set of linearly independent spin orbitals we can always choose the transformation matrix $\mathcal{A}$ such that the resulting spin orbitals are orthogonal to each other.

c. Evaluation of the Energy Expression.

In mathematical language the first step in the HF approximation implies evaluation of the following energy expression

$$\frac{< D|\mathcal{H}|D >}{< D|D >} \qquad \ldots (1.62)$$

where D is given by (1.57) and the Hamiltonian used here is the operator given by (1.7) which if written in atomic units has the form:

$$\mathcal{H} = \frac{1}{2} \sum'_{g,h} \frac{Z_g Z_h}{R_{gh}} - \frac{1}{2} \sum_i \Delta_i - \sum_{g,i} \frac{Z_g}{r_{ig}} + \frac{1}{2} \sum'_{i,j} \frac{1}{r_{ij}} \qquad \ldots (1.63)$$

The individual sums are over all electrons and nuclei and we use the notation $\Delta_i = \nabla_i^2$. Using Slater's rules we obtain

$$< D|D > = 1 \qquad \ldots (1.64)$$

$$\text{and } < D|\mathcal{H}|D > = \frac{1}{2} \sum'_{g,h} \frac{Z_g Z_h}{R_{gh}} - \sum_{k=1}^{n} < k|\frac{1}{2}\Delta_1 + \sum_g \frac{Z_g}{r_{1g}}|k > + \frac{1}{2} \sum_{k,\ell=1}^{n} < k\ell\left|\frac{1-P_{12}}{r_{12}}\right|k\ell > . \qquad \ldots (1.65)$$

d. Derivation of the Hartree-Fock Equations.

The next step involves the application of the variation principle to the wave function (1.57) which implies minimization of the expression (1.65) with respect to the spin orbitals, i.e.

$$\delta < D|\mathcal{H}|D> = 0 \qquad \ldots (1.66)$$

The expression (1.65) has been derived on the assumption that spin orbitals are orthonormal. When we start varying the expectation value of $\mathcal{H}$ we have to introduce a device which keeps them orthonormal, since otherwise Slater's rules are not valid. This is most directly done by introducing a set of undetermined constants $\lambda_{k\ell}$, the so-called Lagrangian multipliers and varying the expression

$$< D|\mathcal{H}|D> - \sum_{k,\ell=1}^{n} \lambda_{k\ell} < k|\ell > \qquad \ldots (1.67)$$

for arbitrary variations $(\delta\psi_1, \delta\psi_2, \ldots, \delta\psi_n)$, which is the method elaborated in many textbooks.

Alternatively we may introduce Lagrangian multipliers in a different way. In the method due to Dahl et al.[8] we firstly obtain with the help of the Slater's rules $\delta < D|\mathcal{H}|D>$ as a difference of $< D|\mathcal{H}|D>_{\psi+\delta\psi}$ and $<D|\mathcal{H}|D>_{\psi}$ where $< D|\mathcal{H}|D>_{\psi+\delta\psi}$ is an energy expression similar to (1.65) where we have replaced spin orbitals ψ by spin orbitals $\psi + \delta\psi$. Ignoring higher than the first order terms in $\delta\psi$ we obtain

$$\delta < D|\mathcal{H}|D> = \sum_{k=1}^{n} \{ < \delta\psi_k|h_1|\psi_k > + <\psi_k|h_1|\delta\psi_k > \} +$$

$$\sum_{k,\ell=1}^{n} < \delta\psi_k\psi_\ell \left|\frac{1-P_{12}}{r_{12}}\right|\psi_k\psi_\ell> + <\psi_k\psi_\ell\left|\frac{1-P_{12}}{r_{12}}\right|\delta\psi_k\psi_\ell > \qquad \ldots (1.68)$$

where $h_1 = -(\frac{1}{2}\Delta_1 + \sum_g \frac{Z_g}{r_{1g}})$.

Using the notation

$$F \equiv F(1) = h_1 + \sum_{\ell=1}^{n} \int \frac{\psi_\ell^*(x_2)(1-P_{12})\psi_\ell(x_2)}{r_{12}} dx_2 \qquad \ldots (1.69)$$

we can write (1.68) as

$$\delta < D|\mathcal{H}|D> = \sum_{k=1}^{n} \{ < \delta\psi_k|F|\psi_k> + < \psi_k|F|\delta\psi_k> \} \qquad \ldots (1.70)$$

where F is a one electron Hartree-Fock operator. We further require that the new spin orbitals $\psi + \delta\psi$ remain orthogonal. That is

$$< \psi_k + \delta\psi_k|\psi_\ell + \delta_\ell> = < \psi_k|\psi_\ell> + <\delta\psi_k|\psi_\ell> +$$
$$< \psi_k|\delta_\ell> + < \delta\psi_k|\delta\psi_\ell> \overset{\sim}{=}$$
$$0 + < \delta\psi_k|\psi_\ell> + < \psi_k|\delta_\ell> + 0 = \delta < k|\ell> = 0 \qquad \ldots (1.71)$$

where we have ignored the second order term and used (1.15). The orbitals satisfying (1.66) and (1.71) are Hartree-Fock spin orbitals. Of these n denoted by Roman subscripts are occupied $[\Psi_1, \Psi_2, \ldots, \Psi_k \ldots, \Psi_\ell, \ldots, \Psi_n]$ and the remaining ones denoted by Greek subscripts are unoccupied or virtual

$$[\Psi_{n+1}, \Psi_{n+2}, \ldots, \Psi_\lambda, \ldots, \Psi_\mu, \ldots].$$

The conditions (1.66) and (1.71) should be valid for all variations $(\delta\psi_1, \delta\psi_2, \ldots, \delta\psi_n)$ of spin orbitals, therefore it must hold for any particular instance, and for our purpose it is sufficient to consider a variation of the form

$$\delta\psi_i = C\Psi_\lambda, \ \delta\psi_k = 0 \text{ for } k \neq i, \qquad \ldots (1.72)$$

where C is a real constant and Ψ_λ is a fixed virtual HF orbital. These variations will certainly satisfy (1.71) because

$$\delta < i|\ell> = < \delta\psi_i|\Psi_\ell> + < \Psi_i|\delta\psi_\ell> =$$
$$\overset{*}{C} < \Psi_\lambda|\Psi_\ell> = 0 \qquad \ldots (1.73)$$

Further, the variations (1.72) imply for (1.66)

$$\overset{*}{C} < \Psi_\lambda|F|\Psi_i> + C < \Psi_i|F|\Psi_\lambda> = 0 \qquad \ldots (1.74)$$

where we have used the notation in (1.70).

Repeating the same procedure with variations when

$$\delta\psi_i = iC\Psi_\lambda \; ; \quad \delta_k = 0 \text{ for } k \neq i \qquad \ldots (1.75)$$

we obtain

$$-iC^* < \Psi_\lambda | F | \Psi_i > + iC < \Psi_i | F | \Psi_\lambda > = 0 \qquad \ldots (1.76)$$

(Note: Symbol i when not used as a subscript denotes a complex number.)

Combining (1.74) and (1.76) we obtain

$$< \Psi_i | F | \Psi_\lambda > = < \Psi_\lambda | F | \Psi_i > = 0 \qquad \ldots (1.78)$$

which holds for any occupied spin orbital Ψ_i and any virtual spin orbital Ψ_υ.

If we now expand $F\Psi_k$ in terms of occupied and virtual HF orbitals we obtain

$$F\Psi_k = \sum_{\ell=1}^{n} \Psi_\ell \varepsilon_{\ell k} + \sum_{\mu=n+1}^{\infty} \Psi_\mu \varepsilon_{\mu k} \qquad \ldots (1.79)$$

then we can show that the coefficients $\varepsilon_{\mu k}$ are zero.

Proof: If we multiply (1.79) by a fixed virtual spin orbital Ψ_μ^* and integrate we get for the LHS

$$\int \Psi_\mu^*(x_1) F(1) \Psi_k(x_1) dx_1 = < \mu | F | k > . \qquad \ldots (1.80)$$

This is equal to zero due to (1.78). The RHS of (1.79) becomes

$$\sum_{\ell=1}^{n} < \mu | \ell > \varepsilon_{\ell k} + \sum_{\upsilon=n+1}^{\infty} < \mu | \upsilon > \varepsilon_{\upsilon k} \qquad \ldots (1.81)$$

(Note that υ and μ are dummy indices.)

Using the orthogonality condition (1.15) the expression (1.81) reduces to $\varepsilon_{\mu k}$ which must be equal to (1.80) hence to zero.

Having proved that $\varepsilon_{\mu k} = 0$ we can write (1.79).

$$F\Psi_i = \sum_{k=1}^{n} \varepsilon_{ki} \Psi_k ; \quad i = 1,2,\ldots n \qquad \ldots (1.82)$$

(Note that k, ℓ and i are dummy indices.)

These n equations (1.82) are Hartree-Fock equations which the orbitals $\psi_1, \psi_2, \ldots \psi_n$ have to satisfy. These equations can be written in the matrix form

$$F\Psi = \Psi\mathcal{E} \qquad \ldots (1.83)$$

where Ψ and $\mathcal{E}$ are 1xn and nxn matrices respectively.

$$\Psi = [\psi_1 \psi_2 \ldots \psi_n] \qquad \mathcal{E} = \begin{bmatrix} \varepsilon_{11} & \varepsilon_{12} \cdots \varepsilon_{1n} \\ \varepsilon_{21} & \cdots \\ \vdots & \\ \varepsilon_{n1} & \varepsilon_{nn} \end{bmatrix}$$

$$\ldots (1.84)$$

The coefficients ε_{ki}, the Lagrangian multipliers, are elements of a Hermitian matrix since F is a Hermitian operator. Therefore $\mathcal{E}$ can be diagonalized by a unitary transformation

$$U^{+}\mathcal{E}U = \mathcal{E}' \; ; \; \varepsilon'_{ij} = \varepsilon'_i \delta_{ij} \qquad \ldots (1.85)$$

where the nxn matrix U satisfies

$$UU^{+} = U^{+}U = 1 \qquad \ldots (1.86)$$

Multiplying (1.83) by U from the right and using (1.85) and (1.86) we get

$$F\Psi' = \Psi'\mathcal{E}' \qquad \ldots (1.87)$$

where $\Psi' = \Psi U$ $\qquad \ldots (1.88)$

We may note that the operator F (1.69) is defined in terms of the original HF orbitals. We shall prove later on however that F is independent of the way in which the orthonormal set $\{\psi_i\}$ is chosen, hence F' = F, therefore we are justified in carrying out the unitary transformation (1.85).

Thus we obtain a set of equations in their canonical form

$$F\psi_i = \varepsilon_i \psi_i \quad i = 1,2,\ldots, n \qquad \ldots (1.89)$$

where we have dropped the primes for notational convenience. Equations of the type (1.89) were first derived by Fock[9] based on the earlier work of

Hartree[10] and are generally known as Hartree-Fock equations. We shall come back to the solution of (1.89) after a brief analysis of the results already derived.

e. The Fock-Dirac Density Matrix.

Fock[9] and Dirac[11] introduced the quantity

$$\rho(x_1,x_2) = \sum_{k=1}^{n} \psi_k^*(x_1)\psi_k(x_2) \qquad \ldots (1.90)$$

where $\{\psi_k\}$ are orthogonal spin orbitals defined in (1.57) and satisfying (1.15). This quantity $\rho(x_1,x_2)$ is called the Fock-Dirac matrix and can be shown to be invariant under a unitary transformation of spin orbitals, i.e.:-

$$\rho(x_1,x_2) = \sum_{k=1}^{n} \psi_k^*(x_1)\psi_k(x_2) =$$

$$= \sum_{k=1}^{n} \psi_k'^*(x_1)\psi_k'(x_2) \qquad \ldots (1.91)$$

where $\Psi' = \Psi U$, $\Psi = [\psi_1\ \psi_2 \ldots \psi_n]$

and U is a unitary matrix satisfying (1.86).

Löwdin[4,5] has shown using Slater's rules that a density matrix of order P defined by (1.47), where $\Psi(x_1,x_2,\ldots,x_n)$ is replaced by D defined in (1.57), is expressible in the form

$$\Gamma^p(x_1'x_2'\ldots x_p'|x_1x_2\ldots x_p) = \frac{1}{p!}\det\{\rho(x_i',x_j)\} \qquad \ldots (1.92)$$

For the particular cases of p = 1 and p = 2 we have

$$\Gamma(x_1'|x_1) = \rho(x_1',x_1) \qquad \ldots (1.93)$$

$$\Gamma^2(x_1'x_2'|x_1x_2) = \frac{1}{2}\begin{vmatrix} \rho(x_1',x_1) & (x_1'x_2) \\ \rho(x_2',x_1) & (x_2'x_2) \end{vmatrix} \qquad \ldots (1.94)$$

These relationships show that the Fock-Dirac matrix is identical to the first order density matrix, and that this determines the higher order

density matrices and hence the entire physical description of the system.

Finally it is useful to deduce a couple of important relationships. It is worthwhile pointing out that $\rho(x_1', x_1)$ is a kernel of a density operator . (For properties of kernels, see e.g. R. McWeeny[7]). The full array $\mathbf{P}$ is a matrix representing the density operator referred to the basis $\{\psi_k\}$. It is trivial to show using (1.90) that

$$\int \rho(x_1, \xi_1)\, \rho(\xi_1, x_2) = \rho(x_1, x_2) \qquad \ldots (1.95)$$

and $$\int \rho(x_1, x_1)\, dx_1 = n \qquad \ldots (1.96)$$

It can also be easily verified[4,5,6] that the relationships expressed in (1.95) and (1.96) lead to the following matrix relationships

$$\mathbf{P}^2 = \mathbf{P} \qquad \ldots (1.97)$$

$$\mathrm{Tr}(\mathbf{P}) = n \qquad \ldots (1.98)$$

which we shall need in the forthcoming sections.

f. Hartree-Fock, Coulomb and Exchange Operators.

We shall now make use of the Fock-Dirac density matrix (1.90) introduced in the previous section. Using (1.91) we may re-write the effective HF operator (1.69) as

$$F \equiv F(1) = h_1 + \int \frac{(1-P_{12})\, \rho(x_2, x_2')}{r_{12}}\, dx_2 \qquad \ldots (1.99)$$

The relationship (1.99) shows that the operator F(1) depends on the spin orbitals $\{\psi_i\}$ entirely through the quantity $\rho(x_2, x_2')$ which we have shown through (1.91) to be invariant under a unitary transformation. Therefore the HF operator F is also invariant under a unitary transformation and the relations (1.83) - (1.88) are justified.

The second term in the expression (1.99) can be written as

$$\int \frac{(1-P_{12})\, \rho(x_2, x_2')}{r_{12}} = C(1) + X(1) \qquad \ldots (1.100)$$

where

$$C(1) = \int \frac{\rho(x_2,x_2)}{r_{12}}\, dx_2 \qquad \ldots (1.101)$$

and

$$X(1) = \int \frac{-P_{12}\rho(x_2,x_2')}{r_{12}}\, dx_2 \qquad \ldots (1.102)$$

C(1) is called the Coulomb operator.

Note that we can remove the prime from the second coordinate in C(1). This Coulomb operator represents the potential at position 1 due to the charge distribution ρ. It is a multiplicative operator which is sometimes referred to as a local operator.

The exchange operator X(1) has a different character. If we operate on an arbitrary function $\phi(x_1)$ we obtain

$$X(1)\phi(x_1) = -\int \frac{P_{12}\rho(x_2,x_2')\phi(x_1)}{r_{12}}\, dx_2$$

$$= -\int \frac{\rho(x_1,x_2')\phi(x_2)}{r_{12}}\, dx_2 = -\int \frac{\rho(x_1,x_2)\phi(x_2)}{r_{12}}\, dx_2 \qquad \ldots (1.103)$$

P_{12} is an operator permuting non-primed coordinates x_1 and x_2. This means that to carry out such an operation it is not sufficient to know ϕ at x_1. We need to know ϕ for all values of its argument since it appears to be in the integral. The exchange operator is non-local. This is an aspect which is important to keep in mind in band theory and in certain recent MO theories.

g. Orbital Energies and the Total Energy.

We can write the total energy of the system in the HF formalism in terms of the Fock-Dirac density matrices. Combining (1.65) and (1.90) we obtain

$$E_{HF} = \langle D|\mathcal{H}|D\rangle = \frac{1}{2}\Sigma'_{g,h}\frac{Z_g Z_h}{R_{gh}} + \int h_1 \rho(x_1,x_1') +$$

$$\frac{1}{2}\int \frac{(1-P_{12})\rho(x_1,x_1')\rho(x_2,x_2')}{r_{12}}\, dx_1 dx_2 \qquad \ldots (1.104)$$

On the other hand from (1.89) and (1.99) we obtain

$$\sum_{k=1}^{n} \varepsilon_k = \sum_{k=1}^{n} \langle \Psi_k | F | \Psi_k \rangle = \int F(1)\rho(x_1,x_1')dx_1$$

$$= \int h_1 \rho(x_1,x_1') + \int \frac{(1-P_{12})\rho(x_1,x_1')\rho(x_2,x_2')dx_1dx_2}{r_{12}} \qquad \ldots (1.105)$$

Comparing (1.104) and (1.105) we obtain

$$E_{HF} = \frac{1}{2} \sum_{g,h}{}' \frac{Z_g Z_h}{R_{gh}} + \sum_{k=1}^{n} \varepsilon_k -$$

$$\frac{1}{2} \int \frac{(1-P_{12})\rho(x_1,x_1')\rho(x_2,x_2')}{r_{12}} dx_1dx_2 \qquad \ldots (1.106)$$

This is a very important relationship showing that the total HF energy E_{HF} is not equal to the sum of orbital energies. This is because the electronic repulsion is counted twice in the sum of orbital energies (1.105). The last term in (1.106) corrects for this.

h. Koopmans' Theorem.[12]

We assume that an atom or a molecule in a certain state is described by the HF determinant

$$D = \mathcal{A}_n[\Psi_1\Psi_2 \cdots \Psi_k \cdots \Psi_n] \qquad \ldots (1.107)$$

with spin orbitals Ψ_i satisfying (1.89). The simplest possible description appropriate for a corresponding ionized system would be a determinant with n-1 rows and columns, in which one of the spin orbitals (Ψ_k) is missing:

$$D_k^+ = \mathcal{A}_{n-1}[\Psi_1\Psi_2 \cdots \Psi_{k-1}\Psi_{k+1} \cdots \Psi_n] \qquad \ldots (1.108)$$

The corresponding Fock-Dirac matrices are related by

$$\rho(x,x') = \rho_k^+(x,x') + \Psi_k(x)\Psi_k^*(x') \qquad \ldots (1.109)$$

Using the expressions (1.105) and (1.106) together with Slater's rules we can show (for an initially closed shell system) that

$$E_{HF,k}^+ - E_{HF} = - \langle k|F|k \rangle = -\varepsilon_k \qquad \ldots (1.110)$$

This implies that the negative of the orbital energies can be interpreted as the ionization potentials. This is often referred to as Koopmans' theorem.[12] We may note however that in deducing (1.110) we have neglected all reorganization of the electrons consequent upon ionization - the so-called relaxation, because the remaining spin orbitals in (1.108) are taken to be the same as in (1.107) which is of course only an approximation. Further details on this topic concerning mainly calculations of ionization energies and the importance and consequences of relaxation (reorganization) phenomena will be discussed in subsequent chapters.

i. The Self-Consistent Field Method.

At this stage we may now discuss the solutions of the Hartree-Fock equations (1.89). The main problem in the solution of these equations is associated with the fact that the Hartree-Fock operator F(1) (1.99) itself depends on the solution ψ_k of the equations (1.89).

Although exact solutions of HF equations are limited to a few special cases, the concept of self consistent fields (SCF) provides in principle a formalism for approximate solutions to any desired degree of accuracy. The general philosophy behind the approach is to 'guess' an initial set of $\{\psi_k^{o}\}$. These can be used to construct the Fock-Dirac matrix

$$\rho^{o}(x,x') = \sum_{k=1}^{n} \psi_k^{(o)}(x)\psi_k^{(o)*}(x') \qquad \ldots (1.111)$$

which gives the first approximation of the effective HF operator $F^{(o)}$ (1.99). Then the next set of approximate spin orbitals $\{\psi_k^{(1)}\}$ is obtained from (1.89) by regarding $F^{(o)}$ as a fixed operator

$$F^{(o)}\,\psi_k^{(1)} = \varepsilon_k \psi_k^{(1)} \qquad \ldots (1.112)$$

The whole procedure is repeated until the Fock-Dirac matrix no longer changes (within a certain tolerance) on further iteration. The orbitals which generate the final Fock-Dirac matrix are then said to be self-consistent with

the potential field they generate and the whole procedure is called the self-consistent field method. In practical calculations there are two main streams in handling the SCF idea: numerical and analytical methods. In the numerical methods the problem is in one way or another reduced to an integro-differential equation which is solved numerically. The analytical methods are characterized by the use of a known set of basis functions. The unknown solutions are expanded in these basis functions, and the problem is reduced to a set of linear equations for the corresponding coefficients.

j. Open Shell Methods.

Most of the expressions derived in this section on the Hartree-Fock method apply strictly speaking to closed shell systems. However calculations on open shell species (in our case on core and valence ionized states) are becoming increasingly important and are part of an essential routine to any theoretical chemist. There are several procedures to tackle the problem of open shell molecules, all based on the HF theory and its various extensions. The most commonly used techniques are:- Roothaan's Open Shell Method,[13] Nesbet's Method,[14] and the UHF method discussed in a later section.

1.5. The LCAO MO Method.

a. Basic Procedure.

The main analytical method for solving the HF equations is the method in which Molecular Orbitals are constructed as Linear Combinations of Atomic Orbitals, the LCAO MO method. In this approach each Hartree-Fock molecular spin orbital is expanded in terms of a set of basis functions

$$\psi_k = \sum_{\mu=1}^{m} \phi_\mu(x) c_{\mu k}; \quad k = 1,2,\ldots, n \qquad \ldots (1.113)$$

where $\Phi = \{\phi_1 \ \phi_2 \ \ldots \ \phi_m\}$ ... (1.114)

is a set of m basis functions whose form will be discussed later. If the complete set Φ is used (i.e. m is infinite), the final result will approach

the Hartree-Fock limit. In practice, however, one truncates the expansion so that m is finite. In order to be able to construct at least n linearly independent solutions, it is necessary that $m > n$.

One way of introducing the LCAO procedure is to use expansion (1.113) as the means of solving equations like (1.112) where the operator F is temporarily fixed. Inserting (1.113) into such equations we obtain

$$\sum_{\mu=1}^{m} F\phi_\mu(x) c_{\mu k} = \varepsilon_k \sum_{\mu=1}^{m} \phi_\mu(x) c_{\mu k} \qquad \ldots (1.115)$$

Multiplying (1.115) from the left by a fixed basis function $\phi_\upsilon^*(x)$ and integrating we obtain

$$\sum_{\mu=1}^{m} F_{\upsilon\mu} c_{\mu k} = \varepsilon_k \sum_{\mu=1}^{m} \Delta_{\upsilon\mu} c_{\mu k} \qquad \ldots (1.116)$$

which can be re-written as

$$\sum_{\mu=1}^{m} [F_{\upsilon\mu} - \varepsilon\Delta_{\upsilon\mu}] c_\mu = 0 \qquad \ldots (1.117)$$

where we have left out the index k for convenience and where

$$F_{\upsilon\mu} = \int \phi_\upsilon^*(x) F\phi_\mu(x)\, dx \qquad \ldots (1.118)$$

$$\Delta_{\upsilon\mu} = \int \phi_\upsilon^*(x) \phi_\mu(x)\, dx \qquad \ldots (1.119)$$

There are m equations of the type (1.117), because $\upsilon = 1,2,\ldots, m$ and they form a set of linear equations which have non-trivial solutions only if the determinant of their coefficients vanishes

$$\det\{ F_{\upsilon\mu} - \varepsilon\Delta_{\upsilon\mu} \} = 0. \qquad \ldots (1.120)$$

The solution of (1.120) yields m eigenvalues ε_k and for each ε_k we get a corresponding set of coefficients $c_{\mu k}$; $\mu = 1,2,\ldots, m$. It is convenient to arrange them in a column matrix

$$\mathbb{C}_k = \begin{bmatrix} c_1^k \\ c_2^k \\ c_\mu^k \\ c_m^k \end{bmatrix} , \qquad \ldots (1.121)$$

and to collect all such columns in a square matrix of dimensions mxm

$$\mathbb{C}' = [\mathbb{C}_1 \mathbb{C}_2 \ldots \mathbb{C}_m] = \qquad \ldots (1.122)$$

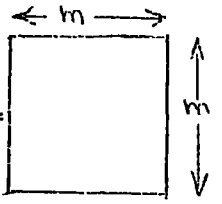

For the original problem we need however only n such vectors, which is why the two concepts occupied and virtual spin orbitals are introduced.
(In most applications the occupancy of orbitals in successive SCF cycles is determined by the Aufbau principle.)

$$\mathbb{C}' = [\overbrace{\mathbb{C}_1 \mathbb{C}_2 \ldots \mathbb{C}_n}^{\mathbb{C}\ (mxn)\ \text{matrix}} \mathbb{C}_{n+1} \ldots \mathbb{C}_m] =$$

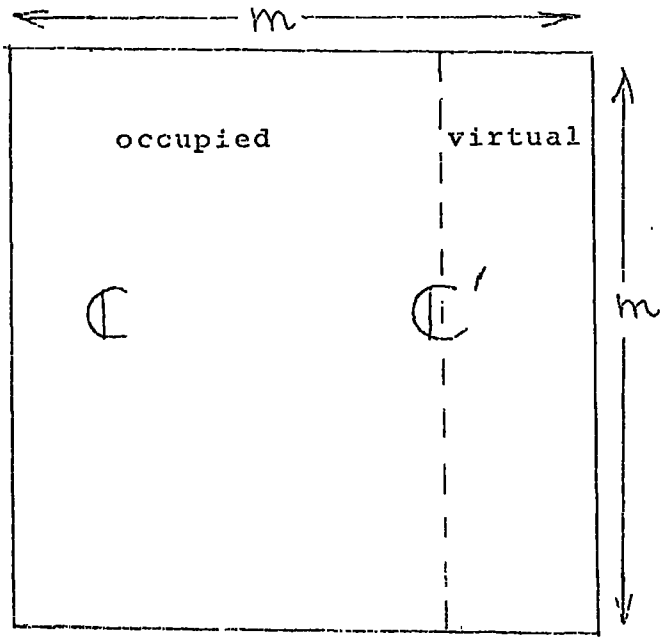

... (1.123)

It is worthwhile to mention briefly the practical solution of the problem (1.120). The evaluation of $\det\{F_{\upsilon\mu} - \varepsilon\Delta_{\upsilon\mu}\}$ is not very practical and therefore we re-write the general expression (1.117) in matrix notation as

$$\mathbb{F}\,\mathbb{C}' = \mathbb{\Delta}\,\mathbb{C}'\mathbb{E} \qquad \ldots (1.124)$$

This is a standard matrix eigenvalue problem which can be tackled by diagonalization of the hermitian matrix . Two well known procedures for this process are Jacobi and Householder methods described e.g. by Cook.[15] The presence of the overlap matrix $\mathbb{\Delta}$ in (1.124) which superficially seems to complicate the diagonalization of the Fock matrix can be overcome by various standard numerical procedures again described e.g. by Cook.[15]

There are several methods used for guessing the initial matrix $\mathbb{C}^{o}$ for the iterative procedure. The simplest way (even if not the most efficient) is to diagonalize the one electron Hamiltonian operator matrix $\mathbb{h}_1$ and the n eigenvectors of lowest eigenvalue will define $\mathbb{C}^{o}$. Note that a general element of the $\mathbb{h}_1$ matrix is

$$h_{1\,\upsilon\mu} = \int \phi^{*}_{\upsilon}(x) h_1 \phi_{\mu}(x)\,dx \qquad \ldots (1.125)$$

$$\text{where } h_1 = -(\tfrac{1}{2}\Delta_1 + \sum_{g} \frac{Z_g}{r_{ig}}) \qquad \ldots (1.126)$$

b. <u>The Charge and Bond Order Matrix.</u>

In the LCAO MO approximation the set of occupied M.O.'s is written in a matrix as

$$\mathbb{\Psi} = [\Psi_1 \Psi_2 \ldots \Psi_n] \qquad \ldots (1.127)$$

Using (1.113) and (1.114) we can write (1.127) as

$$\mathbb{\Psi} = \mathbb{\Phi}\mathbb{C} \qquad \ldots (1.128)$$

The M.O.'s are orthonormal

$$\mathbb{\Psi}^{+}\mathbb{\Psi} = \langle \mathbb{\Psi} | \mathbb{\Psi} \rangle = \mathbb{1} \qquad \ldots (1.129)$$

but the basis functions (1.114) in general are not orthogonal

$$\Phi^{+}\Phi = \langle\Phi|\Phi\rangle = \Delta = 1 \qquad \ldots (1.130)$$

If one thinks of a row function (1.127) as a matrix with the column labelled by discrete indices 1,2,...,n and the rows by a continuous index x, i.e.

$$\Psi = \begin{bmatrix} \psi_1(x_1)\psi_2(x_1)\ldots\psi_n(x_1) \\ \psi_1(x_2)\psi_2(x_2)\ldots\psi_n(x_2) \\ \vdots \quad \vdots \\ \psi_1(x_\infty) \quad \vdots \quad \ldots \quad \psi_n(x_\infty) \end{bmatrix} \qquad \ldots (1.131)$$

then the Fock-Dirac matrix can be written as

$$\rho = \Psi\Psi^{+} = |\Psi\rangle\langle\Psi| \qquad \ldots (1.132)$$

We can rewrite (1.132) in terms of basis functions. Using (1.128) in (1.132) we get

$$\rho = |\Phi\rangle C C^{+} \langle\Phi| = |\Phi\rangle R \langle\Phi| \qquad \ldots (1.133)$$

The matrix

$$R = CC^{+} = \underset{n \times m}{\square} \; \underset{m \times n}{\square} = \underset{n \times n}{\square} \qquad \ldots (1.134)$$

is often referred to as charge and bond order matrix and is in fact the Fock-Dirac matrix in the particular representation . It is trivial to check that the relation (1.97) $\rho^2 = \rho$ implies

$$R \Delta R = R \qquad \ldots (1.135)$$

and the relation (1.98) $\mathrm{Tr}(\rho) = n$ implies

$$\mathrm{Tr}(\Delta R) = \mathrm{Tr}(R \Delta) = n \qquad \ldots (1.136)$$

c. Population Analysis.

The charge and bond order matrix R together with the bond overlap matrix Δ are used in the so-called Mulliken Population Analysis[16] to

analyse the results of LCAO MO calculations.

We shall illustrate the Mulliken procedure for restricted Hartree-Fock (RHF) wave function whose main characteristic is the equivalence restriction. For closed shell species this implies

$$\psi_{2i-1}(k) = \phi_i(k)\alpha(k)$$
$$\psi_{2i}(k) = \phi_i(k)\beta(k) \qquad \ldots (1.137)$$

where ϕ_i is a spatial part and α, β are spin parts associated with spin orbitals ψ_{2i-1} and ψ_{2i} respectively.

Applying (1.15) to ψ_{2i} and ψ_{2j} (or ψ_{2i-1} and ψ_{2j-1}), integrating over the spin factors and using (1.14b) we obtain

$$\langle \phi_i | \phi_j \rangle = \delta_{ij} \qquad \ldots (1.138)$$

The determinant (1.57) now becomes

$$D = \mathcal{A}[\psi_1(1)\alpha(1)\ \psi_1(2)\beta(2)\ \psi_2(3)\alpha(3)\ldots\ \psi_{n/2}(n)\beta(n)] \qquad \ldots (1.139)$$

and we now have to solve $^n/2$ Hartree-Fock equations (1.89)

$$F\psi_i = \epsilon_i \psi_i \quad i = 1,2,\ldots, {}^n/2 \qquad \ldots (1.140)$$

In the LCAO MO approach the $\mathbb{C}'$ matrix (1.123) now has the form

$$\mathbb{C}' = [\underbrace{\mathbb{C}_1 \mathbb{C}_2 \cdots \mathbb{C}_{n/2}}_{\mathbb{C}\ (m \times n/2)\ \text{matrix}}, \quad {}^n/_{2+1} \cdots \quad {}^m] \qquad \ldots (1.141)$$

For closed shell systems with $^n/2$ doubly occupied molecular orbitals (DOMOS) we obtain by using $\mathbb{C}$ from (1.141) in the equation (1.134)

$$\mathbb{R} = \mathbb{C}\,\mathbb{C}^+ \qquad \ldots (1.142)$$

where an element of the above matrix is given as

$$R_{ij} = \sum_{u=1}^{n/2} c_{iu} c_{ju} \qquad \ldots (1.143)$$

We define an overlap population matrix $\mathbb{W}$ with an element

$$W_{ij} = 2R_{ij}\Delta_{ij} \qquad \ldots (1.144)$$

where Δ_{ij} is an overlap integral connecting basis functions i and j defined by (1.119).

In the Mulliken approach

$$V_j = \sum_{i=1}^{m} W_{ij} \qquad \ldots (1.145)$$

corresponds to the population of basis function j.

The charge q_A assigned to the atom A is then given by

$$q_A = Z_A - \sum_{j}^{A} V_j \qquad \ldots (1.146)$$

where Z_A is the atomic number of A, and the sum is taken over all basis functions centred on atom A.

The overlap population matrix $\mathbb{W}$ can also be used to calculate bond overlaps q_{AB} (which can be split into σ and π components) between atoms A and B in a given molecule.

$$q_{AB} = 2 \sum_{j}^{\text{all A}} \sum_{i}^{\text{all B}} W_{ij} \qquad \ldots (1.147)$$

($\sum_{i}^{\text{all B}}$ implies that the summation is taken over all i's which are indices of basis functions centred at B only for a given j which is an index of a given basis function centred at A.) These bond overlaps may be used to give us information about a strength and a geometry of that bond.

Although we have not considered open shell species in any detail, it is worth mentioning that a similar analysis can be carried out for molecules with unpaired electrons. Here in addition to a closed shell density matrix

$$\mathbb{R}_2 = \mathbb{C}_2 \mathbb{C}_2^{+} \qquad \ldots (1.148)$$

we define an open shell density matrix

$$\mathbb{R}_1 = \mathbb{C}_1 \mathbb{C}_1^{+} \qquad \ldots (1.149)$$

where $\mathbb{C}_2$ and $\mathbb{C}_1$ denote eigen vector arrays associated with DOMOS and SOMOS (singly occupied molecular orbitals) respectively. Similarly the overlap population matrix formed from DOMOS $\mathcal{W}_2$ has an element

$$(W_2)_{ij} = 2(R_2)_{ij}\Delta_{ij} \qquad \ldots (1.150)$$

and the corresponding matrix elements of $\mathcal{W}_1$ is

$$(W_1)_{ij} = 1(R_1)_{ij}\Delta_{ij} \qquad \ldots (1.151)$$

In an analogy with the expression (1.145) we define

$$(V_2)_j = \sum_{i=1}^{m} (W_2)_{ij} \qquad \ldots (1.152)$$

$$(V_1)_j = \sum_{i=1}^{m} (W_1)_{ij} \qquad \ldots (1.153)$$

which correspond to the contribution from DOMOS and SOMOS respectively to the Mulliken population of the basis function j. Further

$$V_j = (V_1)_j + (V_2)_j \qquad \ldots (1.154)$$

corresponds to the total Mulliken population of the j^{th} basis function and the equation (1.146) gives again the total charge on atom A. Finally bond overlaps between a pair of atoms from DOMOS and SOMOS can be calculated from the expression (1.147) using appropriate elements of the matrices $\mathcal{W}_2$ and $\mathcal{W}_1$ respectively, and the sum of these can again tell us something about the strength and the geometry of the bond under consideration.

There are a number of weaknesses associated with this approach to elaborating details of electron distributions in molecules. Notably assigning electron population to a given atom, because a basis function is centred on that atom is a simplification, especially if the basis function concerned is diffuse. Further, it is arbitrary to divide the overlap terms equally between the centres concerned (see expressions 1.144, 1.150, 1.151). The next drawback stems from the fact that $\mathbb{R}$ (and $\mathbb{R}_1, \mathbb{R}_2$) is basis set dependent which comes clearly from the invariance property of $\mathcal{P}$ (see (1.91)) and dependence of Δ on basis functions. This clearly implies that charges on atoms (and bond

overlaps between them) are basis set dependent. The classic example is the CO molecule where not only different basis sets give various absolute values of charges, but also give different relative charges (i.e. signs) on carbon and oxygen. This is clearly illustrated in Table 1.1.

Table 1.1.

Charges on Carbon and Oxygen in CO Molecule Calculated with Different Basis Sets. (Details of these Calculations will be Discussed in the Later Chapters)

Basis Set	Charge on Carbon	Charge on Oxygen
STO 4-31G	-0.076	+0.076
Double Zeta Slater	+0.451	-0.451
Extended Slater	+0.356	-0.356

Despite these limitations the Mulliken population analysis is conceptually close to qualitative ideas about charge distributions in molecules, and as we shall see in the next chapters, it can be very useful to a theoretical chemist when cautiously used; particularly if the emphasis is on interpreting trends and differences for a series of closely related molecules.

Often a more useful method of looking at the electronic charge distribution in a molecule is by use of density contour maps. In this approach the electronic density at a point in space r is evaluated

$$\rho(r) = \sum_{ij} 2R_{ij}\phi_i(r)\phi_j(r) \qquad \ldots (1.155)$$

(This expression is for closed shell systems. For open shell molecules we have to consider again

$$\rho_2(r),\ \rho_1(r),\ (R_2)_{ij} \text{ and } (R_1)_{ij}.)$$

An arbitrary grid of densities is usually produced and from these contours are built up by employing an interpolation procedure. We shall be using these

contours (and in particular difference contours) to indicate changes of electron densities in different regions of a molecule as a consequence of electronic reorganizations accompanying photoionization.

d. Basis Function and Basis Sets.

We have already mentioned that in the LCAO-MO procedure each molecular orbital is expanded according to (1.113) in terms of a set of basis functions. Exponential or Gaussian functions are most frequently employed for this purpose.

Exponential Functions.

The use of exponential functions was first suggested by Slater[17] and functions of the type

$$Ar^{n-1}e^{-\zeta r} \qquad \ldots (1.156)$$

are therefore called Slater functions or Slater-type orbitals (STO's), where A is a normalization factor, n is a principal number and ζ is an orbital exponent. Angular dependence is usually introduced by multiplying (1.156) by the appropriate spherical harmonic $Y_{lm}(\theta,\phi)$.

Gaussian Functions.

The use of Gaussian functions or Gaussian type orbitals (GTO's) in electronic structure calculation was first suggested by Boys.[18] By analogy with (1.156) the radial dependence of a Gaussian function may be written as

$$Br^{n}e^{-\alpha r^{2}} \qquad \ldots (1.157)$$

where n is the analogue of the principal quantum number in the Slater function case. Angular dependence may be again introduced by a factor $Y_{lm}(\theta,\phi)$. However the more usual form of Gaussians including both radial and angular dependence is often introduced by a function of the form

$$Cx^{p}y^{q}z^{s}e^{-\alpha r^{2}} \qquad \ldots (1.158)$$

where p, q, s are integers. Functions of the type (1.158) are called Cartesian Gaussians. If, for example p = q = 0 and s = 1, the function is of P_z symmetry.

The main attraction of Gaussian functions is their well known property[19] which is: that the product of two Gaussian functions G_a and G_b centred on different points a and b is itself a Gaussian function centred at a point e located on the line joining these points.

Thus

$$< G_a G_b \left| \frac{1}{r_{12}} \right| G_c G_d > \; = \; < G_e \left| \frac{1}{r_{12}} \right| G_f > \qquad \ldots (1.159)$$

Therefore three- or four-centre integrals which are very time consuming in LCAO MO calculations are reduced to relatively simple two-centre integrals.

The major drawback to the use of Gaussian functions is that they do not resemble atomic orbitals very closely. In particular the S type Gaussian function lacks a cusp at the nucleus and also its property at large distance is very different from a true behaviour. Figure 1.1 clearly illustrates this where a comparison is made with a Slater type orbital, the latter being a somewhat better approximation.

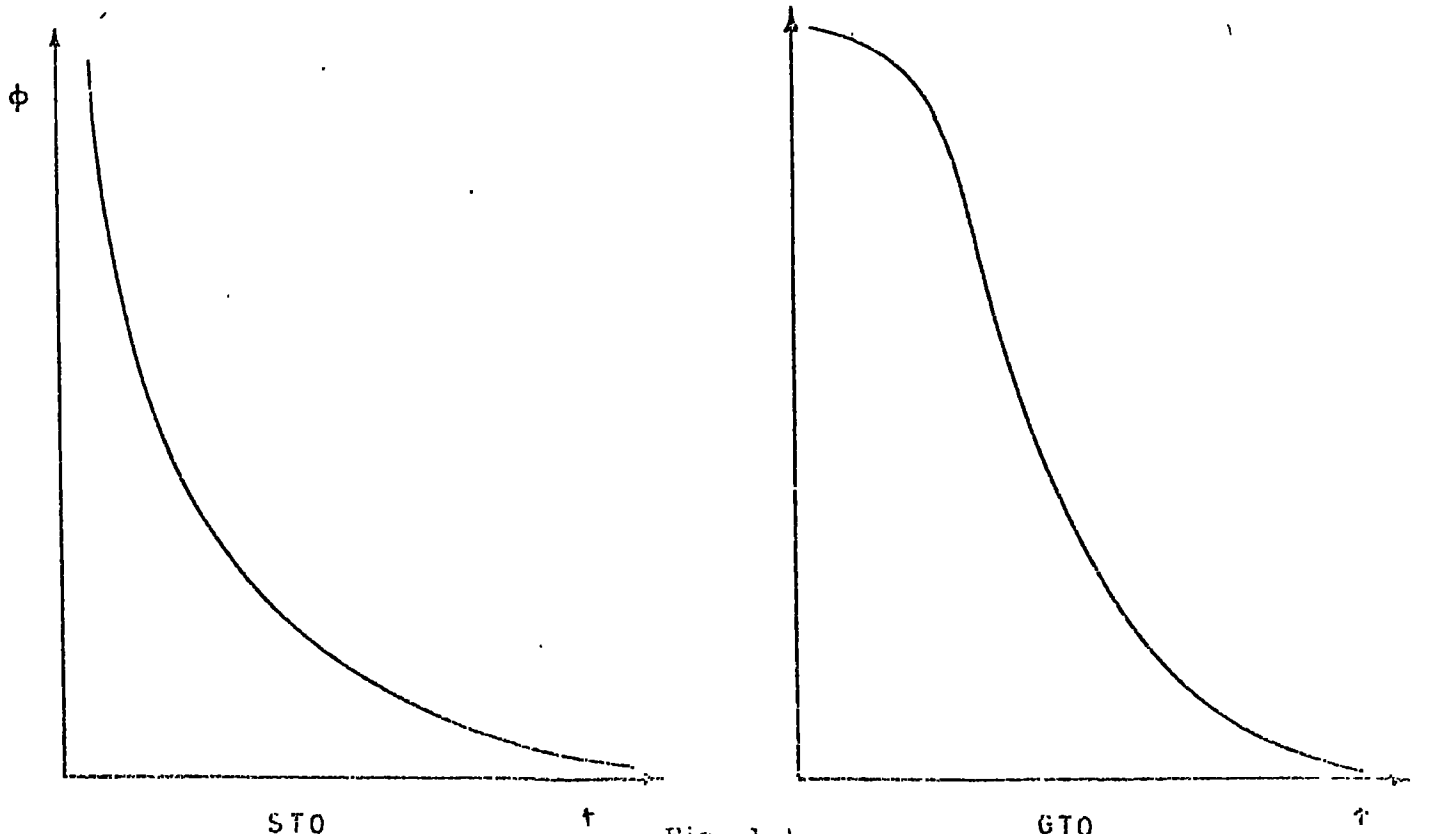

Fig. 1.1.

The Minimal Basis Set.

The basis set is usually described as minimal if it contains only one function for each atomic orbital occupied or partly occupied in the atomic ground state. For molecules with only first row atoms a minimal basis set consists of a 1s function for hydrogen and 1s, 2s, 2px, 2py, 2pz functions for the other atoms. The functions in a minimal basis set are usually Slater functions.

The most important problem is to find the values of exponents ζ for various atoms. The original method for finding these makes use of empirical rules deduced by Slater.[17] The present modern procedures consist of variation of ζ values in repeated atomic SCF calculations for the ground electronic state of each atom until a set of ζ's is obtained giving the lowest possible minimal basis energy. Clementi[20,21] and his co-workers have produced tables containing such best atom exponents, and the exponents in reference 20 have been used in this present work and are reproduced in Appendix 1. Atom optimized basis set exponents are usually used directly in MO calculations even if a molecular environment is often quite different from that of a free atom, because optimization of exponents in molecular environments is generally not computationally practical. Therefore it is preferred to extend the size of a basis set if a greater accuracy of calculation is desired.

A minimal Slater basis set is conceptually simple, but requires a computation of complicated multicentre two-electron integrals. To overcome this problem, Foster and Boys[22] suggested to expand each STO in terms of linear combinations of n Gaussian functions (the STO-nG method). This scheme was extensively tested by Pople and his co-workers.[23,24] In their technique the coefficients and exponents of the Gaussians are optimized by a least squares method to fit a Slater orbital of unit exponent. The

Slater exponent is then chosen and the Gaussian exponent scaled accordingly (scaled Gaussian exponent = least squared optimized exponent X (Slater exponent)^2). The coefficients of the Gaussians obtained from the least squares expansion and the scaled exponents are then used in the STO-nG expansion.

Stewart[25] has also obtained an expansion of Clementi[26] STO SCF AO's (which are Hartree-Fock orbitals) in terms of Gaussian functions for the first row atoms by the method of least squares. The coefficients and exponents of the Gaussians from this expansion form ingredients of the so-called HF-nG minimal basis set which closely resembles the STO-nG set. The HF-nG expansion is primarily useful in calculations on molecules containing electronegative atoms like oxygen or fluorine, because it is well known that the shapes of the atomic orbitals of these elements are not very well reproduced by a simple exponential function.

Split Valence Basis Set.

Pople and co-workers[27] have introduced a slightly more flexible basis set, the so-called split valence 4-31G basis set. In this set each inner shell is represented by a single basis function taken as a sum of four Gaussians, and each valence orbital is split into inner and outer parts described by three and one Gaussian functions, each part being varied independently. Depending on the way the expansion coefficients and Gaussian exponents are determined we obtain STO 4-31G,[24] HF 4-31G[25] and LEMAO (least energy minimal atomic orbitals) 4-31G[27] split valence basis sets.

These split valence basis sets are relatively economical to use and are capable of describing the main features of the changes of atomic size and angular distortion which occur in a molecule. We shall see later on that when the concept of an equivalent core atom is incorporated into these

split sets, then they can be useful in calculating fairly accurately wave functions of core hole state species.

Double Zeta and Extended Basis Sets.

An improvement in the overall SCF energy can be obtained with double zeta basis set. This set includes exactly twice as many Slater functions as the minimal basis. For the first, second and third row atoms double zeta basis sets have again been determined by successive ground state SCF calculations until the best possible sets of $\{\zeta$ values are obtained.[28,29,30] Appendix 1 contains exponents for double zeta basis set used in this work, which have been taken from reference 28.

In order to approach the Hartree-Fock limit triple or extended basis sets (E.B.S.) have to be employed. In this work the extended basis set (E.B.S.) have employed best atom exponents due to McLean and Yoshimire.[31] The values of these exponents are again tabulated in Appendix 1.

Gaussian Basis Set.

A large body of literature with carefully optimized Gaussian basis sets of various sizes is well known.[32,33,34] These sets have been optimized for ground state of atoms by varying the Gaussian exponents α in (1.157) or (1.158) and minimizing the SCF energy.

It is already been pointed out (Figure 1.1) that a STO provides a more adequate description of atomic functions than a GTO. For this reason it is necessary to use a larger number of Gaussian functions compared with Slaters in order to achieve the same accuracy. If there are m basis functions then it can be shown that in the LCAO MO procedure

Number of one-electron integrals (p) $= \frac{m(m+1)}{2}$

Number of two-electron integrals (t) $= \frac{p(p+1)}{2} =$

$\frac{1}{8}(m^4 + 2m^3 + 3m^2 + 2m) \simeq m^4$

Even if it is easier to evaluate a 'large' number of 2-electron integrals over Gaussians than relatively 'fewer' such integrals over Slaters, a relatively large number of Gaussians introduces a problem of storage space for the integrals. Further the time required to build up and diagonalize a Fock matrix (1.124) rapidly increases (the fastest diagonalization procedures are roughly proportional to the cube of the matrix dimensions), and the iterative process converges very slowly when large basis sets are used. The above problems have led to the use of contracted Gaussians, linear combinations of Gaussians with fixed coefficients.[35,36] In this technique, then, only the integrals over the contracted functions are stored and in solving the SCF equations only the coefficients in each MO of the contracted functions must be determined. This approach allows one to exploit the analytical properties of Gaussians in integral evaluation and yet save on storage space and keep the time required for the SCF iteration at a reasonable level. How much accuracy is lost as a result of such contractions depends a great deal on the skill with which the initial basis of the Gaussians is contracted. This problem is discussed elsewhere.[35,36,37]

It is worthwhile noting that most calculations in this work have been performed with split valence 4-31G basis sets which are relatively small, but incorporate the advantageous principles discussed above. Integration is done over Gaussian functions which are contracted, a fair amount of flexibility is retained in the valence region (which is in principle of double zeta quality) and the idea of atomic orbitals is preserved.

Polarization Functions.

As we have already pointed out a Hartree-Fock limit can only be achieved in principle with an infinitely large basis set. This is not a

very practical suggestion, and a majority of calculations are done only with basis functions representing each atomic orbital occupied or partly occupied. However as emphasized by Nesbet[38] inclusion of 'higher functions' (e.g. 2p for H, 3d for Cl, 4d for Br) can lead to a substantial decrease in SCF energy and an improvement of some computed expectation values of various properties of the molecule. Fortunately these properties are not too sensitive to small variations in exponents of polarization functions, and it is often enough to make reasonable choices of these exponents based on optimized small molecule calculations[39] or even to refer to simple empirical rules such as Slater's[17] or Burns'[40] rules.

e. Semi-Empirical LCAO MO Methods.

The main difficulty in using the LCAO MO method for actual calculations is to compute the matrix elements of the Hartree-Fock operator (1.118) which involves a computation of a large number of three- and four-centre two-electron integrals. In the so-called ab initio methods all integrals are computed, but in semi-empirical procedures a number of integrals is either set to zero (e.g. some two centre and all three and four centre integrals) or estimated empirically from parameters of different kinds taken from experimental data. Consequently a great amount of accuracy is lost but the computation time is drastically reduced thus allowing larger systems to be studied.

Various semi-empirical schemes have been devised over the years differing mainly in the degree of approximation involved. The methods for a treatment of π electrons explicitly are Hückel (HMO) and PPP methods.[41] The well known methods which include all valence electrons are known in their abbreviated form as CNDO, INDO, NDDO, MINDO, EHMO techniques.[42]

The nature of the projects presented in the following chapters are such that only a non-empirical treatment is feasible. But one should not underestimate semi-empirical methods because presently and also in the near future a great majority of the problems in chemistry will be computationally impossible to be tackled by ab initio methods. Knowing their advantages, limitations and pitfalls, semi-empirical methods can be a valuable tool to any theoretically minded chemist.

1.6. Beyond the Hartree-Fock Limit.

a. The Statement of the Problem.

The experimental energy of a molecule is different from the Hartree-Fock energy due to spin, relativistic and correlation effects. We can write

$$E_{expt} = E_{HF} + E_{corr} + E_{relat} + E_{spin} \qquad \ldots (1.160)$$

The approximations inherent in using a non-relativistic spin free hamiltonian are negligible for molecules containing first row atoms as far as the work in this thesis is concerned. Therefore E_{relat} and E_{spin} can be ignored in terms of their contribution to the total energy.

By contrast the inclusion of correlation effects is of some importance since although the absolute magnitude of E_{corr} is small compared with E_{HF} for the systems of interest in as far as this thesis is concerned the contribution to energy differences can often be significant.

b. Correlation of Electrons.

Ignoring spin and relativistic effects equation (1.160) now becomes

$$E_{expt} = E_{HF} + E_{corr} \qquad \ldots (1.161)$$

The exact expression (equation (1.55) where Ω is replaced by the Hamiltonian defined in (1.63)) for total energy may now be written as

$$\langle \mathcal{H} \rangle = E_{HF} + E_{corr} \qquad \ldots (1.162)$$

where E_{HF} is the Hartree-Fock energy defined by (1.104), and E_{corr} is the correlation energy. According to (1.162) the correlation energy is defined as the difference between the exact energy and the energy at the HF limit. This definition is due to Löwdin.[43] Correlation energy is therefore a mathematical quantity telling us the error in the energy at the HF limit. The physical reason for this error can be easily seen from the following consideration. The HF treatment neglects instantaneous repulsions between pairs of electrons and instead considers an average interaction. In reality an electron in a molecule (or an atom) will have instantaneous interactions with all other electrons due to Coulombic repulsions. These interactions will not be the same as the average interaction included in the HF procedure. The difference of these two interactions is the origin of the correlation error which is partly accounted for in the case of electrons of the same spin by the antisymmetrizer (1.12). The antisymmetrizer correlates electrons of the same spin, because it does not allow more than one electron of a certain spin to occupy a given spatial orbital. Löwdin[43] has demonstrated this quantitatively using the second order density matrices.

The problem of correlation can be basically handled in two ways. Either we ignore the errors associated with correlation or we try to estimate them.

c. Cases where a Correlation Error can be Ignored.

There are many problems in chemistry where we can ignore with confidence the effects of electronic correlation. In this work Hartree-Fock energies have been primarily used to calculate potential energy surfaces (PES's) and ionization energies of some molecules.

i) Some important aspects of PES's, namely equilibrium geometries and force constants can be successfully predicted within the

Hartree-Fock formalism. This comes clearly from Fig. 1.2,

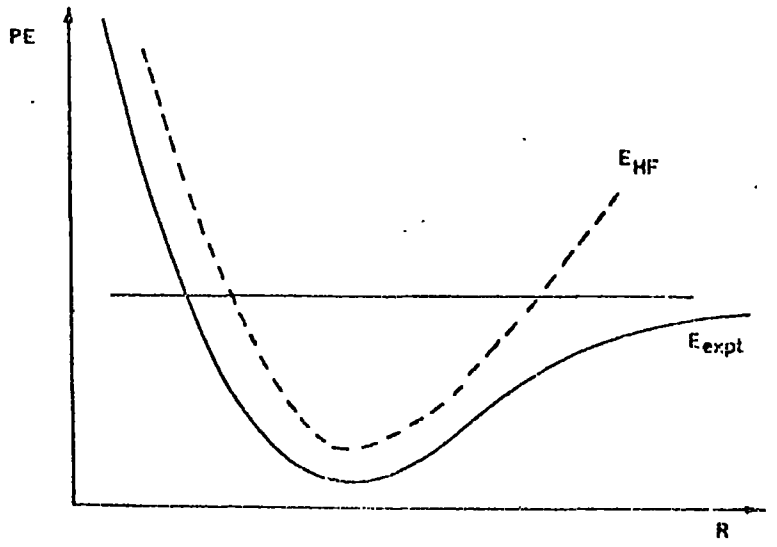

Fig. 1.2

Experimental and HF PES for a diatomic molecule

where we have sketched a computed and an experimental potential energy curves of a diatomic molecule. The point to be noticed is that the HF curve lies above the experimental, but the shape of the two curves is pretty well the same around the minimum, one being almost parallel to the other. Consequently the computed Re values (equilibrium bond distances) are normally close to the observed values (usually few hundredths of an Angström too small) and also the vibrational frequencies (thus the force constants) are well reproduced by HF functions, being usually slightly larger as the size of basis set decreases. These aspects of PES's have been quantitatively discussed e.g. by Cade[44] and his co-workers. The same situation occurs in multidimensional PES's of polyatomic molecules where equilibrium geometries and force constants can be successfully computed from HF wave functions.

ii) One of the main methods for calculating ionization potentials is the Δ SCF method. In this technique ionization potentials are given by

$$IP = E^{HF}_{(ion)} - E^{HF}_{(neutral)} \qquad \ldots (1.163)$$

where it is assumed that correlation corrections uniformly lower the total energy of the ground and ionized states of a given molecule. We shall discuss this in slightly more detail in the context of calculations of ionization potentials.

There are also other quantities of chemical interest such as barriers to rotation[45] or heats of isodesmic reactions[46] where changes in correlation energies are small.

However the most important drawback of the HF treatment is its incorrect behaviour at large internuclear separations. This is also illustrated in Fig. 1.2. The reason for this can be readily appreciated by expanding the determinental wave function and this reveals the contribution at large internuclear distances of spurious ionic terms. Therefore we cannot describe bond breaking and stretching. Further, heats of atomization, dissociation energies and heats of reactions (apart from isodesmic reactions) are inadequately described within the Hartree-Fock formalism.

d. Methods for Treating Electronic Correlation.

Many of the current approaches to the correlation energy problem derive from the pioneering studies of Hylleraas in the very early days of the development of quantum chemistry.

i) The Pair Population Method.

In this technique which is originally due to Hollister and Sinanoglu[53] the correlation energy is evaluated from

$$E_{corr} = \sum_i c_{ii}\rho_i + \sum_{i>j} c_{ij}\rho_i\rho_j \qquad \ldots (1.164)$$

where ε_{ij}'s are atomic pair correlation energies weighted by the atomic orbital pair populations ρ_i's. (The value of a particular ρ_i is conveniently obtained from the Mulliken population analysis. It is in fact a population of the atomic orbital i obtained as a sum of populations of basis functions (1.145) compromising this orbital.) We can further split E_{corr} into inter- and intra-atomic terms,

$$E_{corr} = E_{corr\text{-}inter} + E_{corr\text{-}intra} \qquad \ldots (1.165a)$$

depending on whether the pairs of orbitals are located on the same or different atoms.

Snyder and Basch[49] have employed this method to estimate correlation corrections to some values of heats of reactions. They used Nesbet's work[50] to guide them in preparing a set of ε_{ij}'s for atomic orbitals of the first row atoms, which are listed in Table 1.2. However only ε_{ij}'s corresponding to atomic orbitals on the same atom can be calculated by Nesbet's method, and therefore only the $E_{corr\text{-}intra}$ component can be evaluated. However the same authors[49] have also estimated empirically values of ΔE_{corr}^{inter} for the already mentioned reactions and they showed that this was in general of the same order of magnitude as ΔE_{corr}^{intra} but of opposite sign.

It is clear from this work that ΔE_{corr}^{inter} is strongly dependent on the connectivity and that although for isomeric straight chain or cyclic systems ΔE_{corr}^{inter} was approximately constant in comparing cyclic with acyclic compounds marked differences were apparent. The relevance of this will become more apparent when we come to discuss the relative importance of correlation energy corrections to calculated ionization potentials by the ΔSCF method.

The expression (1.164) applies strictly to closed shell species. For open shell molecules with one unpaired electron (e.g. core and valence hole states) an extra term has to be subtracted from it. Thus

$$E_{corr}^{intra}(\text{hole state}) = \sum_i \tfrac{1}{2}\rho_i\varepsilon_{ii} + \sum_{i>j}\rho_i\rho_j\varepsilon_{ij} - \sum_i \tfrac{1}{2}\rho_i^{\lambda}\varepsilon_{ii} \qquad \ldots (1.165b)$$

Table 1.2.

Atomic Orbital Pair Correlation for the First Row Atoms and Hydrogen in Atomic Units

Pair ij	C	N	O	F	Ne	H
1s 1s	-0.0409	-0.0409	-0.0402	-0.0398	-0.0399	-0.0409
1s 2s	-0.0015	-0.0013	-0.0014	-0.0014	-0.0013	
1s 2p	-0.0015	-0.0014	-0.0012	-0.0016	-0.0017	
2s 2s	-0.0284	-0.0136	-0.0129	-0.0119	-0.0108	
2s 2p	-0.0139	-0.0139	-0.0118	-0.0084	-0.0068	
2p 2p	-0.0258	-0.0258	-0.0258	-0.0258	-0.0258	
2p 2p'	-0.0123	-0.0123	-0.0123	-0.0123	-0.0123	

where ρ_i^{λ} corresponds to the contribution from the SOMO denoted by λ to the Mulliken population of the i^{th} atomic orbital. The last term in (1.165b) will compensate for the hypothetical correlation of ½ an electron of α and ½ an electron of β spin in λ which is included in the first term.

We have been using this Pair Population Method in our laboratory with a reasonable success,[51,52] and therefore the present work also makes use of this technique of estimation of correlation energies.

ii) Removal of the Symmetry Constraint from the Conventional Hartree-Fock Scheme

In the conventional Hartree-Fock scheme, which we have so far discussed, it has always been assumed that if the system studied has certain symmetry properties contained in the total Hamiltonian , the solutions to the Hartree-Fock equations would always be symmetry-adapted, i.e. form a basis for the irreducible transformation. Mathematically this is expressed in an eigenvalue equation

$$\Lambda D = \lambda D \qquad \ldots (1.166)$$

where Λ is a symmetry operator. However confusion arises from the fact that the exact eigenfunction Ψ and the approximate eigenfunction D have different properties. We know that if

$$\mathcal{H}\Lambda = \Lambda\mathcal{H} \qquad \ldots (1.167)$$

is fulfilled then

$$\Psi = \lambda\Psi \qquad \ldots (1.168)$$

is essentially a consequence of

$$\mathcal{H}\Psi = E\Psi \qquad \ldots (1.169)$$

For the approximate eigenfunction D one replaces the eigenvalue relationship (1.169) by the variational principle

$$\delta \langle D | \mathcal{H} | D \rangle = 0 \qquad \ldots (1.170) \equiv (1.66)$$

However no rigorous proof has been presented which would allow one to deduce the relationship (1.166), therefore the relationship (1.166) should be considered as a constraint which necessarily raises the energy above the absolute minimum $< \mathcal{H} >$ (1.162). In the conventional treatment of the Hartree-Fock scheme due to Roothaan[13,54] often referred to as RHF (Restricted Hartree Fock) one starts out from the two basic equations

$$\delta < D | \mathcal{H} | D > = 0; \quad \Lambda D = \lambda D \qquad \ldots (1.171)$$

but if one drops the symmetry constraint and considers only the relationship

$$\delta < D | \mathcal{H} | D > = 0 \qquad \ldots (1.172)$$

one obtains unrestricted Hartree-Fock (UHF) scheme, and the corresponding HF functions are no longer symmetry adapted. This is a symmetry dilemma in the Hartree-Fock scheme discussed more fully by Löwdin.[55] If one looks for the absolute minimum of the energy one loses the symmetry properties and since the correlation energy (1.162) essentially refers to the difference between the exact energy and the energy in the conventional (RHF) Hartree-Fock scheme a very large part of this correlation energy depends on the symmetry constraint (1.166).

We can look at this UHF scheme from a different angle. In this technique the total wave function is approximated by a single determinant where electrons with different spins may have different orbitals. Solution of this problem is described in many texts[6,42] and the energy lowering over the corresponding RHF wavefunction can be substantial. The smaller correlation error associated with the UHF scheme can physically be interpreted to originate from the fact that if we let electrons with different spins occupy different orbitals in space then they got a chance to avoid each other in accordance with the influence of the Coulombic repulsion and their motions are partly correlated. However this extra degree of freedom is reflected in the inability of the total wavefunction to represent a

pure spin state, in other words the single-determinantal wavefunction is not an exact eigenfunction of the spin operator S^2.

It is worthwhile pointing out that RHF and UHF wavefunctions give the same energies for any closed shell species. This derives straightforwardly from the variational and Pauli exclusion principles, since if 2 electrons of opposite spins are indistinguishable then they have the same spatial wavefunction. Table 1.3 clearly shows this for Cl^-. Further, the data in Table 1.3 indicates that the difference between the energies of core hole state species as calculated from RHF and UHF wavefunctions is minute. The reason for this is that the correlation between core and valence orbitals is quite small as can readily be seen from the atomic orbital pair correlation energies displayed in Table 1.2.

Table 1.3.

A comparison between RHF and UHF calculations of ground state energy and core binding energies of Cl^- ion. (The basis set used was uncontracted basis set of 10s and 6p optimized gaussian functions taken from A. Veillard, Theoretica Chim. Acta, 12, 405 (1968)).

	RHF	UHF
E_{total}	12501.159 eV	12501.159 eV
Be_{1s}	2810.22 eV	2809.94 eV
Be_{2s}	266.24 eV	266.18 eV
Be_{2p}	196.03 eV	195.93 eV

Binding energies computed as energy differences between ground state and relevant core hole states.

There are other more sophisticated methods based on similar ideas to the UHF technique which further lower the HF energy and can at the same time preserve certain symmetry properties while retaining the independent particle model (one orbital per electron) e.g. PUHF, SEHF, SOHF.[56]

The basic theory has been elaborated in each case however not all of the computational aspects have been considered.

iii) Correlated Wave Functions.

This method is based on the idea of introducing the interelectronic distance r_{12} in the wave function itself which is then called a 'correlated wave function'. We shall not discuss the details of this technique[43] as it is not directly relevant to the present work.

iv) Superposition of Configurations.

One of the most common procedures to go beyond the Hartree-Fock limit is to abandon the independent particle model and introduce superposition of configurations. In the HF scheme we truncate the expansion (1.21) after one term. In the method of superposition of configurations we keep more than one determinant in the expansion and then optimize that finite expansion.

Basic idea - CI

The best known procedure within the content of a superposition of configuration is the method of configuration interaction (CI) formalism. In principle a starting point is a complete set of known spin orbitals which we can choose to be orthonormal (1.15). They can be, and indeed most usually are, obtained for example from HF calculations. Then a set of coefficients C_K (cf. (1.21)) can be found such that the expansion (1.21) is the exact solution of the n-electron Schrödinger equation

$$\mathcal{H}\Psi = E\Psi \qquad \ldots (1.173)$$

In practice we work only with a finite number $M > n$ of spin orbitals

$$\psi_k(x); \quad k = 1,2,\ldots,M \qquad \ldots (1.174)$$

With these we can construct all possible nxn determinants and use an expansion of these

$$\Psi_M = \sum_{k=1}^{f_M} C_K D_K \qquad \ldots (1.175)$$

as the trial function in a variational calculation. There are

$$f_M = \binom{M}{n} = \frac{M!}{n!(M!-n!)} \qquad \ldots (1.176)$$

such determinants, but in practice the expansion (1.176) can be further reduced by symmetry. Minimization of the expectation value

$$\langle \mathcal{H} \rangle = \frac{\langle \Psi_M | \mathcal{H} | \Psi_M \rangle}{\langle \Psi_M | \Psi_M \rangle} \qquad \ldots (1.177)$$

with respect to unknown coefficients C_K leads to a well known set of linear secular equations

$$\sum_{L=1}^{f_M} [H_{KL} - E\delta_{KL}] C_L = 0; \quad K = 1,2,\ldots, f_M \qquad \ldots (1.178)$$

where the integrals

$$H_{KL} = \langle D_K | \mathcal{H} | D_L \rangle$$

$$S_{KL} = \langle D_K | D_L \rangle \qquad \ldots (1.179)$$

are calculated using Slater rules. These equations have non-trivial solutions only if the determinant of the coefficients vanishes

$$\det\{H_{KL} - E\delta_{KL}\} = 0 \qquad \ldots (1.180)$$

A CI calculation is in principle computationally simpler than a HF procedure once we have obtained a set of spin orbitals (1.174), because it is a linear problem. The difficulties with many-centre integrals are the same but the solution of (1.178) and (1.180) is not a great problem nowadays, because several numerical procedures exist in finding the lowest eigenvalues of the matrix $\{H_{KL}\}$. The major difficulties in any CI calculation is the problem of finding the most important configurations which represent the maximum amount of electronic correlation if one is to obtain reasonably good energy values using only a few configurations.

MC-SCF.

In the HF method we put one of the coefficients C_K equal to 1 and all others to zero, and then optimize the spin orbitals. In CI we fix the spin orbitals, but optimize the coefficients C_K. The Multi Configuration-SCF procedure offers a combination of these two ideas. A relatively small number of configurations is often adequate to choose, and the corresponding expectation value of the total Hamiltonian is minimized with respect to both spin orbitals and coefficients. The resulting wavefunction is very accurate but unfortunately demands an enormous amount of computer time for molecular systems and the method is often computationally unstable.

Valence bond method.

While on the subject of superposition of configurations it is only logical to discuss briefly similar ideas which are involved in the Valence Bond (VB) method. The literature on the theory of the VB method is enormous and has its origin in the very beginning of quantum chemistry. In summary, the steps in the full VB method are:

i) Take the set of all atomic orbitals of the atoms in the molecule together with the spin factors α, β and form a set of spin orbitals.

ii) Form determinants from selection of spin orbitals which reflect the likely electronic structure of the molecule.

iii) Form a linear combination of these determinants (cf. (1.175)) and optimize the numerical coefficients C_K.

The last step is a linear problem which has the form (1.178) and (1.180), where however D_K's are the determinants of step (ii).

The rules for evaluation of the matrix elements (1.179) involving determinants of step (ii) were derived by Löwdin and they are often referred to as Löwdin rules.[4] These matrix elements are very complicated indeed because they consist of integrals involving non-orthogonal spin orbitals,

and their computation is the greatest handicap of the V.B. method.

The VB wavefunction describes bond breaking correctly (provided the requisite pairing schemes are included) as it does not emphasize ionic terms at large internuclear distances (for a simple discussion of H_2 see e.g. reference 57), but its behaviour at equilibrium distances in many cases is not as good as that of the HF wavefunction. This is indicated for H_2 in Fig. 1.3. To get around this problem Goddard and his co-workers have started to use the generalized valence bond (GVB) method.[57] The wavefunction used in this technique is of a similar nature as in the traditional VB method, but in addition we solve for the orbitals self-consistently at each R (internuclear distance) just as in the Hartree-Fock method. This combines the best attributes of both the HF and VB methods and leads to a wavefunction that adequately describes potential energy surfaces at both short internuclear distances and at the dissociation limit. The three curves for H_2 (HF, VB and GVB) are sketched in Fig. 1.3.

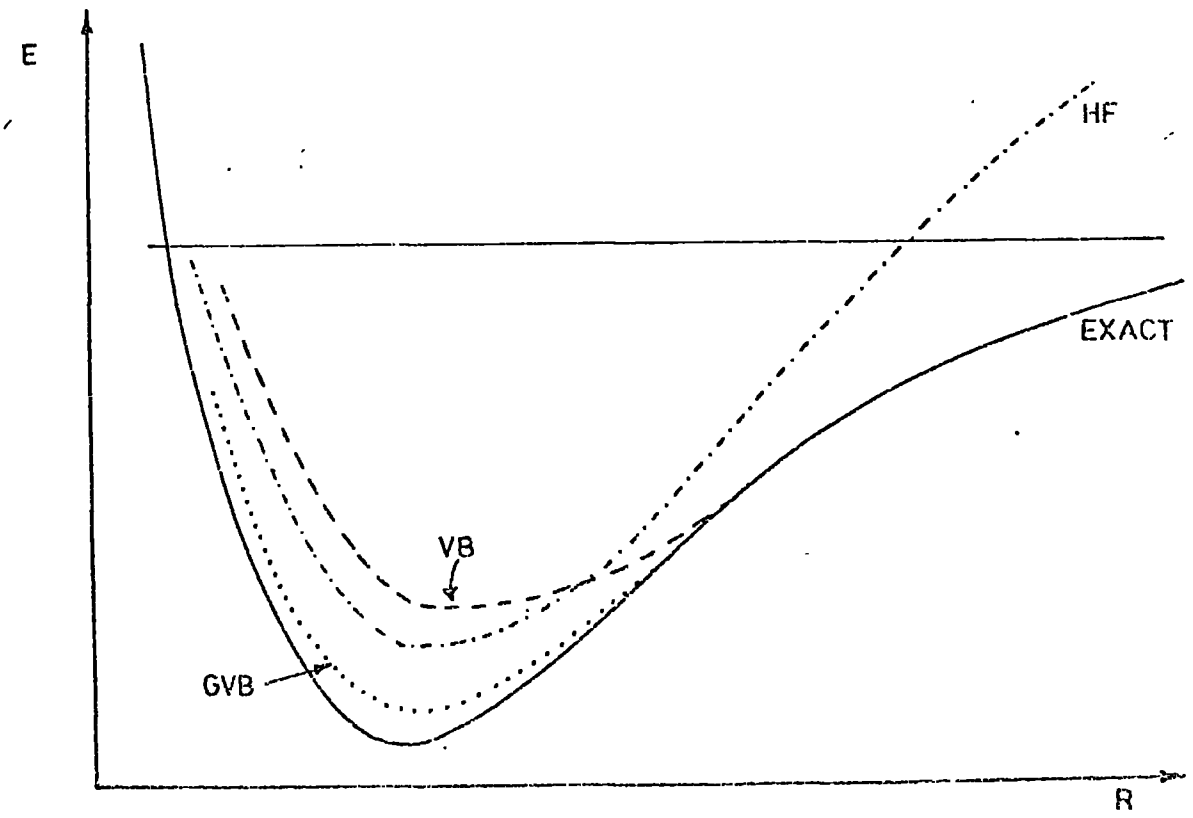

Fig. 1.3.

HF, VB, GVB and exact energies for H_2.

It is worth pointing out that there is little difference between MC-SCF and GVB methods when they are both carried out to their full extent.

1.7. Computer Programs for Ab Initio Calculations.

a. Introduction.

The theories behind Quantum Mechanics with a special emphasis on MO theory were largely elaborated during the 1920's and 30's, but it is only with the help of modern electronic computers and appropriate computer programs both devised in the second part of this century that people have been able to use these theories to solve certain problems in physics, chemistry and biology. The writing and the development of ab initio programs requires a lot of labour by various teams of people. Some of the familiar names are IBMOL, POLYATOM, ATMOL, MOLECULE, ALCHEMY and they are usually available through international organizations such as Quantum Chemistry Program Exchange (QCPE). In this section we shall limit ourselves to a brief description of the ab initio program ATMOL 2 which has been used entirely throughout this work.

b. Description of ATMOL 2.

ATMOL consists of several programs (packages) which were originally devised by Hillier and Saunders in the late 1960's as extensions to the POLYATOM and IBMOL systems. Several additions and improvements have been done since namely by Saunders, Guest, Chiu and Rodwell working presently at the Atlas Computing Laboratory, Chilton, Didcot, Berks, U.K.

As in most ab initio programs ATMOL 2 has the following essential stages.

i) Computation of integrals over basis functions and if required transformation of these integrals over contracted functions.

ii) Assembly of the Fock matrix and its diagonalization. This step is iteratively repeated until required self-consistency is obtained.

iii) Analysis of a molecular wave function in the form of e.g. producing Mulliken population analysis, generation of electron density and molecular electrostatic contours, calculation of expectation values of some 1-electron operators (e.g. dipole and quadrupole moments) etc.

There are two integral packages in ATMOL 2. The first one is used for computation of molecular integrals over GTO's which are then stored in a contracted form using either normal Gaussian basis sets or STO-nG, HF-nG, STO 4-31G, HF 4-31G basis sets. Stewart's least square minimization results[24] described in section 1.5d are used in both STO-nG and HF-nG expansions. They are permanently stored in a standard library. The other package computes integrals over STO's and is an adaptation of a system due to R.M. Stevens (Harvard University). We have found the latter package particularly efficient for calculations on linear molecules with double and extended Slater basis sets. Both packages make use of symmetry properties of a molecule since in a highly symmetric molecule many integrals will be zero or equal within a sign and these do not have to be re-calculated.

The iterative part of the ATMOL 2 can be implemented with three different packages. Firstly, the closed shell (RHF) SCF program which has been used in calculating the energies of ground states of molecules. The open shell cases are usually tackled by the (RHF) SCF package for 'half closed' open shell species. The open shell program has been used for calculating energies of mainly core and some valence ionized states of certain molecules. This was achieved with the help of Lock directive which causes iterated molecular orbitals to be selected on the principle of maximum overlap with trial molecular orbitals thus over-riding the Aufbau principle. The third iterative package is the (UHF) SCF program.

This program is mainly useful for calculating wave functions of free radicals, and as was pointed out in section 1.6d it has no advantage over the (RHF) SCF packages as far as calculations of core binding energies is concerned.

Use has also been made of the Mulliken population analysis program for calculating charges and bond overlaps and the package for the graphical analysis of molecular wave functions to generate electron density contour plots.

Presently work is being undertaken to generate a CI package which will be useful in the context of this work to calculate potential energy surfaces of valence excited ionized states (so-called shake-up states). The ATMOL manual which contains all the details concerning the ATMOL 2 programs and further information concerning the development of the more advanced ATMOL 3 system can be obtained from:-

Atlas Reception Desk,
Science Research Council,
ACL,
Chilton, Didcot, Berkshire,
OX11 OQY, ENGLAND - U.K.

All the calculations in this work have been performed on the IBM 370/195 computer at the Rutherford Laboratory via the remote satellite station GEC 2050 in Durham.

CHAPTER II

PHOTOIONIZATION AND RELATED PHENOMENA

Abstract.

This chapter is divided into two parts. Firstly we shall discuss the fundamental concepts behind core and valence electron ionizations and the two well-known spectroscopic techniques ESCA and UPS for measuring binding energies (ionization potentials) of these electrons. Multielectron processes (shake-up and shake-off) which accompany core and valence electron ionizations are also considered.

The second part of the chapter deals with various methods for calculating binding energies. Firstly the methods based on Koopmans' theorem and the Δ SCF technique are introduced. They form a theoretical background for the discussion of electronic and nuclear relaxation accompanying photoionization. The importance of the sudden approximation is stressed, and its consequences with regard to the theory of multi-electron processes are considered. It is pointed out that transitions involved in photoionization processes are vertical and that the core hole states are localized in nature.

The rest of the chapter deals briefly with some other methods for calculation of ionization potentials. They include the relaxed Koopmans' model, the equivalent cores approach, the transition operator method, various potential models, the MS Xα technique, and the approach based on the one-particle propagator.

2.1. Photoionization Processes.

a. Core Electron Ionization and ESCA.

Localized electrons which do not take part in chemical bonding are predominantly either of s or p character, e.g. 1s in C; 1s, 2s, 2p in Cl and they are referred to as core electrons. Their importance has been stressed with the development of ESCA[58-60] (Electron Spectroscopy for Chemical Analysis) which is an experimental technique for measuring their energies which are often referred to as binding energies (BE) or ionization potentials (IP) (i.e. an energy or potential to remove an electron from its orbital to infinity).

In order to knock out a core electron from its orbital we need a high energy photon source such as $MgK\alpha_{1,2}$ (1253.7 eV) or $AlK\alpha_{1,2}$ (1486.6 eV) which can be with the state of the art of instrumentation highly monochromatic.[60] Nowadays it is true enough that studies of gaseous and solid samples are considered to be straightforward experimental routine whereas liquid phase studies require special instrumentation associated with the necessity for differential pumping. Therefore studies of liquid samples have only been applied in a small number of cases.[60]

If the incident beam has energy hυ and KE is the kinetic energy of the ejected electron then the binding energy is given by

$$BE = h\upsilon - KE \qquad \ldots (2.1)$$

where we have neglected the recoil energy of the sample. This relationship is unambiguous for gaseous samples, but for solids the situation is more complex. If one is interested in the binding energy relative to the solid sample's vacuum level one must correct for the contact potential[58] between the sample and the spectrometer (provided the sample and the spectrometer are in electrical contact, that is both have the same Fermi level), which is just the difference between their work functions.

$$BE\ (fermi) = h\upsilon - KE\ (spect) - \phi\ (spect) \quad \ldots (2.2)$$

$$BE\ (vacuum) = h\upsilon - KE\ (spect) - \phi\ (spect) + \phi\ (sample) \quad \ldots (2.3)$$

Here ϕ denotes a work function, KE (spect) is the kinetic energy of the electron when it enters the spectrometer (analyser). On entering the analyser the electron is accelerated by an energy $[\phi(sample) - \phi\ (spect)]e$. However binding energies as calculated by theoretical methods presented in the next sections refer strictly speaking to isolated gaseous molecules and appropriate corrections for heats of sublimation, $\Delta H(sub)$, must be made to make a detailed comparison between a binding energy of a molecule in a gaseous and a solid state as is indicated on the Born cycle diagram shown in Fig. 2.1. Electronic reorganization (relaxation) effects consequent upon core electron ionizations will be discussed in some detail later in this chapter, but it is worthwhile pointing out at this stage that the method which will be presented adequately describes intramolecular reorganization energies. However reorganization energy in a solid sample has in addition an intermolecular term which can slightly modify binding energies of solids in comparison with gases such that direct theoretical comparison is inappropriate even when due allowance has been made for work function and lattice sublimation terms. To summarize, in order to compare binding energies of solid samples which are experimentally measured with respect to the fermi level (2.2) (for operational convenience) with absolute binding energies of gaseous isolated molecules (2.1) we must take into account the work function of the sample, heats of sublimation of the neutral and the core hole state molecule and in any theoretical comparison we must also consider intermolecular reorganization effects. However the last two effects are of a minor importance and they will tend to cancel together with the work function correction when we make comparisons between chemical shifts (differences of binding energies for a certain core hole level) measured experimentally with respect to the fermi level (ΔBE (fermi)) and chemical shifts of gaseous species.

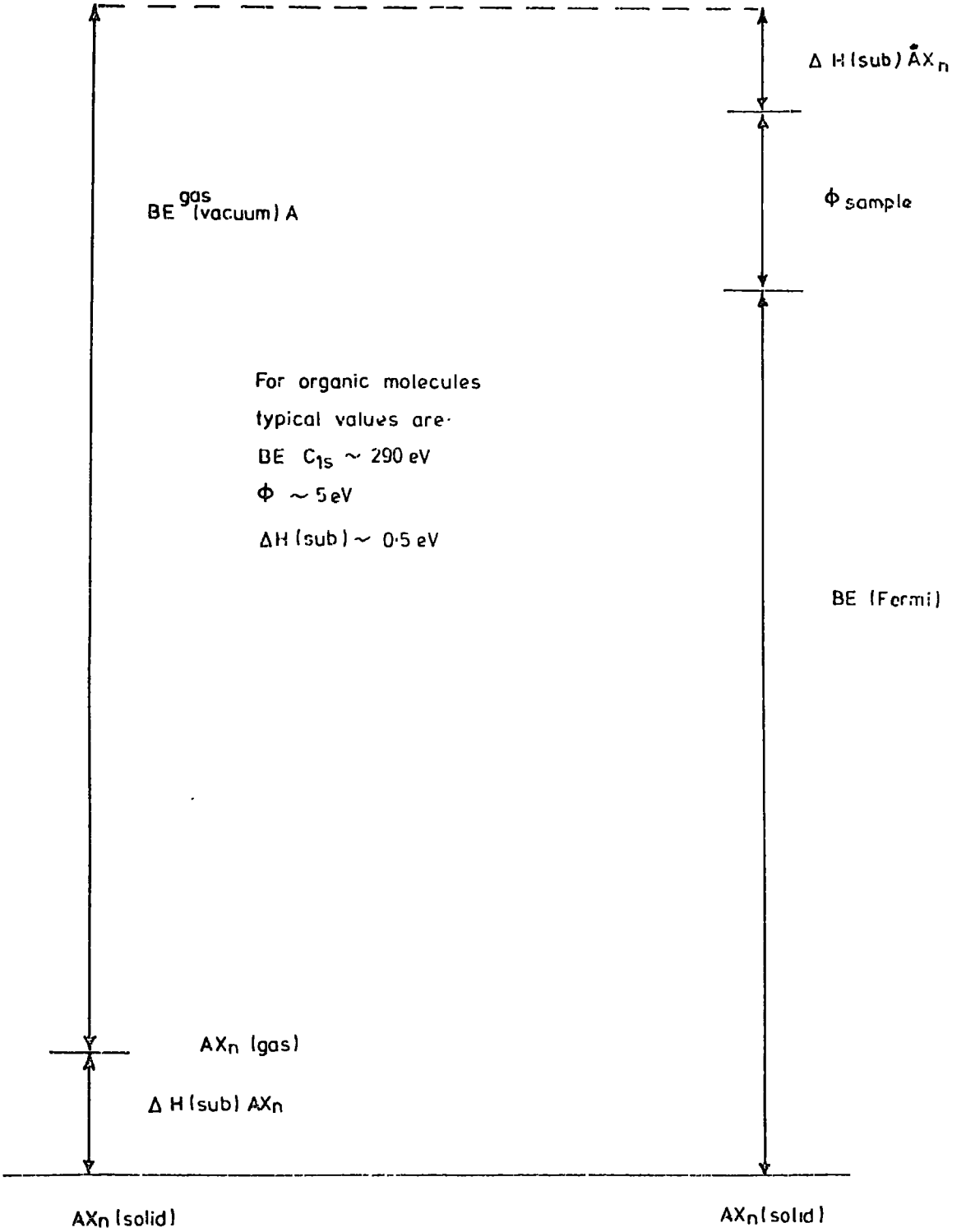

Fig. 2.1.

Relationship between energy levels of a gaseous and a solid sample AX_n (covalent with no strong intermolecular interaction) with a core hole on the atom A.

After a loss of a core electron from a molecule (or atom) A by the process

$$A + h\upsilon_1 \longrightarrow (A^+)^* + \bar{e}_1 \qquad \ldots (2.4)$$

the hole state $(A^+)^*$ species in their ground electronic state can relax by two fundamental processes.

i) X-ray emission[58]

$$(A^+)^* \longrightarrow A^+ + h\upsilon_2 \qquad \ldots (2.5)$$

where electronic transition occurs from a higher orbital to fill a core hole.

ii) Auger process[61]

$$(A^+)^* \longrightarrow A^{++} + \bar{e}_2 \qquad \ldots (2.6)$$

Auger emission is radiationless process in which an electron from a higher orbital undergoes a transition to fill the hole in a lower orbital and simultaneously a second electron is ejected from the system. The Auger process is much more likely for light elements whereas heavy atoms usually relax by X-ray emission. These relaxation processes must not be mixed with electronic and nuclear relaxation (reorganization) phenomena accompanying core electron ionization.

b. Valence Electron Ionization and UPS.

Electrons occupying valence orbitals (e.g. π in CO) are usually of a delocalized nature. They determine important chemical and physical properties of molecules (e.g. their shape, bonding, reactivity) and the development of photoionization techniques in particular ESCA and UPS (Ultraviolet Photoelectron Spectroscopy) which measure binding energies (ionization potentials) of these electrons has considerably improved our knowledge of these properties.

i) ESCA.

We have discussed this technique in the context of core electron ionization. Even if ESCA is mainly a tool for looking at core levels, its relative importance in studies of valence electrons has been emphasized in

many texts.[59,60]

ii) UPS.

The major difficulty with ESCA is the relatively high inherent linewidth of a conventional ionizing source. Even if monochromatization techniques[60] are gradually overcoming this problem it is still convenient in many cases to study valence electrons with low energy (thus narrow natural linewidth) photon sources in the vacuum U.V. region, namely He(I) and He(II) discharges with photon energies 21.2 eV and 40.8 eV respectively. Such spectra can reveal considerable details concerning vibrational fine structure accompanying photoionization of a molecule. The technique is commonly referred to as Ultraviolet Photoelectron Spectroscopy (UPS)[62] and it is a sister technique to ESCA, because the principles involved in measuring binding energies are the same in both techniques. Whereas ESCA is suitable mainly for studying samples in the solid and gas phases, samples for UPS are usually handled in the gas phase though they may be studied as condensed films.

An interesting point is that the linewidth of peaks corresponding to a given valence photoionization is different when studied by ESCA and UPS and in addition the relative intensities differ substantially because the photoelectric cross-section is strongly dependent on the energy of the ionizing source.

c. Multielectron Processes.

It is well known that an electron ionization is very often accompanied by simultaneous excitation (shake-up) or emission (shake-off) of a valence electron.[59,64] These multielectron processes give rise to satellite peaks with lower kinetic energy than the direct photoionization peaks,

$$KE = h\upsilon - BE - E_d \qquad \ldots (2.7)$$

where E_d is the energy of the shake-up or the shake-off process. This is illustrated in Fig. 2.2 for a core electron ionization. We shall be discussing intensities of these satellite peaks with respect to the main peak within the sudden approximation in slightly more detail in the next section.

2.2. Methods of Calculating Binding Energies.

a. Koopmans' Method.

It has already been pointed out in Chapter I, Section 1.4.b. that the negative of the orbital energies for an initially closed shell system can be set equal to the ionization potentials

$$BE = - \varepsilon_k \qquad \ldots (2.8)$$

This comes clearly from Koopmans' theorem (1.110), whose major deficiency is that it assumes no changes in spatial distribution of molecular spin orbitals on photoionization. We shall be showing in several examples in the following chapters that this approximation not only predicts absolute values of binding energies incorrectly, but even in some cases the chemical shifts are wrongly described with this model.

b. The Δ SCF Technique and Electronic Relaxation.

The major drawback of Koopmans' theorem is that it relies solely on the ground state properties of a wave function. Binding energy however depends as much on the properties of the final (ionized) state as it does on the properties of the ground state wave function. In the Δ SCF technique we calculate the binding energy of an electron as the difference between the energy of the ionized and the ground state of an atom or a molecule

$$BE = E^{ion} - E^{ground} = \Delta E \qquad \ldots (2.9)$$

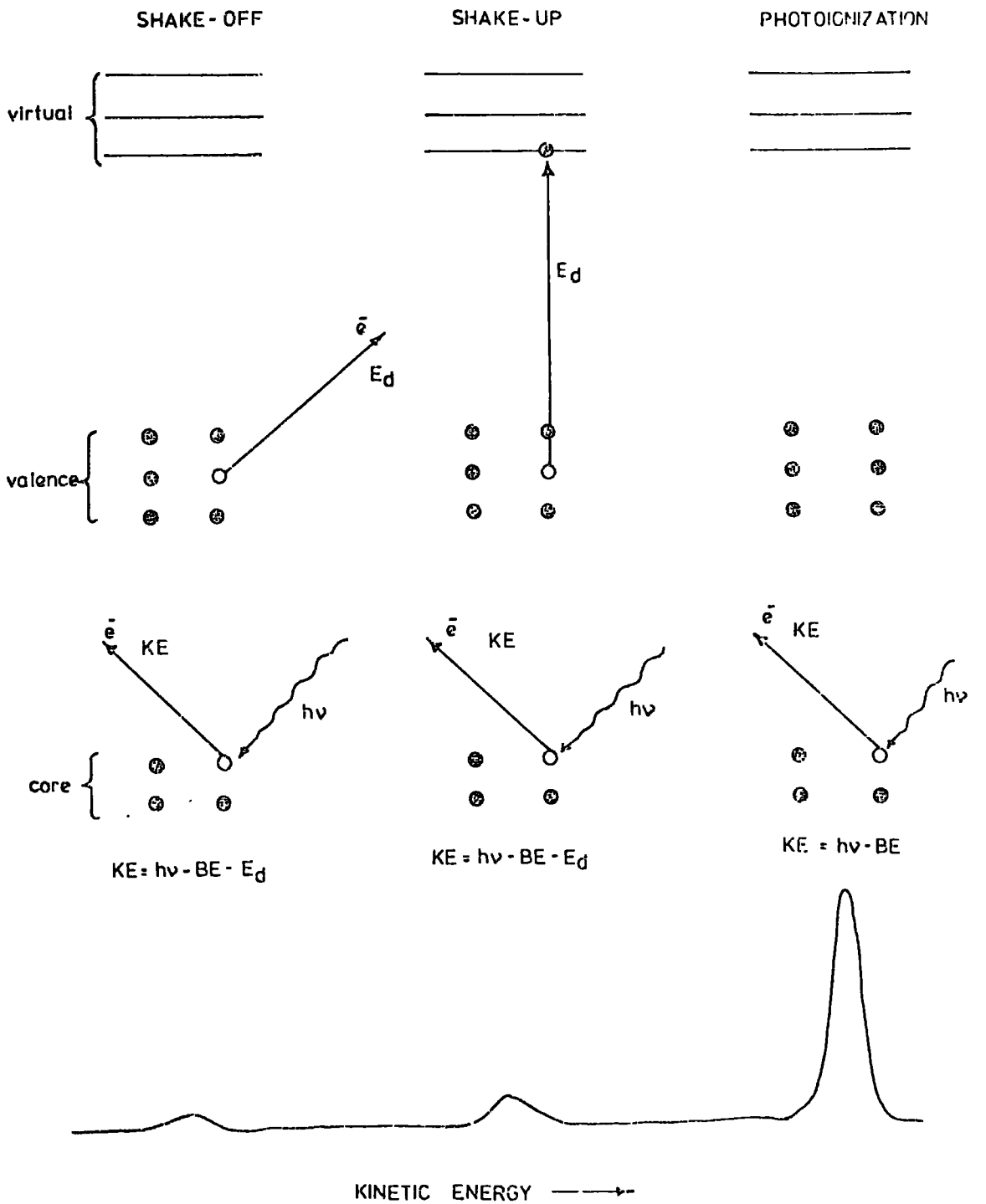

Fig. 2.2.

Shake-up, shake-off and the main photoionization process. The three peaks in the kinetic energy curve correspond to the three processes.

Within the Hartree-Fock formalism the experimental energy of a molecule or ion can be written as a sum

$$E_{expt} = E_{HF} + E_{corr} + E_{relat} + E_{spin} \quad \ldots \quad (2.10) \equiv (1.160)$$

It has been pointed out in Chapter I, Section 1.6.a. that E_{spin} and E_{relat} are approximated to be zero, therefore (2.9) becomes

$$BE = (\Delta E)_{HF} + (\Delta E)_{corr} \quad \ldots \quad (2.11)$$

$(\Delta E)_{relat}$* for a valence electron ionization can be ignored with some confidence as the relativistic energy stems primarily from the core electrons. Veillard and Clementi[65] have estimated E_{relat} for the first and the second row atoms. For carbon (with C_{1s} BE $\sim$ 300 eV) they arrive at the value of 0.188 eV and for Argon (with Ar_{1s} BE $\sim$ 3200 eV) 23.958 eV. (Both of these values include spin effects.) Therefore $(\Delta E)_{relat}$ for core electron ionization can to a good approximate be neglected for first row atoms but for accurate values of absolute binding energies of heavier atoms $(\Delta E)_{relat}$ can be of some importance. $(\Delta E)_{relat}$ can however be ignored for these latter elements if we are interested in the values of chemical shifts (i.e. differences in binding energies), because $\Delta(\Delta E)_{relat}$ then approaches zero.

We have briefly discussed the correlation energy term (E_{corr}) in the previous chapter, and it was pointed out that this quantity is of considerable importance in discussing various molecular properties. Fortunately correlation energy for ground and core hole state species is in many cases similar, and the net effect amounts to $(\Delta E)_{corr} \simeq 0$. One would normally expect $(\Delta E)_{corr} > 0$ because $|E_{corr}|$ should be somewhat larger for the neutral system with an extra electron than for the ion

---

* Many authors include spin effects into the relativistic effect.

(correlation energy is a negative quantity). This is usually the case, however for valence electrons of widely differing localization characteristics it is possible for the correlation energy to be larger* for the ionized species. As a simple example Table 2.1. shows the computed correlation energy changes for core and valence ionizations in water. In the particular case of the $2a_1$ (O_{2s}) valence orbital the correlation energy increases on ionization.

Table 2.1.

$(\Delta E)_{corr}$ in eV for H_2O. Taken from U. Gelius, Physica Scripta, 9, 133 (1974)

Orbital	$1a_1$ (O_{1s})	$2a_1$	$1b_2$	$3a_1$	$1b_1$
$(\Delta E)_{corr}$	0.5	-1.9	1.3	1.4	1.4

Further examples are provided by the work of Clementi[66] and Bagus[67] who have pointed out that E_{corr} depends not only on the number of electron pairs, but also on the electron distribution which can change substantially on ionization. It is clear from the above discussion that $(\Delta E)_{corr}$ can be neglected in many situations, this is true in particular if we are interested in chemical shifts. Consequently in core levels (2.11) becomes

$$BE = (\Delta E)_{HF} \qquad \ldots (2.12)$$

The quantity defined on the R.H.S. of 2.12 since it is computed as an energy difference from SCF calculations is often referred to as the Δ SCF value.

Therefore we write (2.12) as

$$BE = (\Delta E)_{HF} = \Delta \text{ SCF} \qquad \ldots (2.13)$$

* In this context 'larger' means greater in magnitude thus disregarding the negative sign.

Bagus[67] was first to use the Δ SCF method. His calculations on F^-, Ne, Na^+, Cl^-, Ar and K^+ were successful and this method is now very popular amongst ab initio chemists. The present work relies heavily on the Δ SCF technique, and it will be shown in the following chapters that binding energies and especially their shifts are very well predicted with this method even with relatively small basis sets (e.g. 4 - 31G).

Having defined Δ SCF we shall now define a quantity called relaxation energy which is sometimes referred to as re-organization energy (RE)

$$RE = - \varepsilon_k - \Delta \text{ SCF} \qquad \ldots (2.14)$$

Relaxation energy as defined by (2.14) is a positive quantity indicating the difference between binding energies of an electron k defined by Koopmans' theorem and the Δ SCF method. The relationship between the experimental, Koopmans' and Δ SCF binding energies is schematically shown in Fig. 2.3. Relaxation energies are by no means negligible even for valence levels. For carbon atoms with approximate core BE ∿ 300 eV they have values ∿ 13 eV. We shall be studying properties of relaxation energies in much greater detail in the forthcoming chapters. A physical interpretation of relaxation energies is made clear from the following consideration. If an electron is ejected from a core or a valence level, the remaining electrons will experience an increased potential at the nucleus and relax (reorganize) to minimize the energy. This relaxation process changes the spatial distribution of the remaining n-1 orbitals which is taken into account in the Δ SCF method but not in Koopmans' theorem. A change of the potential at the nucleus will be much larger if a core rather than a valence electron is ionized because core electrons have a larger screening coefficient. This is reflected in the values of relaxation energies which are usually smaller by a factor of ten for valence as compared with core electrons. (As an illustration, values of RE's for the

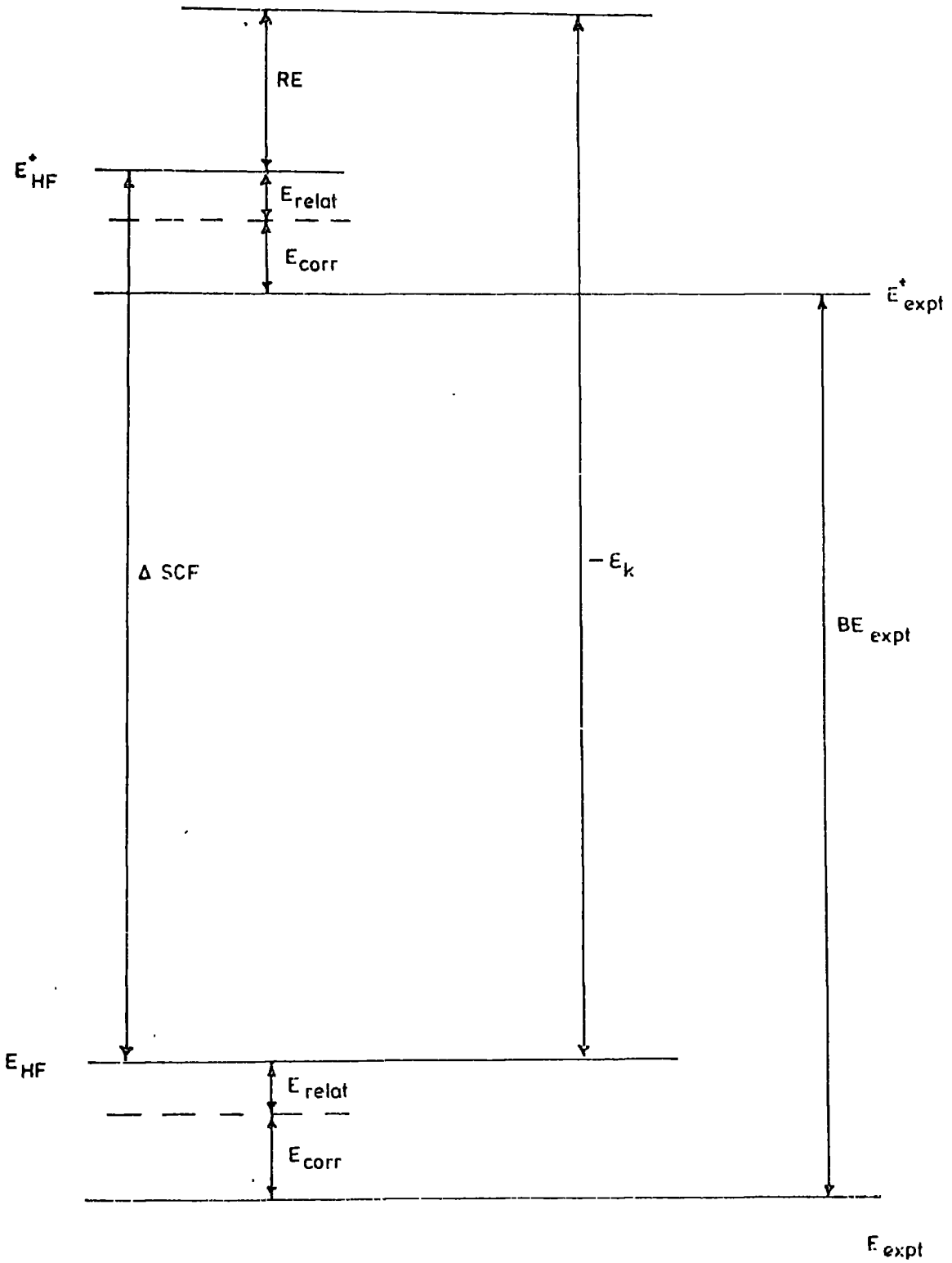

Fig. 2.3.

Relationship between the experimental (BE_{expt}), Koopmans' ($-\varepsilon_k$) and the Δ SCF binding energies.

C_{1s} and 1π orbitals in CO calculated with a double zeta basis set are 11.4 eV and 1.8 eV respectively).

Goscinski and Pickup[68] have expressed this in a quantitative way. Following their notation, i,j,k... denote occupied and a,b,c unoccupied spin orbitals for the neutral molecule. For an ionization process associated with spin orbital i they showed that through second order in perturbation theory

$$-\Delta SCF = \varepsilon_i + \sum_{j,a} \frac{|\langle ij||ia\rangle|^2}{(\varepsilon_a - \varepsilon_j)} \qquad \ldots (2.15)$$

where the integral symbol $\langle ij||ia\rangle$ stands for

$$\langle ij \left| \frac{(1-P_{12})}{r_{12}} \right| ia \rangle$$

The second term on the L.H.S. of (2.15) represents electronic relaxation consequent upon an electron ionization, and a careful investigation of this expression indicates that its magnitude is larger on core rather than valence electron ionization. The expression (2.15) will also be of some importance during the discussion of the transition operator method which will be presented at a later stage in this chapter.

Although relaxation energy is a theoretical quantity because transitions to Koopmans' states are not experimentally observed, it can however be shown[69] that the weighted average over the energies of the direct ionization and associated shake-up and shake-off peaks is equal to the binding energy appropriate to the unrelaxed system as would be obtained from Koopmans' theorem. A fundamental assumption in this argument is that the n electron Hamiltonian is <u>suddenly</u> replaced by an n-1 electron Hamiltonian and thus that a description in terms of time independent theory is valid. The theoretical criterion for the validity of the <u>sudden approximation</u> is that[70]

$$[E^f(n\ell,n'\ell') - E^f(n\ell)]\ \tau/h << 1 \qquad \ldots (2.16)$$

where $E^f(n\ell,n'\ell')$ is the total final state energy resulting from a two electron transition, $E^f(n\ell)$ is the total final state energy for a one electron transition involving electron $n\ell$ and τ is the time of transit of the $n\ell$ photoelectron past the $n'\ell'$ subshell in leaving the atom. The energy difference on the L.H.S. of (2.16) is just the separation of the intense one electron photoelectron peak from a certain two electron satellite at lower kinetic energy (cf. Fig. 2.1). In a typical ESCA experiment $\tau/h \simeq 1/65\ eV^{-1}$ thus for satellite separations as large as, or more than 65 eV, the sudden approximation would appear to be violated. Very few satellite peaks are so far away from the main peak, and thus the intensity model presented below is justified. This would not be the case in a UPS experiment where τ/h approaches unity and thus the energies of the observed satellite peaks do not satisfy (2.16).

The initial wave function of the n electron system is denoted by $\Psi^i(n)$ and is expressed as an antisymmetrized product of the $n\ell^{th}$ one electron orbital and a remainder. That is

$$\Psi^i(n) = \mathcal{A}\psi_{n\ell}\Psi_R(n-1) \qquad \ldots (2.17)$$

The wave function $\Psi^i(n)$ satisfies equation

$$\mathcal{H}^i(n)\Psi^i(n) = E^i\Psi^i(n) \qquad \ldots (2.18)$$

where $\mathcal{H}^i(n)$ is the n electron Hamiltonian. If the $n\ell$ electron has been ejected rapidly then the resulting n-1 electron state is not an eigenstate of the final Hamiltonian but a mixture of such eigenstates. That is

$$a_m\Psi^i(n) = \Psi_R(n-1) = \sum_{j=o}^{\infty} C_{mj}\Psi^f_j(n-1) \qquad \ldots (2.19)$$

where a_m is an operator annihilating an electron from the $n\ell^{th}$ orbital

and the wave functions $\Psi_j^f(n-1)$ satisfy

$$\mathcal{H}^f(n-1)\,\psi_o^f(n-1) = E_o^f(n\ell)\,\Psi_o^f(n-1) \quad (j = o) \qquad \ldots (2.20)$$

$$\mathcal{H}^f(n-1)\,\Psi_j^f(n-1) = E_j^f(n\ell,n'\ell')\;\Psi_j^f(n-1) \quad (j=1,2,\ldots) \qquad \ldots (2.21)$$

Index j is used to distinguish final states, and we have arbitrarily chosen j=o to represent one electron transition final state with a fully relaxed electronic cloud corresponding to the main peak of the photoelectron spectrum. Integrating (2.19) from the left by a fixed function $\Psi_k^f(n-1)$, assuming that $< \Psi_k^f \mid \Psi_j^f > = \delta_{kj}$ one obtains

$$C_{mj} = < \Psi_j^f(n-1) \mid \Psi_R(n-1) > \qquad \ldots (2.22)$$

The probability that the (n-1) electron system is in a state j after the annihilation of an electron m is thus

$$P_{mj} = C_{mj}^{\,2} = < \Psi_j^f(n-1) \mid \Psi_R(n-1) >^2 \qquad \ldots (2.23)$$

where $\sum_{j=o}^{\infty} P_{mj} = 1$

In order for two wavefunctions to overlap they must have the same symmetry properties.

That is

$$\Delta J = \Delta L = \Delta S = \Delta M_j = \Delta M_s = 0 \qquad \ldots (2.24)$$

Therefore the selection rules for transitions between two states with the same number of particles are monopole allowed with a unit operator as a perturbing operator. Substituting (2.22) into (2.19) we obtain

$$\Psi_R = \sum_{j=o}^{\infty} < \Psi_j^f \mid \Psi_R > \Psi_j^f \qquad \ldots (2.25)$$

Writing the energy expectation value for $\Psi_R(n-1)$ with the help of (2.25) we obtain

$$E^{R}_{(n-1)} = \langle \Psi_R | \mathcal{H}^{f}_{(n-1)} | \Psi_R \rangle = \sum_{j=o}^{\infty} E^{f}_{j} \langle \Psi^{f}_{j} | \Psi_R \rangle^2 \quad \ldots (2.26)$$

or in terms of ionization potentials as

$$(IP)_R = E^{R}_{(n-1)} - E^{i} = \sum_{j=o}^{\infty} \langle \Psi^{f}_{j} | \Psi_R \rangle^2 \; (IP)_j \quad \ldots (2.27)$$

where $(IP)_j = E^{f}_{j(n-1)} - E^{i}$. If $\Psi^{i}_{(n)}$ is given in the H-F approximation, then $(IP)_R$ is the energy of the unrelaxed system as obtained from Koopmans' theorem. The relation between $(IP)_R$ and the ionization energy $(IP)_o$ relating to the fully relaxed state represented by Ψ^{f}_{o} can be written as

$$(IP)_R = (IP)_o + \sum_{j=1}^{\infty} \langle \Psi^{f}_{j} | \Psi_R \rangle^2 \; [(IP)_j - (IP)_o] \quad \ldots (2.28)$$

The second term on the L.H.S. of (2.28) represents relaxation energy as defined by (2.14). It is a weighted average over the shifts of various multi-electron processes with respect to the main photoionization peak. The coefficients are just the transition probabilities, or in turn, the experimental peak heights corresponding to each $\Psi^{f}_{j(n-1)}$. The relationship (2.28) suggests that relaxation energies can be obtained from experimental data. Strictly speaking this may be true, but practical difficulties in calculating the weighted average from an experimental spectrum make the relationship (2.28) of a purely theoretical interest. Manne and Aberg[69] have estimated the relaxation energy of 1s Ne^{+} species from an experimental spectrum measured by Krause and his co-workers,[64] and they arrived at a value of $(RE)_{expt}$ = 16 eV, whereas a more detailed approach by Meldener and Perez[71] relying on more accurate data by Siegbahn et al.[59] yielded $(RE)_{expt}$ = 22 eV which favourably compares with the theoretical value by Bagus[67] $(RE)_{cal}$ = 23 eV.

So far we have assumed when calculating binding energies by the Δ SCF method that both the molecule and the ion are in their vibrational ground states, and zero point energies have not been considered. The latter chapters will contain discussions on vibrational effects accompanying core and valence ionizations in some detail, however it is worthwhile noting that accurate values of vertical and adiabatic ionization potentials as obtained by the Δ SCF method require a detailed knowledge of the potential energy surfaces of ground and ionized state species in particular equilibrium geometries, force and sometimes anharmonicity constants. By a vertical transition we mean a transition which involves the most likely vertical change from a vibrational level v = 0 whereas an adiabatic transition represents a vertical change from v" = 0 to v' = 0 level. Note, that the term 'vertical change' implies that no changes in nuclear geometry occur during the emission of the photoelectron which is the main assumption behind the use of the Franck-Condon Principle.[72-74] This assumption is substantiated by the fact that photoemission occurs on a time scale of around 10^{-17} sec.[75] whereas a typical vibrational frequency is of the order of $\sim 10^{-13}$ seconds.[76]

Siegbahn et al. have demonstrated[77] that intensities of various vibrational components in the main photoionization peak for core levels in simple molecules are governed by Franck-Condon factors (Fig. 2.4) which were originally discussed by Franck[72] and Condon[73,74] in calculating intensities of vibrational components in electronic spectra. Clark and Adams[78] have suggested that vibrational excitation plays an important part in the band shape of some shake-up peaks and a theoretical analysis by Gelius[79] has indicated that Franck-Condon factors must be taken into account when determining a transitional probability between a ground state and a vibrationally excited shake-up state.

FRANCK CONDON TRANSITIONS

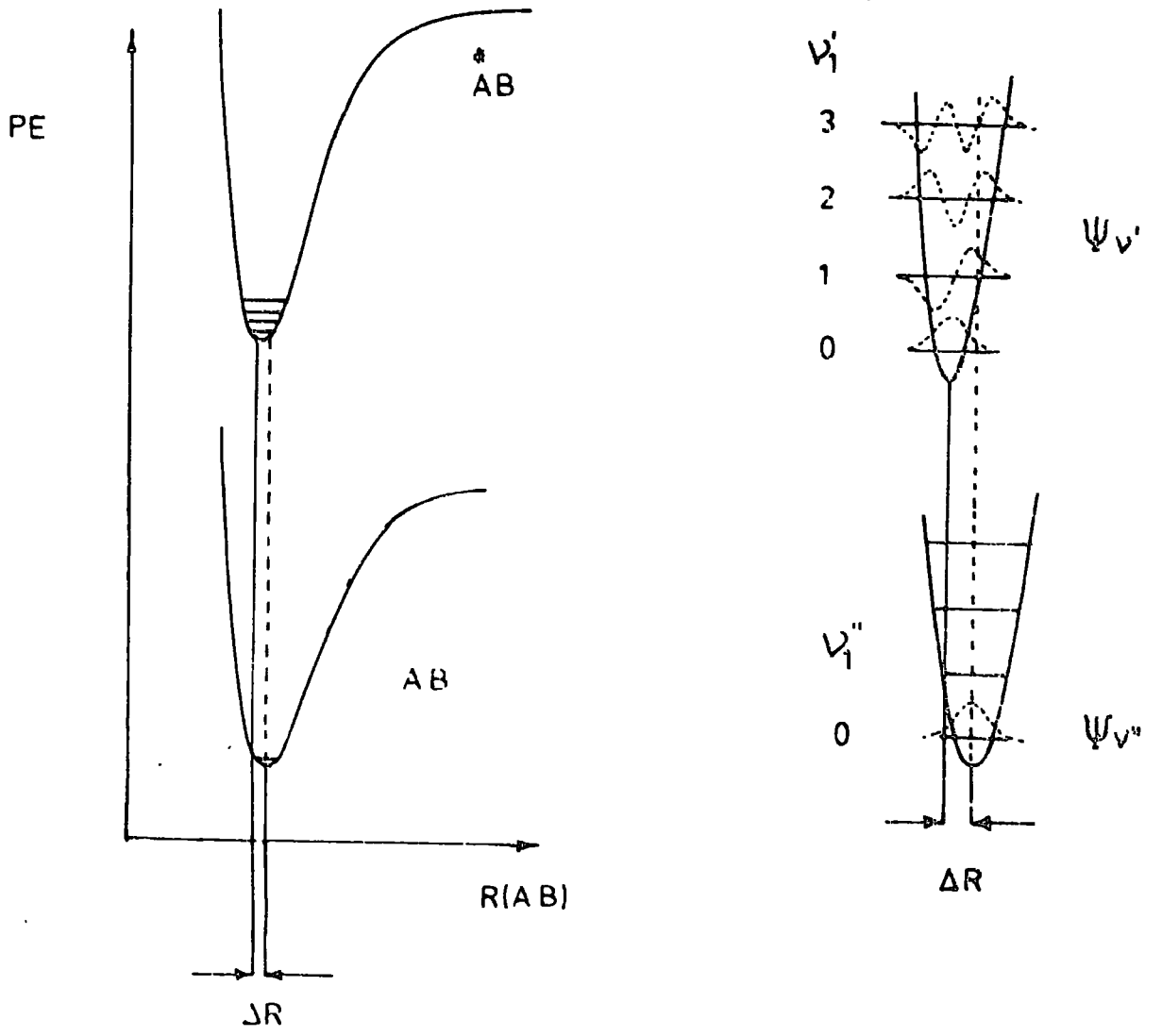

$$P_{v'v''} \propto \left| \int \psi_{v'} \psi_{v''} \, d\tau \right|^2$$

Fig. 2.4.

A schematic representation of the vibrational excitation in a hypothetical molecule AB. Franck-Condon factors are governed by the values of $P_{v',v''}$.

While on the subject of the Δ SCF method it is worthwhile briefly discussing the symmetry properties of core holes, in particular whether they are localized to a specific atom in a molecule or not. In molecules containing no equivalent centres there is no doubt of the local nature of the core hole since the ground state core orbitals are very localized indeed. The situation in molecules with two or more equivalent nuclear centres is less clear-cut because of the delocalized nature of the core orbitals in the HF approximation. For example if we remove a core electron from O_2 do we represent the ion by a structure $O^{\frac{1}{2}+}\!\!-\!\!-O^{\frac{1}{2}+}$ or by a structure $O^{+}\!\!-\!\!-O$ with equal chances of finding the positive charge on each atom. An overwhelming body of evidence in the literature[80-84] indicates that in these cases the correct description of the HF wavefunction is achieved with core holes localized at one of the equivalent centres.

The first evidence of this kind came from Bagus and Schaefer[80] who performed calculations on localized and delocalized 1s hole states of O_2^+ molecular ion. They found that the hole state calculations with g or u symmetry imposed on the 1s hole states gave a BE = 554.4 eV. When the symmetry restriction was relaxed the HF equations yielded two solutions at BE = 542 eV corresponding to 1s hole on each oxygen which favourably agrees with the experimental value of 543.1 eV. The authors pointed out that a total wavefunction of proper Σ_g or Σ_u symmetry can be formed from these two localised hole states.

Snyder's model[81] based on atomic shielding constants states that delocalization of a hole over t centres produces a hole charge of $\frac{1}{t}$ on each centre with relaxation energy per centre of approximately $\frac{1}{t^2}$ that for a localized hole. The total relaxation energy for t centres would be $\frac{1}{t}$ that for a localized hole. This model predicts relaxation energy for N_{1s} hole 13.7 eV which would be reduced to 6.8 eV if the hole were delocalized. Shifts in

core binding energies between N_2 and NH_3 as well as between CH_4 and C_2H_4 are both well predicted from Koopmans' theorem[85] thus indicating that relaxation energies must be very similar in each of the two pairs which can only be true if the holes are localized. HF calculations of binding energies by the Δ SCF method in our laboratory on systems like N_2, C_2H_4, F_2, C_2H_2 and others correspond to experimental values only if the core hole states are localized.

Another line of evidence supporting the localized nature of core holes comes from an elegant study by Murrell and Ralston[82] who computed potential energy curves for the He_2^+ ion. Their study indicates that the MO function, which has the wrong dissociation limit, has a higher energy than the simplest VB function for internuclear separation larger than 2 a.u. showing that the contraction energy from a localized positive charge is appreciably more than that from two half charges even when hole exchange is important. The comparison of core ionized N_2^+ with He_2^+ at large internuclear separations where the 1s overlap integrals are comparable clearly indicates that the N_{1s} core hole species of N_2 are best represented by a function which takes into consideration the localized nature of the core hole.

Hillier and his co-workers[83] tried to interpret shake-up spectra of the C_{1s} peaks in C_2O_3 and the O_{1s} peak in CO_2 using the relation (2.23)$^{--}$ in a simplified form and they came to the conclusion that certain satellite peaks could only be interpreted with a localized hole state model.

An interesting study by H. Siegbahn[84] indicates that the difference between the energies of localized and delocalized holes for a given system disappears when a CI procedure (which takes into account correlation effects) starting either from localized or delocalized Hartree-Fock equations is adapted.

Many important points have been introduced in this section and we shall discuss some of their aspects and consequences in the chapters to follow. Now we shall return to other methods for interpreting ionization potentials.

c. Relaxed Koopmans' Ionization Potentials.

Liberman has suggested[86] that the binding energy is essentially the arithmetic mean of the orbital energies for the K^{th} orbital in the ground and hole state, that is

$$(BE)_k = -\tfrac{1}{2}(\varepsilon_k + \varepsilon_k^*) \qquad \ldots (2.29)$$

We shall refer to binding energies calculated in this way as relaxed Koopmans' ionization potentials (binding energies). From a computational point of view no extra labour is saved over the Δ SCF method because calculations on both ground and ionic states must be performed. Liberman used the relationship[86] (2.29) to calculate the BE of the Ar_{1s} hole. The value obtained with this method (118.0 A.U.) is in very good agreement with the experimental value[59] 117.8 A.U.

The empirical relationship (2.29) has been theoretically justified by Hedin and Johansson.[87] In their method based on a polarization potential, they derived an expression for a binding energy of an electron in an orbital k.

$$-BE = \varepsilon_k + \tfrac{1}{2} \langle k | V_R | k \rangle \qquad \ldots (2.30)$$

where $|k\rangle$ is the k^{th} one electron orbital and V_R is a relaxation (or sometimes called polarization) potential arising from the difference between the Hartree-Fock potential V_ℓ of passive orbitals in the final (k-hole) state and the initial state. Specifically

$$V_R = \sum_{\ell \neq k} (V_\ell^{(f)} - V_\ell^{(i)}) \qquad \ldots (2.31)$$

They went on to prove that the relationship (2.30) is nearly equivalent to Liberman's empirical rule (2.29). Finally it is worthwhile pointing out

that the relationship (2.15) derived by Goscinski and Pickup is a generalization of (2.30).

d. Other Techniques.

There are other methods for calculation of binding energies apart from the ones already mentioned but we shall discuss them only briefly giving illustrative rather than comprehensive references as these techniques have not been used in the present work.

i) The Equivalent Cores Approach.

The equivalent cores method of predicting shifts in binding energies from thermodynamic data was developed by Jolly and Hendrickson.[88] It is based on the principle that

'When a core electron is removed from an atom, molecule or ion, the valence electrons relax as if the nuclear charge on the atom had increased by one unit.'

Consider, for example, the shift in C_{1s} binding energy between CH_4 and CH_3F.

$$CH_4 \longrightarrow \overset{*}{C}H_4^+ + \bar{e}; \quad \Delta E = (BE)_{CH_4} \qquad \ldots (2.32)$$

where * indicates a core hole vacancy (C_{1s} in this case).

$$\overset{*}{C}H_4^+ + N^{5+} \longrightarrow NH_4^+ + \overset{*}{C}^{5+} \quad \Delta E = \delta_o \qquad \ldots (2.33)$$

The reaction (2.33) is the exchange of the $\overset{*}{C}^{5+}$ core and the equivalent core species N^{5+}, and the energy δ_o for this exchange process is called the energy of core exchange. Summing up (2.32) and (2.33) we obtain

$$CH_4 + N^{5+} \longrightarrow NH_4^+ + \overset{*}{C}^{5+} + \bar{e}; \quad \Delta E = (BE)_{CH_4} + \delta_o \qquad \ldots (2.34)$$

Similarly for CH_3F we obtain

$$CH_3F + N^{5+} \longrightarrow NH_3F^+ + \overset{*}{C}^{5+} + \bar{e}; \quad \Delta E = (BE)_{CH_3F} + \delta_1 \qquad \ldots (2.35)$$

Subtracting (2.35) - (2.34) we get

$$CH_3F + NH_4^+ \longrightarrow NH_3F^+ + CH_4^+; \quad \Delta E = (BE)_{CH_3F} - (BE)_{CH_4} + (\delta_1 - \delta_o) \ldots (2.36)$$

It is assumed that δ_o and δ_1 are small quantities because $\overset{*}{C}H_4$ and NH_4^+, $\overset{*}{C}H_3F$ and NH_3F^+, $\overset{*}{C}^{5+}$ and N^{5+} are chemically equivalent. In the strong form of the equivalent core approximation δ_o and δ_1 are put to zero, but it is sufficient to have $\delta_1 - \delta_o = 0$ (the weak form) to determine a chemical shift. Therefore according to the weak form of the equivalent core approximation the chemical shift between CH_4 and CH_3F is given by the heat of reaction (2.36). Such heats and corresponding shifts in binding energies can be obtained either from thermodynamical data[88-90] or from ab initio[91,92] or semi-empirical[93] LCAO MO SCF calculations.

It has been mentioned in Chapter I, Section 1.5.d. that small basis sets like 4-31G and 3G can be very useful in describing core hole state HF wave functions if the equivalent core model is incorporated into them. McWeeny and Velenik[94] were the first to suggest that accurate binding energies can be calculated with small basis sets using the ΔSCF method if the core hole state wave function is calculated with valence exponents appropriate to the equivalent core species (e.g. N for C with core electron deficit). This is a reasonable suggestion because the valence electrons of the hole state (e.g. $\overset{*}{C}H_4^+$) and the equivalent core species (e.g. $\overset{+}{N}H_4$) experience a similar potential due to the nucleus and the core electrons associated with it which is different from that of the neutral molecule (e.g. CH_4). Investigation of such core hole state wave functions in conjunction with calculations of binding energies, relaxation energies and force constants will be presented in the chapters to come. Basis sets based on this idea are referred to as optimized basis sets.

ii) The Transition Operator Method.

Goscinski and his co-workers[95] have argued that if according to Koopmans' theorem eigenvalues ε_i's of the Fock operator (1.99)

$$F = h_1 + \sum_j < j(2)||j(2) > \qquad \ldots (2.37)$$

correspond to negative values of ionization potentials then an eigenvalue equation associated with a transition operator (for an i-hole)

$$F_i^T(1) j^T(1) = \varepsilon_j^T j^T(1) \qquad \ldots (2.38)$$

must give us ionization potentials which incorporate electronic relaxation. The operator in (2.38) is defined as

$$F_i^T(1) = h_1 + \sum_{j\neq i} < j^T(2)||j^T(2) > + \tfrac{1}{2} < i^T(2)||i^T(2) > \qquad \ldots (2.39)$$

where $j = 1,2,\ldots,i,\ldots n$ (n is number of electrons).
This is a reasonable suggestion because the operator F_i^T describes a half-ionized state. An operator of this nature is called a transition operator. They went on[95] to expand an orbital energy ε_i^T through second order in perturbation theory and thus obtained

$$\varepsilon_i^T = \varepsilon_i + \sum_{j,a} \frac{< ij||ia >}{(\varepsilon_a - \varepsilon_j)} \qquad \ldots (2.40)$$

which according to (2.15) is equal to ΔSCF for an i-hole. Thus we obtain

$$-\varepsilon_i^T = \Delta_i \text{ SCF} \qquad \ldots (2.41)$$

Therefore it is evident that the eigenvalue of the transition operator F_i^T corresponds to the Δ_i SCF result. The direct subtraction of large numbers is avoided but unfortunately as in the ΔSCF method one must make a separate calculation for each hole state. Whereas the eigenvalues ε_j^T for $j\neq i$ of F_i^T do not have a special importance the orbitals j^T (for all j) may be utilized in the calculation of generalized overlap

amplitudes and transition probabilities.[96] Accuracy of ionization potentials calculated by the transition operator method has been well demonstrated by Goscinski and his co-workers[95,97] who have also pointed out the difficulties in the present model in describing localized core hole states.[97] The use of this transition formalism is justified not so much for reduction of computer time but on account of its conceptual framework which in particular leads to a transition potential model for chemical shifts discussed further on in this section.

iii) Potential Models.

The first model proposed for calculating binding energies, and in particular their shifts, based on electrostatic potential is the charge potential model. This model relates core electron binding energies with the charge on the atom from which core ionization takes place and the potential from the charges in the rest of the molecule

$$E_i = E_o + kq_i + \sum_{i \neq j} \frac{q_j}{r_{ij}} \qquad \ldots (2.42)$$

where E_i is binding energy of atom i

q_i is charge on atom i

r_{ij} is interatomic distance between atoms i and j

E_o is a reference level

k is a constant which is approximately equal to the one centre Coulomb integral between a core and a valence electron on atom i.

The relation (2.42) was originally derived from purely classical electrostatic consideration by Siegbahn and his co-workers.[59] It can however be derived from Koopmans' theorem[98] and for this reason it, in principle, suffers from the same deficiency notably that the binding energies obtained by this method depend only on ground state properties of molecules hence do not take into account electronic relaxation. This difficulty can be

partly overcome if we consider k and E_o as adjustable parameters determined from a least squares fit of a series of similar molecules whose binding energies have been measured experimentally. The charges q_j are obtained from the Mulliken population analysis and the use of semi-empirical methods (such as CNDO) is particularly useful in predicting chemical shifts in large systems which would be computationally too expensive or impracticable to calculate from ab initio wave functions.[99-101] Alternatively we can use (2.42) to obtain 'experimental' ground state charge distributions from experimentally measured shifts in binding energies.[102]

The charge potential model given by (2.42) is just one particular approach to calculate chemical shifts from ground state properties of a molecule using electrostatic arguments. An alternative model is that due to Swartz.[103] Methods of this kind are generally called ground-state potential models (GPM).[104] Basch showed[105] that a shift in potential energy of an electron at a nucleus, ΔV_n, provides a good approximation to the shift in orbital energy $\Delta\varepsilon^k$

$$\Delta\varepsilon^k \simeq \Delta V_n \qquad \ldots (2.43)$$

Writing

$$V_n = kq_i + \Sigma\frac{q_j}{r_{ij}} \qquad \ldots (2.44)$$

will give us an alternative derivation of the charge potential model (2.42) for predicting chemical shifts.

Shirley and Davis[104] have used Liberman's relationship (2.29) to derive the relaxation potential model (RPM) which depends not only on the ground state but also on the core hole state properties of a molecule thus incorporating into it electronic relaxation. Starting with (2.29) and using (2.43) we obtain

$$(BE)_k = -\tfrac{1}{2}(\epsilon_k + \epsilon^*_k) \qquad \ldots (2.45)$$

$$\Delta(BE)_k = -\tfrac{1}{2}(\Delta\epsilon_k + \Delta\epsilon^*_k) \qquad \ldots (2.46)$$

$$\Delta(BE)_k = -\tfrac{1}{2}(\Delta V_n + \Delta V_n^*) \qquad \ldots (2.47)$$

Invoking the equivalent cores approximation one obtains

$$\Delta(BE)_k = -\tfrac{1}{2}(\Delta V_n + \Delta V_n(Z+1)) \qquad \ldots (2.48)$$

where $V_n(Z+1)$ is the potential energy of a core electron at an equivalent core nucleus.

Thus the GPM gives

$$\Delta(BE)_k = -\Delta V_n \qquad \ldots (2.49)$$

and the RPM defined in (2.48) gives

$$\Delta(BE)_k = -\Delta V_n - \Delta V_R \qquad \ldots (2.50)$$

where

$$V_R = \tfrac{1}{2}[V_n(Z+1) - V_n] \qquad \ldots (2.51)$$

is the relaxation energy in the RPM approximation which incidentally can be combined with ab initio orbital energies to give an alternative way of calculating binding energies. Davis and Shirley[104] have discussed some results obtained from the GPM and the RPM based on CNDO wave functions and they have shown as expected that in general the RPM version gives better agreement with experimental results.

An alternative potential model for calculating core binding energies which incorporates electronic relaxation is the transition potential model (TPM) developed by Goscinski and his co-workers.[106,107] They base their arguments on the transition operator technique discussed earlier in this chapter. They point out that if the ordinary charge potential model (2.42) depending on the ground state properties of a molecule can be deduced from Koopmans' theorem by considering an expectation value of the Fock operator[98] (2.37) then an equivalent expression

$$E_i^T = E_o^T + k^T q_i^T + \sum_{i \neq j} \frac{q_j^T}{r_{ij}} \qquad \ldots (2.52)$$

can be derived by considering an expectation value of the transition operator (2.39) where

E_i^T is the binding energy of atom i incorporating relaxation effects of valence electrons

q_i^T is a transition charge on i discussed below and

E_o^T and k^T are constants of the same nature as defined in (2.42).

The transitions charges q_i^T's are obtained from a CNDO wave function which must be slightly modified, namely that Z_i^*, the effective reduced charge of atom i usually defined as the nuclear charge Z_i minus the number of core electrons (e.g. for C_{1s} ionization $Z_c^* = 4$) is within the TPM mechanism defined as the nuclear charge Z_i minus the average number of core electrons before and after ionization (e.g. for C_{1s} ionization $Z_c^* = 4.5$). This implies that the atomic CNDO parameters for atom i are interpolated between Z_i and Z_i+1. We can also use the TPM to calculate relaxation energy which is given by

$$(RE)_i = E_i - E_i^T \qquad \ldots (2.53)$$

The most attractive feature of the TPM is that one calculation per ionized hole is needed which is 'safer' than subtraction of potentials derived from two semi-empirical calculations. The TPM method has so far been tested to calculate core binding and relaxation energies of some carbon and boron compounds[106,107] and seems to give more accurate results than Shirley's RPM technique.[104,108]

iv) Multiple-Scattering - X_α Method.

Slater has suggested[109] that it is possible to approximate the solutions of HF equations by replacing the non-local operator (1.102) with a local exchange potential called X_α. The electronic equations obtained

in this way are usually solved by the method known as the multi-scattering (MS) or scattered-wave method. The MS X_α technique has the great advantage that it requires relatively small computer time and therefore it can be used successfully to describe electronic structure of large systems[110] which are of chemical interest (e.g. SF_6) but its main purpose lies in the field of solid state physics. The greatest disadvantage of this method is the fact that the results of the MS X_α technique depend on the initial choice of X_α potential and on the boundary conditions.

Thus although the method describes valence ionized states reasonably well for core hole states both absolute and relative binding energies can be considerably in error. The strong dependence on parametrization and inconsistent nature of the results suggests that the technique is unsuitable for studying photoionization phenomena in general.

v) Green's Function Method.

A new viable alternative to more established wavefunction methods for obtaining information about molecular structure and especially photoelectron spectra is what is believed a more superior method based on a direct calculation of the one-particle propagator or Green's function.[112] The advantage of the propagator formalism is that it involves a direct method of calculating ionization energies and if necessary it can take into account electronic relaxation and correlation.[68] Green's function itself has been known in mathematics for a long time, but its application to quantum chemistry is relatively new and so far only few albeit successful calculations have been reported particularly by Cederbaum and his co-workers[113-115] and the Florida group led by Ohrn.[11,116,117] Further developments in this method especially with emphasis on computer programs should bring more successful results in this exciting field of quantum chemistry.

CHAPTER III

INVESTIGATIONS OF ELECTRONIC RELAXATIONS ACCOMPANYING CORE IONIZATIONS

Abstract.

Ab initio calculations have been carried out on an extensive series of molecules for both the neutral species and core ionized states. Substituent effects on C_{1s}, N_{1s}, O_{1s} and F_{1s} levels have been investigated and where available comparison has been drawn with experiment. Comparison with Koopmans' theorem has allowed a relatively detailed study of changes in relaxation energies as a function of substituent effect on a given core level. Whilst for C_{1s} levels the computed shifts in core binding energies are approximately linearly related to differences in relaxation energies, for the N_{1s}, O_{1s} and F_{1s} levels, the relative electronegativity of the substituent can invert the correlation. The empirical correction of Koopmans' theorem for differences in relaxation energies at different sites has been investigated for large molecules. The results compare well with the direct hole state calculations.

A theoretical analysis has also been made of differences in relaxation energies for photoionization from the core levels of the series X_2, HX for X = F, Cl, Br. It is demonstrated that whilst the change in relaxation energies is largest for F_2 with respect to HF, the contribution to the shifts in core levels is relatively larger for the series X_2 and HX for X = Cl, Br. It is further shown that shifts in binding and relaxation energies show very little dependence on core levels studied.

3.1. Substituent Effects on Binding Energies.

(a) Introduction.

As we have previously indicated there have been numerous theoretical calculations on core binding energies. However, there has been no previous systematic study of a large range of substituent effects on different core levels studied with a comparable basis set. For this reason substituent effects on C_{1s}, N_{1s}, O_{1s} and F_{1s} core levels in a range of both saturated and unsaturated compounds have been investigated using the ΔSCF method.[67]

Experimentally determined geometries[118] were employed where available, otherwise they were estimated using tables of standard bond distances and angles.[118] Preliminary studies indicated, however, that binding energies are relatively insensitive to small variations in geometry. (e.g. computed C_{1s} binding energies with STO 4 - 31G basis set for staggered and eclipsed conformers of CH_3OH are 306.67 eV and 306.66 eV respectively.) The emphasis in these particular calculations has been on shifts in binding energies rather than absolute values and therefore we have chosen a rather small basis at the 4 - 31G level whose limitations are in this case (i.e. in considering shifts) to some extent relatively minor as has been previously shown in our laboratory.[119] (STO 4 - 31G expansions[24] with Clementi's best atom exponents[20] were used for all elements except fluorine which has been investigated with a comparable HF 4 - 31G basis[25] as was suggested in Chapter I, Section 1.5.d.). As a preliminary check the absolute binding energy for the C_{1s} levels of CH_4 is calculated to be 294.3 eV. In the next sections a detailed discussion of relaxation energies will be given but at this stage it should be emphasized that by comparison with the results from Koopmans' theorem the basis underestimates the magnitude of the relaxation energy. As we have already

pointed out this relaxation energy is associated almost solely with the valence electrons and the underestimation of this quantity with the 4 - 31G basis is readily understandable since the exponents are optimised with respect to the neutral species. That this is the case may readily be demonstrated by re-computing the total energy for the hole state with exponents appropriate for the valence atomic orbitals of the equivalent core (viz. N in CH_4). The excellent agreement (Table 3.1) for the absolute binding energies for the molecules studied by this approach is most encouraging and indicates a computationally less expensive means of calculating absolute binding energies, as compared to large basis computation. In a subsequent chapter a detailed investigation of the basis set dependence of both absolute and relative binding energies and relaxation energies will be presented. At this stage, however, we may note that differences in both binding and relaxation energies are adequately described with calculations at the 4-31G level at least as far as systems based on elements of the first row of the periodic table are concerned.

Now we shall turn our attention to a discussion of substituent effects in saturated and unsaturated systems.

(b) Binding Energies in Saturated Systems.

The range of substituents which have been studied are indicated in Tables 3.2 and 3.3 with the primary substituent effect with respect to the methyl substituent taken as standard. This is more reasonable than employing hydrogen substituent as reference since it is not clear in cases where strong hydrogen bonding is possible that the experimental results refer to the free molecule. (Ground state energies of all molecules investigated are tabulated in Appendix 2. Using these together with values in Tables 3.2, 3.3, 3.6, 3.7, 3.10 and 3.11 will give us energies of

Table 3.1.

Effect of Optimised Core Valence Atomic Orbital Exponents on Core Binding Energies (in eV)

X	Unoptimised	Optimised†	Experimental[a]
$\underline{CH_4}$	294.18	290.71	290.8
$\underline{H_2O}$	545.49	539.12	539.4
$\underline{CO}$	548.47	541.89	542.3
$\underline{CO}$	300.78	296.71	296.2

† In this context optimised is taken to mean that the valence atomic orbital exponents correspond to the equivalent core species for the hole state.

[a] T.D. Thomas, J. Chem. Phys., 1970, 53, 1744.

Table 3.2.

Substituent Effects on Carbon Core Binding Energies (in eV)

Carbon:

	X	Calc.	Exptl.[a]	Exptl.[e]
$\underline{C}H_3$-X	CH_3[d]	(0)	(0)	0
	H	0.23	0.2	0.2
	CH_2F	0.61	-	0.43
	CHF_2	1.26	-	0.86
	CF_3	1.96	2.2[b]	1.31
	CHO	0.57	0.8	-
	NH_2	0.89	0.9[c]	-
	OH	1.55	1.8	2.1
	F	3.46	3.0	3.0
$\underline{C}H_2$=X	CH_2	0.22	0.3	0.1
	CHF	0.80	-	0.34
	CF_2	1.54	-	0.57
	NH	1.97	-	-
	O	3.87	3.4	-
HC≡$\underline{C}$-X	H	1.18	0.6	0.6
	F	4.46	-	-

	X	Calc.	Exptl.[a]	Exptl.[e]
X$\underline{C}$HO	CH_3	3.40	3.4	-
	H	3.87	3.4	-
	NH_2	4.30	-	-
	OH	5.32	5.2	-
	F	7.28	-	-
	Miscellaneous			
	$CH_3\underline{C}H_2F$	2.96	-	2.63
	$CH_3\underline{C}HF_2$	6.04	-	5.29
	$CH_3\underline{C}F_3$	9.13	-	7.88
	$F_2\underline{C}O$	10.73	-	-
	HC$\underline{C}$F	2.03	-	-
	FC$\underline{C}$F	5.29	-	-
	$CH_2\underline{C}HF$	3.17	-	2.72
	$CH_2\underline{C}F_2$	6.29	-	5.34

[a] Schwartz and Switalski, J. Amer. Chem. Soc., 1972, 94, 6298. Collection of experimental data from references: D.W. Davis, D.A. Shirley and T.D. Thomas, J. Chem. Phys., 92, 4184 (1970); T.D. Thomas, J. Amer. Chem. Soc., 92, 4184 (1970); D.W. Davis, J.M. Hollander, D.A. Shirley and T.D. Thomas, J. Chem. Phys., 52, 3295 (1970); K. Siegbahn et al., 'ESCA Applied to Free Molecules', North Holland, Amsterdam (1969).

[b] Estimated from thin film measurements on benzotrifluoride and benzene, Cf. D.T. Clark, D. Kilcast and W.K.R. Musgrave, J. Chem. Soc. (D), 516 (1971).

[c] Estimated from thin film measurements on pyrrole, Cf. D.T. Clark and D.M.J. Lilley, Chem. Phys. Lett., 9, 234 (1971).

[d] Calculated absolute binding energy is 293.95 eV.

[e] D.W. Davis, M.S. Banna and D.A. Shirley, J. Chem. Phys., 60, 237 (1974).

Table 3.3.

Substituent Effects on N, O, F Core Binding Energies (in eV)

NITROGEN								
NH_2-X	X	Calc.	Exptl.[a]	Exptl.[g]	BE(1s)	Calc.	Exptl.[a]	Exptl.[g]
	CH_3[d]	(0)	(0)	-	CH_2NH	0.40	-	-
	H	0.78	0.5	-				
	CHO	1.17	1.0	-				
	NH_2	0.88	-	-				
	OH	1.44	-	-				
	F	3.75	-	-				
OXYGEN								
HO-X	CH_3	(0)[e]	(0)	-	CH_2O	0.60	-1.3	-
	H	1.0	0.8	-	CF_2O	3.12	-	-
	CHO	1.77	1.5	-	CH_3CHO	-0.30	-1.3	-
	NH_2	0.49	-	-	NH_2CHO	-1.37	-	-
	OH	1.30	-	-	OHCHO	-0.17	-0.1	-
	F	4.52	-	-	OHCHO	1.78	1.5	-
					FCHO	1.84	-	-
FLUORINE								
F-X	CH_3	(0)[f]	-	(0)	F_2CO	3.16	-	-
	H	2.24	1.6[b]	-	CH_2CHF	0.40	-	0.34
	CH_2CH_3	-0.28	-	-0.60	CH_2CF_2	1.78	-	1.52
	$CHFCH_3$	0.77	0.9[c]	0.38	HCCF	2.84	-	-
	CF_2CH_3	1.84	1.4[c]	1.97	FCCF	3.29	-	-
	CHO	1.41	-	-				
	NH_2	0.58	-	-				
	OH	0.89	-	-				
	F	4.0	4.3[b]	-				

[a] Values as Table 3.2.(a).

[b] R.W. Shaw and T.D. Thomas, Chem. Phys. Lett., 22, 127 (1973).

[c] Extrapolated from experimental data on fluoromethanes (see text).

[d] Calculated absolute binding energy is 409.07 eV

[e] Calculated absolute binding energy is 544.49 eV

[f] Calculated absolute binding energy is 713.14 eV

[g] D.W. Davis, M.S. Banna and D.A. Shirley, J. Chem. Phys., 60, 237 (1974).

hole state species and respective Koopmans' values.) Where direct experimental data is available,or where it may be inferred,the agreement between theory and experiment is good. The shifts in binding energies are in accord with chemists' intuitive ideas concerning the nature of substituent effects viz. at the two extremes replacing H by Me or F results in a shift to lower and higher binding energies respectively for all core levels. Of some interest is the fact that substituent effects are such that in progressing across the series from C_{1s} to F_{1s} core levels there is generally relatively little variation due to Me, NH_2, OH and F substituents. The net effect is that the difference in shifts arising from these substituents remains relatively constant for the different core levels.

There is sufficient data available to consider both primary and secondary substituent effects on core binding energies and these results are shown in the case of fluorine substitution in Table 3.4. The marked consistency of primary and secondary shifts at carbon of $\sim$ 3.0 eV and $\sim$ 0.7 eV respectively are in excellent agreement with available experimental data obtained from studies of simple monomers and for homopolymers,[120] based on fluorocarbon monomers. It is clear that for fluorine, the primary and secondary substituent effects, in not only saturated but also unsaturated systems are essentially constant in accord with the observed shifts in the fluorobenzenes.[121] By employing appropriate primary and secondary substituent effects it is possible to estimate shifts in core binding energies for other systems. In difluoroacetylene for example, a shift of 4.06 eV is anticipated with respect to acetylene in accord with a calculated value of 4.12 eV. The experimentally observed gas phase shifts in the fluoromethanes by comparison with the fluoroethanes are also well reproduced by this data for both the C_{1s} and F_{1s} core binding energies.

Table 3.4.

Effect of Fluorine Substitution on α and β Core Binding Energies†

	Primary (α)	Secondary (β)
CH_3-CH_3	(0)	(0)
CH_2F-CH_3	2.96 (2.96)	0.61 (0.61)
CHF_2-CH_3	6.04 (3.08)	1.26 (0.65)
CF_3-CH_3	9.13 (3.09)	1.96 (0.70)
$CH_2=CH_2$	(0)	(0)
$CHF=CH_2$	2.95 (2.95)	0.58 (0.58)
$CF_2=CH_2$	6.07 (3.12)	1.32 (0.74)
H-C≡C-H	(0)	(0)
F-C≡C-H	3.20	0.86
$H_2C=O$	(0)	(0)
HFC=O	3.41 (3.41)	1.24 (1.24)
$F_2C=O$	6.86 (3.45)	2.40 (1.16)
H-C≡N	(0)	(0)
F-C≡N	3.3	1.09

† The values in brackets refer to successive shifts w.r.t. the preceding molecule.

(c) Binding Energies in Unsaturated Systems.

A similar analysis has been undertaken for some unsaturated species (see Table 3.4). Reasonable agreement is again evident between the calculated and experimental results where available. Introduction of a double or triple bond to the core ionized centre is seen to have little effect on the primary and secondary shifts with the notable exception of the O_{1s} shifts in the carbonyl compounds where the shift is approximately twice as large. The primary shifts at the carbonyl carbon correlate quite well with those observed at a saturated carbon, the shifts (with respect to CH_3) being slightly larger.

3.2. Substituent Effects on Relaxation Energies.

(a) Introduction.

The computational expense of performing calculations on core hole states for each core level has meant that considerable emphasis in the literature has been placed on the interpretation of shifts using Koopmans' theorem. As we have already indicated the energy lowering due to the relaxation of the valence electrons in going from the neutral molecule to the core ionized species is quite appreciable in absolute terms (of the order of 10 - 30 eV for first row atoms). Previous investigations in which comparisons have been made between Koopmans' theorem and hole state calculations have shown that the relaxation energies are closely similar for a given core level in a closely related series of molecules.[119] Experimental data is available however which suggests that for different bonding environments there may be significant contributions to shifts in core binding energies arising from differences in relaxation energies. A particular example is the shift in carbon 1s levels for the methyl and carbonyl carbons in acetaldehyde. Experimental

measurements both in the gas and solid phase give a shift between 2.7 and 2.9 eV. The shifts however computed from Koopmans' theorem are always smaller by approximately 0.4 eV, independent of the basis set, provided a suitably balanced basis is employed. By contrast the hole state calculations reported here are in excellent agreement with the measured shift in C_{1s} levels for acetaldehyde thus suggesting a small but significant difference in relaxation energy at the two carbon atoms. In studying an extensive series of molecules covering a number of core levels and a variety of bonding situations we may investigate the importance of differences in relaxation energy in contributing to these shifts.

(b) Relaxations Consequent upon Ionizations of C_{1s} Levels.

Firstly considering the data for core ionization at carbon, Fig. 3.1. shows a plot of calculated shifts in binding energies versus differences in relaxation energies covering C_{1s} levels in both saturated and unsaturated systems. It is interesting to note that binding energies span a range of $\sim$ 7 eV whilst the corresponding range for the relaxation energies is $\sim$ 1.5 eV. We have pointed out in the previous chapter that relaxation energy corresponds to weighted mean over all multielectron photoionization processes. The fact that for the series of molecules studied here the relaxation energies fall in a narrow band leads to two conclusions. Firstly, that only shake-up and shake-off transitions of appreciable intensity must fall quite close in energy to the weighted mean and secondly, that in general the changes in relative intensities and transition energies for the multi-electron processes must be quite subtle functions of electronic environment such that the weighted mean remains constant.

Figure 3.1 clearly illustrates that there is a trend established between shifts and relaxation energies and this has also been noted recently

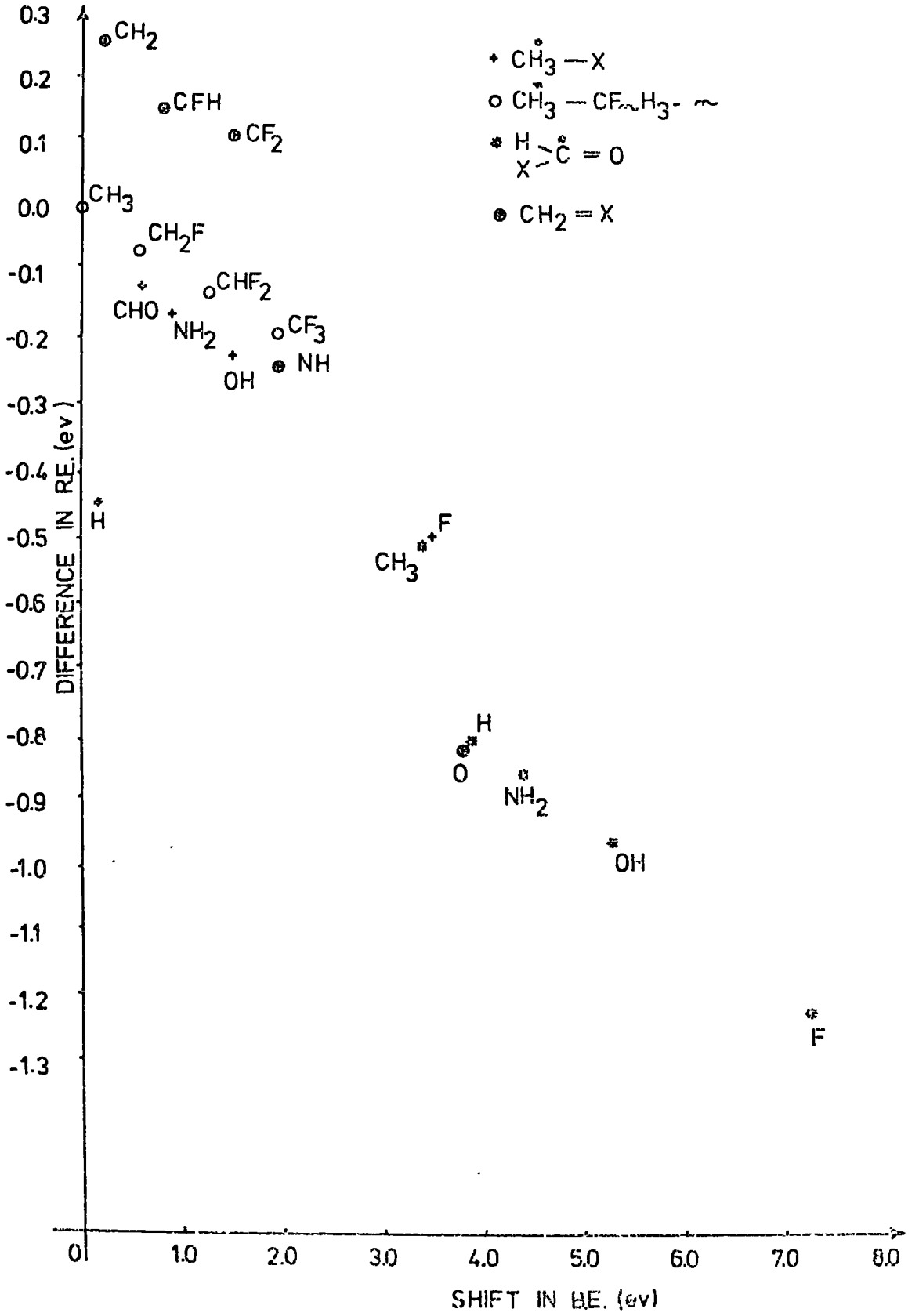

Fig. 3.1.

Plot of computed differences in relaxation energy versus shifts in binding energy (both with ethane as standard) for some C_{1s} levels.

for a limited series of molecules by Hillier and co-workers.[124] Good linear correlations are observed for the four individual series of molecules studied. The relaxation energies are obviously lowest for those core levels corresponding to the largest shifts in binding energy. This is not unreasonable since the valence electron clouds will already be somewhat contracted in the neutral molecule. The good overall correlation between shifts in binding and relaxation energies goes some way to rationalizing why in general the charge potential model works so well. Indeed this is not unexpected in the light of a recent analysis[98,125] of the contributions to relaxation energies in terms of local and neighbouring atom contributions. Both the former and the latter contain charge dependent terms (Eqn. 3.1),

$$E_A^{relax}(mol) = E_A^{contr}(mol) + E_A^{flow}(mol) \qquad \ldots (3.1)$$

where $E_A^{relax}(mol)$ is the total molecular relaxation energy for an ionization in the core of atom A, $E_A^{contr}(mol)$ is the relaxation energy arising from the contraction of the local electron density around the centre A as a result of the increasing electron-nuclear attraction and $E_A^{flow}(mol)$ is the additional relaxation energy which originates from the charge distribution in the whole molecule. Gelius and Siegbahn[98,125] have further shown from the work of Snyder[126] that $E_A^{contr}(mol)$ may be further expressed as

$$E_A^{contr}(mol) = kq_A + \ell_A \qquad \ldots (3.2)$$

where q_A is charge on atom A in the neutral molecule, k is constant and ℓ_A is the relaxation energy due to orbital contraction around the neutral atom. As is evident from equation (3.2) the potential model as given in equation (2.42) does indeed take this reorganization term into account since parameters k and ℓ are adjustable and are obtained from a least squares fit involving theoretically calculated charge distribution binding energies.

For C_{1s} levels another feature which is of interest is the variation of relaxation energy in going from what may be formally described as carbon in sp^3 to sp^2 and sp hybridization. The series which have been studied are displayed in Table 3.5a. The data in Table 3.5a show that there is a consistent increase in relaxation energy in going from carbon in sp to sp^3 and sp^2 environments. This is true for both primary and secondary carbons in both mono and disubstituted species. Electronic relaxation, as was noted above, depends on the amount of electronic cloud associated with it and also on its mobility. Carbons in sp^2 environment might be expected to be particularly favourable in this respect since they are surrounded by a substantial electron density which partly consists of mobile π electrons.

Table 3.5b shows shifts in relaxation energy for primary and secondary carbons at sp, sp^2 and sp^3 environments. The shifts are again consistent, and indicate that as the number of fluorine atoms attached to a carbon centre increases (regardless of its hybridization) relaxation energy for both primary and secondary carbons decreases.

There has been a previous discussion in the literature in the particular case of the fluoromethanes of the relative constancy of the relaxation energy as a function of increasing number of fluorine substituents.[119] In this case the constancy was attributed to the cancellation of charge dependent terms arising from local and nearest neighbour charge distirbutions. For the particular case of the simple fluoro-substituted ethanes a similar analysis has been pursued. The data are collected in Table 3.6. Considering firstly the effect of substituents on the $\underline{C}H_3$ core levels in proceeding from CH_3 to CF_3 as substituent, the binding energy increases by 1.96 eV and the relaxation energy decreases by 0.19 eV. From Mulliken population analyses the changes in valence electron population in going from neutral molecule to the hole state have been computed for both the atom on which the core hole

Table 3.5a.

Shifts† in Relaxation Energy (eV) for Primary and Secondary Carbons at Different Electronic Environments

				Primary (α)		Secondary (β)			Primary (α)	Secondary (β)
CH_3-CH_3	0		CH_3-CH_2F	0		0		CH_3-CHF_2	0	0
$CH_2=CH_2$	0.26	(0.26)	$CH_2=CHF$	0.30	(0.30)	0.22	(0.22)	$CH_2=CF_2$	0.31	0.24
$HC\equiv CH$	-0.44	(-0.70)	$HC\equiv CF$	-0.39	(-0.69)	-0.43	(-0.65)			

Table 3.5b.

Shifts in Relaxation Energy (eV) for Primary and Secondary Carbons at Different Electronic Environments

	(Primary (α)		Secondary (β)			Primary (α)		Secondary (β)			Primary (α)	Secondary (β)
CH_3-CH_3	0		0		$CH_2=CH_2$	0		0		$HC\equiv CH$	0	0
CH_3-CH_2F	-0.14	(-0.14)	-0.07	(0.07)	$CH_2=CHF$	-0.1	(-0.1)	-0.11	(-0.11)	$HC\equiv CF$	-0.09	-0.06
CH_3-CHF_2	-0.21	(-0.07)	-0.13	(-0.06)	$CH_2=CF_2$	-0.16	(-0.06)	-0.15	(-0.04)			

† The values in brackets refer to successive shifts w.r.t. the preceding molecule.

Table 3.6.

Core	ΔBE	ΔRE	q	$\Delta(\Delta_{pop})^a$	$\Delta(\Delta n_i)^b$
$\underline{C}H_3-CH_3$ [c]	(0)	(0)	-0.061	(0)	(0)
$\underline{C}H_3-CFH_2$	0.6	-0.07	-0.116	+0.026	+0.004
$\underline{C}H_3-CF_2H$	1.26	-0.13	-0.164	+0.048	-0.005
$\underline{C}H_3-CF_3$	1.96	-0.19	-0.209	+0.060	-0.021
$\underline{C}FH_2-CH_3$	2.96	-0.14	0.439	-0.033	+0.029
$\underline{C}F_2H-CH_3$	6.04	-0.21	0.905	-0.088	+0.089
$\underline{C}F_3-CH_3$	9.13	-0.19	1.344	-0.169	+0.183

ΔBE - shift in binding energies

ΔRE - difference in relaxation energy

q - charge on $\underline{C}$ in neutral molecule

a - Δ_{pop} = el.pop $\underline{C}^*$ - el.pop $\underline{C}$ (-ve indicates increased flow of electronic charge)

b - Δn_i = sum over bonded atoms (pop X* - pop X)

c - Δ_{pop} = -1.074, Δn_i = 0.773

is located and the nearest neighbour atoms. There is little change across the series in population of this carbon atom in the neutral molecule. In going to the hole state, whilst the change in nearest neighbour populations is effectively constant, there is considerably less electron flow in the case of CF_3 as substituent than for CH_3 and the relaxation energy decreases. By contrast the effect of methyl substituent in the series CF_nH_{3-n} - CH_3 is such that the change in population at the atom concerned and on the nearest neighbours are similar in magnitude and opposite in sign. The large decrease in population in the neutral molecule however results in the smaller calculated relaxation energies in accord with equation (3.2).

(c) Relaxation Consequent upon Ionizations of N_{1s}, O_{1s} and F_{1s} Levels.

In Figures 3.2 and 3.3 are shown similar plots of differences in relaxation and shifts in binding energies for some N, O, and F core hole states with the data for carbon included for comparison. Although for the C_{1s} levels there is a clear correlation between the two (as was previously discussed) for the N_{1s}, O_{1s} and F_{1s} core levels the relationship is less clear cut. Of some interest however is the change in slope for the core hole states of O and F. This can be most simply rationalized by consideration of a prototype system MX-Y where the core hole on X is being investigated as a function of change in substituent Y (with M remaining unchanged). Thus when the effective electronegativity of Y is greater than X there is a decrease in relaxation energy with an increase in binding energy and vice-versa with the effective electronegativity of Y less than X. This has been investigated for the C, N, O and F holes with a similar range of substituents by means of a population analysis, the results of which are shown in Table 3.7. For the neutral molecules the effect of the very electronegative fluorine is to polarize the valence electrons. In going to the F_{1s} hole state then there is a less effective increase in polarising

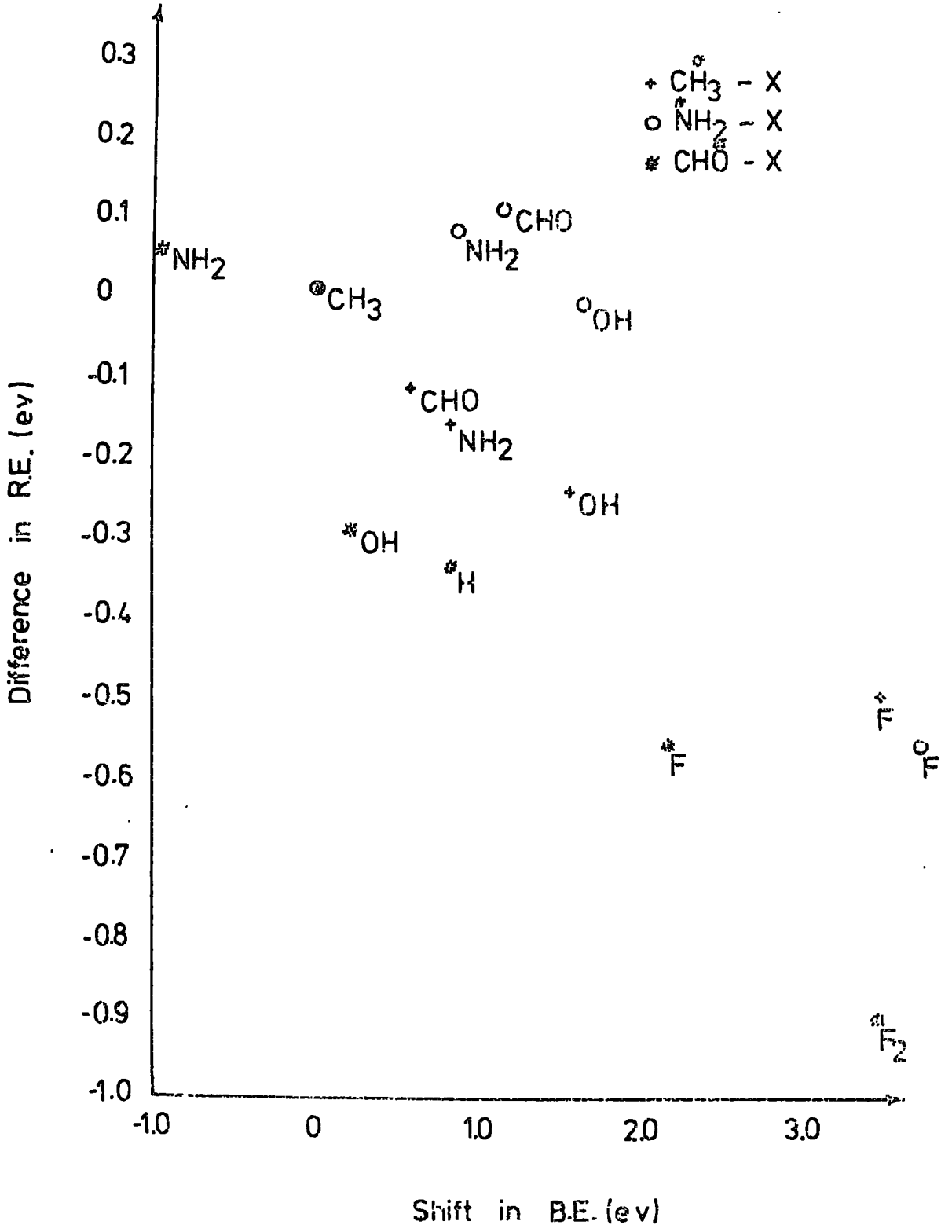

Fig. 3.2.

Plot of computed differences in relaxation energy versus shifts in binding energy (both w.r.t. CH_3 substituent as standard) for some C_{1s}, N_{1s}, O_{1s} levels.

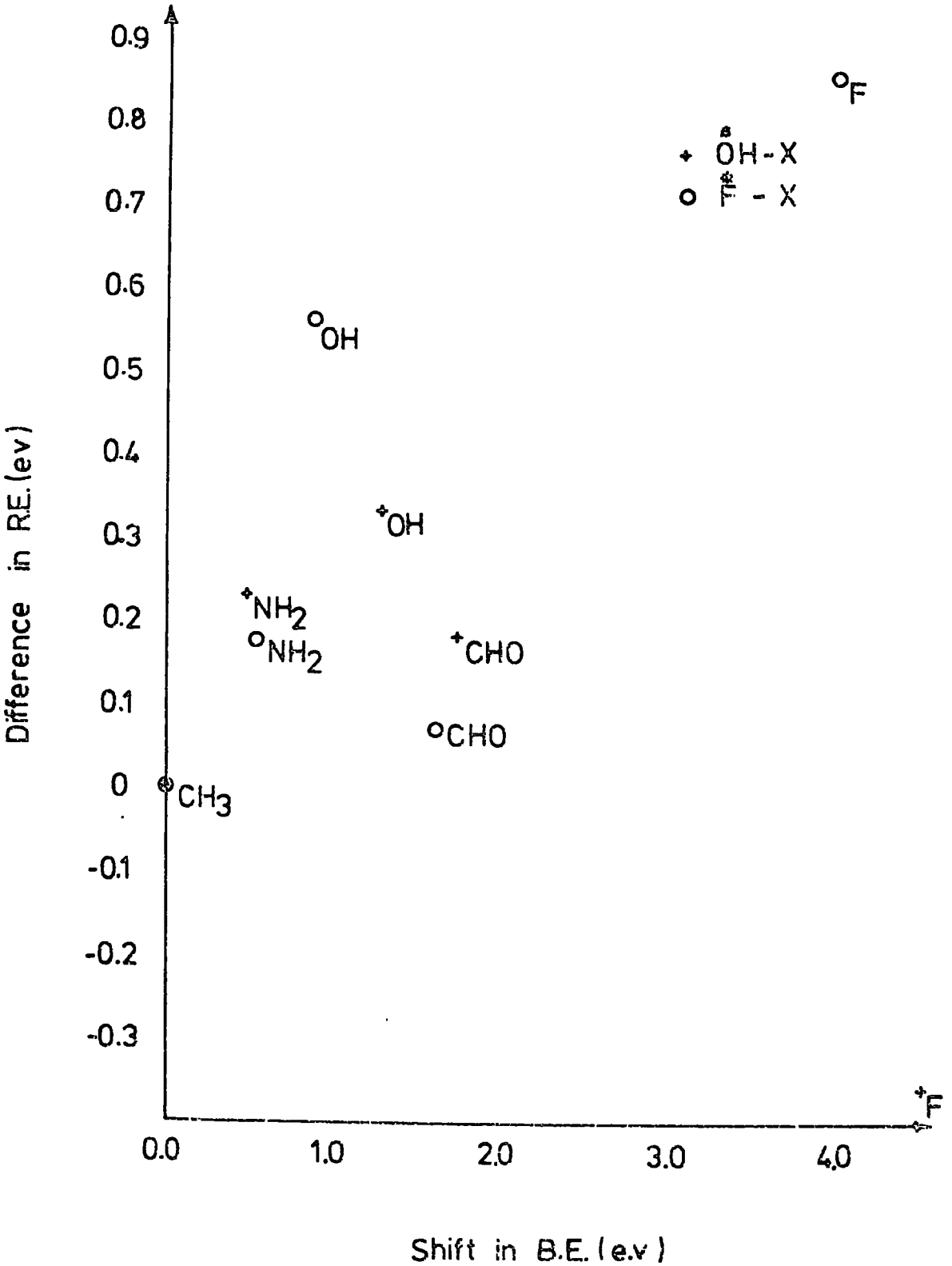

Fig. 3.3.

Plot of computed differences in relaxation energy versus shifts in binding energy (both w.r.t. CH_3 substituent as standard) for some O_{1s} and F_{1s} levels.

Table 3.7.

Substituent Effects on Reorganization Energies and Electronic Charge

Core	ΔRE	q	$\Delta(\Delta_{pop})$
$\underline{CH_3}$-H	-0.46	-0.146	+0.026
$\underline{CH_3}$-CH_3 [a]	(0)	-0.061	(0)
$\underline{CH_3}$-CHO	-0.12	-0.093	+0.052
$\underline{CH_3}$-NH_2	-0.16	-0.027	-0.066
$\underline{CH_3}$-OH	-0.25	0.029	-0.099
$\underline{CH_3}$-F	-0.50	0.331	-0.043
$\underline{NH_2}$-H	-0.63	-0.409	+0.024
$\underline{NH_2}$-CH_3 [b]	(0)	-0.287	(0)
$\underline{NH_2}$-CHO	0.10	-0.206	+0.063
$\underline{NH_2}$-NH_2	0.07	-0.288	-0.050
$\underline{NH_2}$-OH	-0.01	-0.278	-0.085
$\underline{NH_2}$-F	-0.56	0.039	-0.055
$\underline{OH}$-H	-1.06	-0.419	+0.078
$\underline{OH}$-CH_3 [c]	(0)	-0.276	(0)
$\underline{OH}$-CHO	0.14	-0.177	+0.021
$\underline{OH}$-NH_2	0.24	-0.261	-0.056
$\underline{OH}$-OH	0.33	-0.233	-0.100
$\underline{OH}$-F	-0.36	0.033	-0.105
$\underline{F}$-H	-1.42	-0.489	+0.085
$\underline{F}$-CH_3 [d]	(0)	-0.483	(0)
$\underline{F}$-CHO	0.07	-0.405	-0.001
$\underline{F}$-NH_2	0.18	-0.395	-0.087
$\underline{F}$-OH	0.56	-0.307	-0.166
$\underline{F}$-F	0.86	0.0	-0.311

[a] Calculated absolute relaxation energy is 11.42 eV

[b] Calculated absolute relaxation energy is 14.18 eV

[c] Calculated absolute relaxation energy is 16.40 eV

[d] Calculated absolute relaxation energy is 19.48 eV

power from the core ionized fluorine atom and a similar decrease in electronic flow to this centre is observed. The flow will be smallest when the effective electronegativity of the substituent is lowest, and from the form of Figs. 3.2 and 3.3 will be in the opposite sense to the trend exhibited by the C_{1s} levels and hence contribute more to the relaxation energy. This is apparent for the O_{1s} levels where with Y < X a positive slope is observed which is reversed for the very electronegative F. It is of interest to note that whilst the carbonyl oxygen exhibits considerably larger differences in relaxation energies (than for the comparable HOX series) the correlation with shift in binding energy is closely linear and the slope negative. This is understandable on the basis that the combined effective electronegativity of the =CHX group is consistently less than that of oxygen. Table 3.8 exhibits the results of Mulliken population analysis on the remainder of the molecules studied.

It is of a considerable interest that for the series HX and X_2 (X = CH_3, NH_2, OH, F) the relaxation energy differences [RE(X_2) - RE(HX) 0.46, 0.70, 1.39. 2.28 eV] are comparable to the calculated differences in binding energy [BE(X_2) - BE(HX) - 0.23, 0.10, 0.30, 1.8 eV]. This supports the suggestion by Jolly and Perry[1.27] that the former energies may account for the small observed shifts in the analogous species with X = Cl, Br in comparison with X = F and this will be investigated in the final section of this chapter.

Table 3.8.

Substituent Effect on Flow of Electronic Charge Consequent Upon Core Electron Ionization

Core	Δ pop^{TOTAL} [a]	Δ pop^{SIGMA} [b]	Δ pop$^{\pi}$ [c]	Δn_i [d]
$\overset{*}{C}H_3-CH_3$	-1.074	-	-	0.773
$\overset{*}{C}H_3-H$	-1.048	-	-	1.048
$\overset{*}{C}H_3-NH_2$	-1.140	-	-	0.955
$\overset{*}{C}H_3-OH$	-1.173	-	-	1.081
$\overset{*}{C}H_3-F$	-1.116	-	-	1.116
$H_2\overset{*}{C}=CH_2$	-1.050	-0.564	-0.487	0.770
$H_2\overset{*}{C}=NH$	-1.100	-0.662	-0.438	0.970
$H_2\overset{*}{C}=O$	-1.106	-0.745	-0.361	1.106
$HF\overset{*}{C}=O$	-1.120	-0.754	-0.366	1.120
$H\overset{*}{C}\equiv CH$	-0.820	-0.230	-0.590	0.694
$H\overset{*}{C}\equiv CF$	-0.801	-0.249	-0.552	0.614
$F\overset{*}{C}\equiv CH$	-0.897	-0.301	-0.596	0.731
$H\overset{*}{C}\equiv N$	-0.861	-0.394	-0.466	0.861
$\overset{*}{N}H_2\equiv CH_3$	-0.797	-	-	0.427
$\overset{*}{N}H_2-H$	-0.782	-	-	0.782
$\overset{*}{N}H=CH_2$	-0.887	-0.341	-0.546	0.564
$\overset{*}{N}\equiv CH$	-0.786	-0.079	-0.708	0.786
$\overset{*}{O}H-CH_3$	-0.632	-	-	0.170
$\overset{*}{O}H-H$	-0.554	-	-	0.554
$\overset{*}{O}H-F$	-0.736	-	-	0.736
$\overset{*}{O}=CH_2$	-0.740	-0.531	-0.209	0.740
$\overset{*}{O}\equiv C$	-0.691	-0.119	0.286	0.691

[a] Δ pop = el. pop X* - el. pop X (-ve indicates increased flow of electronic charge).

[b] Δ pop^{SIGMA} = sigma el. pop X* - sigma el. pop X.

[c] Δ pop$^{\pi}$ = π el. pop X* - π el. pop X.

[d] Δn_i = sum over bonded atoms (pop Z* - pop Z).

3.3. Estimation of Shifts in Binding Energies from Koopmans' Theorem and Relaxation Energy Corrections

We have stressed above the importance of electronic relaxation concomitant upon core ionization and that between certain core hole states there is an appreciable calculated error in their shifts if this is not taken into consideration. There appears however in these small molecules to be fairly systematic variations in the reorganization energies of a particular atom in similar environments which may be quite general for the nearest neighbour environment. The possibility then arises of making systematic corrections to core level ionization energies as calculated from Koopmans' theorem to estimate the core binding energies. This is of considerable importance for comparison with ESCA studies of larger molecules since computation with a basis set of comparable size would require considerable computer time if the individual core hole states were to be studied. As a suitably complex test case we have the studied biologically important 5-aza-uracil. Experimental studies[128] of core binding energies for an extensive range of pyrimidine bases has allowed, by direct correlation, an assignment of core binding energies in the order:

$$C_{1s} \quad C_2 > C_4 > C_6$$

$$N_{1s} \quad N_1 > N_3 > N_5$$

The charge potential model (CNDO/2 charges) and Koopmans' theorem correctly predict the ordering of N_{1s} levels, however the shifts between C_4 and C_6 is calculated to be small and in both cases in the opposite sense to that inferred from the experimental correlations. It should be emphasized of course that the measurements refer to the solid phase and that extensive hydrogen bonding may modify the pattern of binding energies that might be expected from the free molecule. This will be discussed in detail elsewhere.[129]

In studying relaxation energies as a function of structural type however, it is clear that significant differences in relaxation energies might be expected at different sites within the molecule. Direct hole state calculations (ΔSCF method) have therefore been carried out and, from the series of small molecules exhibiting the appropriate structural features, estimates have been made of differences in relaxation energies, which may be used as corrections to Koopmans' theorem. The results are presented in Table 3.9. The corrected Koopmans' theorem results are in excellent agreement with direct hole state calculations and in complete agreement with the experimentally determined ordering of C_{1s} and N_{1s} levels.

The agreement between the estimated and calculated binding energies by the ΔSCF method is most encouraging and therefore offers an alternative method for estimating binding energies in larger molecules consisting of H, C, N, O and F elements.

Table 3.9.

Shifts in Core Binding Energies (eV) in 5-Azauracil

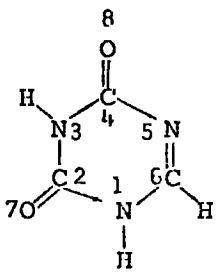

Core	Koopmans' Theorem	Hole State	Estimated RE	Estimated BE[a]
N1	2.08	2.52	-0.43[b]	2.51
N3	1.15	1.82	-0.43[b]	1.58
N5	(0)	(0)	(0)[c]	(0)
C2	0.83	1.70	-0.60[d]	1.43
C4	-0.19	0.54	-0.60[d]	0.41
C6	(0)	(0)	(0)[e]	(0)
O7	0.54	0.92		
O8	(0)	(0)		

[a] BE = Koopmans - RE

[b] Estimated from $\underline{NH}_2CHO$ (14.29)

[c] Estimated from $\underline{NH}{=}CH_2$ (14.72)

[d] Estimated from $NH_2\underline{C}HO$ (10.56)

[e] Estimated from $HN{=}\underline{C}H_2$ (11.16)

3.4. Investigation of Electronic Relaxations Accompanying Core Ionizations in the Series X_2 and HX (X = F, Cl, Br).

(a) Introduction.

We have noticed at the end of the Section 1.3. an interesting trend in relaxation energy differences for X_2 with respect to HX for the series X = CH_3, NH_2, OH and F for data pertaining to the C_{1s}, N_{1s}, O_{1s} and F_{1s} levels respectively. The calculated relaxation energy differences of 0.46, 0.70, 1.39 and 2.28 eV for this series closely parallel the calculated differences in core binding energies -0.23, 0.10, 0.30 and 1.8 for X = CH_3, NH_2, OH and F respectively. These trends might naively be interpreted in terms of simple electronegativity arguments in that the greater the electronegativity difference between H and X and the smaller the polarizability of X (being both a substituent and the atom on which the core hole is located) the larger we might expect the relaxation energy difference between HX and X_2 to be.

Jolly and Perry[127] have investigated differences in relaxation energies arising from core ionization in germanium compounds by a combination of ESCA, Auger spectroscopy and theoretical analysis of model systems. On the basis of these investigations the suggestion has been made[127] that in the series X_2, HX (X = F, Cl, Br) the small shifts in core binding energies for chlorine and bromine compared to fluorine arise from a much larger difference in relaxation energy for X_2 with respect to HX. On the basis of the work presented in the previous section this suggestion would seem to be implausible, since we would expect even on the grounds of a simplistic rationalization that the relaxation energy difference between X_2 and HX would be in the order X = F > Cl, Br.

To investigate this situation ab initio calculations have been carried out on the series X_2, HX (X = F, Cl, Br) for the neutral molecules and hole

states in an attempt to resolve ambiguities in the interpretation of the relevant experimental data. Additional points of interest which have arisen from this work are a comparison of atomic versus molecular relaxation energies and the investigation of shifts in core binding energies for different core levels of the same element.

(b) Computational Details.

Two series of calculations have been carried out. Firstly for F_2, HF, Cl_2 and HCl computations were performed on the neutral molecules and core hole states with double zeta Slater basis sets with Clementi's best atom exponents[28] and using the ATMOL adaptation of Stevens' integral package. Secondly to enable a direct comparison to be made with bromine compounds, calculations were carried on the complete series (X_2, HX, for X = F, Cl, Br) with more restricted basis sets. Clementi's best atom exponents[20] were used for H, Cl and Br in STO 4 - 31G expansion whilst for fluorine an HF 4 - 31G expansion was employed. Polarization functions of d type on Cl and Br and p type on hydrogen were also used in STO 3G expansions. The d exponents for the halogens were estimated from Burns' rules[40] (the values obtained were 1.166 and 1.125 for Cl and Br respectively), whereas the value of 1.1 used by Pople[130] was taken for the p exponent of hydrogen.

The results detailed in the sub-sections to follow pertain to the experimental geometries[118] in each case.

(c) Double Zeta Calculations of Relaxations Accompanying Core Ionizations in F_2, HF, Cl_2 and HCl.

The calculated absolute binding energies and relaxation energies are given in Table 3.10. Both the absolute binding energies and shifts are in excellent agreement with experiment indicating the overall adequacy of the basis set. It is clear that the shifts in molecular core binding

Table 3.10.

Calculated Core Binding Energies and Relaxation Energies for F_2, HF, Cl_2 and HCl (in eV)

	Core level	Calculated B.E. (ΔSCF)	Exptl. B.E.	Calculated shift	Exptl. shift	R.E.	ΔRE
F_2	1s	696.04	696.7[b]	(0)	(0)	23.39	(0)
HF	1s	693.95	694.0[b]	-2.09	-2.7	20.78	-2.61
F	1s	-	-	-	-	22.0[a]	-1.39
Cl_2	1s	2822.63	-	(0)	(0)	31.9	(0)
	2s	278.54	278.7[c]	(0)	(0)	10.8	(0)
	2pσ	208.71	-	(0)	(0)	11.7	(0)
	2pπ	208.57	-	(0)	(0)	11.7	(0)
HCl	1s	2822.09	-	-0.54	-	30.5	-1.5
	2s	278.13	278.3[d]	-0.41	-0.4	9.4	-1.4
	2pσ	208.34	-	-0.37	-	10.3	-1.4
	2pπ	208.13	-	-0.44	-	10.3	-1.3
Cl	1s	-	-	-	-	30.7[a]	-1.2
	2s	-	-	-	-	9.3[a]	-1.5
	2pσ	-	-	-	-	10.4[a]	-1.3
	2pπ	-	-	-	-	10.4[a]	-1.3

[a] U. Gelius and K. Siegbahn, Faraday Discuss. Chemical Soc., 54 (1972).

[b] R.W. Shaw and T.D. Thomas, Chem. Phys. Lett., 22, 127 (1973).

[c] T.X. Carrol and T.D. Thomas, J. Chem. Phys., 60, 2186 (1974).

[d] W.B. Perry and W.L. Jolly, Chem. Phys. Letters, 23, 529 (1973).

energies are calculated to be closely similar for all core levels. The results do suggest however that small but subtle differences may be detectable in shifts in going from one core level to another and indeed recent high resolution studies tend to support this view.[60] The close similarity of the shifts is interesting however since it is clear in considering the core levels of chlorine that the binding energies and relaxation energies span a substantial range.

Considering now the changes in relaxation energies it is instructive to compare the results for the molecular species with those previously reported for the free atoms by Siegbahn and co-workers.[125,132] The results fit into a consistent pattern. Thus for both X = F and Cl the relaxation energies for HX and the atomic species are calculated to be lower than for X_2.[133]

For X = F the relaxation energy for HX is considerably lower than for the atom whilst for the less electronegative chlorine the corresponding energies are about the same. From Table 3.10 we see that the ratio of ΔRE to ΔBE for Cl_2 and HCl is much larger than the corresponding ratio for F_2 and HF. Therefore it would be correct to say that small changes in binding energies for Cl_2 and HCl are accompanied by large changes in relaxation energies to compare with F_2 and HF, but on an absolute scale it is clear that differences in relaxation energies and binding energies between Cl_2 and HCl (∿ 1.5, ∿ 0.5) are smaller than between F_2 and HF (2.6, 2.1) which is in accordance with our results for X_2 and HX (X = CH_3, NH_2, OH, F) reported in a previous section.

(d) Limited Basis Set Calculations of Relaxations Accompanying Core Ionizations in the Series F_2, HF, Cl_2 and HCl.

Since it did not prove computationally feasible to extend the double zeta Slater basis set calculations to Br_2 and HBr, for comparison purposes

more restricted computationally inexpensive basis sets have been employed as detailed above. This can be justified by the work of Clark and Adams[119] and further substantiated by the work presented in Sections 3.1. - 3.4. of this chapter which shows that absolute magnitude of binding and relaxation energies vary with the size of a basis set but the differences and trends in these quantities are much less subject to such variations.

The results of the calculations are shown in Table 3.11. It is clear that to varying degrees the absolute binding energies are over-estimated since the computed relaxation energies are too small. Shifts in core binding energies however are such that in the series X_2 - HX the computed and experimental shifts are overall in reasonable agreement, the order being F >> Cl > Br. Using the double zeta quality calculation on the fluorine and chlorine compounds as yardsticks it is evident that whilst the absolute magnitudes of relaxation energies are too small for the restricted basis sets, the differences in relaxation energies are well reproduced. It is therefore inferred from the data in Table 3.11 that the relaxation energy differences for X_2 with respect to HX are in order F > Cl $\sim$ Br which seems chemically very reasonable.

Table 3.11.

Calculated Core Binding Energies and Relaxation Energies for F_2, HF, Cl_2, HCl Br_2 and HBr (in eV)

	Core level	B.E. (ΔSCF)	Shift	Exptl.	R.E.	ΔRE
F_2	1s	697.66	(0)	(0)	20.34	(0)
HF	1s	695.90	-1.76	-2.7	18.06	-2.3
Cl_2	1s	2834.32	(0)		13.1	(0)
	2s	277.98	(0)	(0)	8.2	(0)
	2pσ	209.79	(0)		8.6	(0)
	2pπ	209.64	(0)		8.6	(0)
HCl	1s	2834.07	-0.25		12.0	-1.1
	2s	277.70	-0.28	-0.4	7.2	-1.0
	2pσ	209.53	-0.26		7.6	-1.0
	2pπ	209.36	-0.28		7.6	-1.0
Br_2	1s	13283.00	(0)		8.9	(0)
	2s	1737.90	(0)		7.6	(0)
	2pσ	1580.88	(0)		7.8	(0)
	2pπ	1580.85	(0)		7.8	(0)
	3s	248.65	(0)		5.6	(0)
	3pσ	190.87	(0)		5.6	(0)
	3pπ	190.59	(0)		5.6	(0)
HBr	1s	13282.89	-0.12		7.9	-1.0
	2s	1737.91	-0.01		6.6	-1.0
	2pσ	1580.83	-0.05		6.8	-1.0
	2pπ	1580.80	-0.05		6.8	-1.0
	3s	248.58	-0.07	-0.1*	4.6	-1.0
	3pσ	190.80	-0.07		4.6	-1.0
	3pπ	190.53	-0.06		4.6	-1.0

* Reference d in Table 3.10. (It is not clear to which level this value refers).

CHAPTER IV

THEORETICAL INVESTIGATIONS OF POTENTIAL ENERGY SURFACES AND OF VIBRATIONAL FINE STRUCTURE RESULTING FROM CORE IONIZATIONS IN N_2 AND CO

Abstract.

Ab initio calculations have been carried out on CO and N_2 and relevant core hole states with different basis sets to investigate differences in potential energy surfaces (PES's), and in particular equilibrium geometries and quadratic force constants. From these calculations vibrational band profiles of the core level ESCA spectra for these molecules have been interpreted, obviating the need to rely on data pertaining to the equivalent core species. The agreement with experimental profiles is found to be excellent. The O_{1s} levels of CO, which have not been subjected to detailed theoretical analysis previously, are predicted to show substantial vibrational fine structure in excellent agreement with recently acquired experimental data. The effect of temperature on the band profiles has also been considered. Theoretically derived core binding and relaxation energies of these systems have been investigated both as a function of basis set, and of internuclear distance. Density difference contours have been computed and give a straightforward pictorial representation of the substantial electronic reorganizations accompanying core ionizations. Small basis sets with valence exponents appropriate to the equivalent core species when used in hole state calculations describe bond lengths, force constants, core binding and relaxation energies with an accuracy comparable to that appropriate to the corresponding extended basis set calculations.

4.1. Introduction.

The advent of high resolution ESCA instrumentation incorporating efficient X-ray monochromatization has recently revealed for the first time vibrational effects accompanying core ionization.[60,77,79,134,135] The most detailed experimental and theoretical studies to date relate to CH_4, N_2 and CO.[60,77,79,134,135] The experimental data pertaining to photoionization of the C_{1s} and N_{1s} core levels in these systems have been interpreted semi-quantitatively in terms of computed Franck-Condon factors with vibrational frequencies and bond lengths being derived from experimental data of neutral and equivalent cores species.[60,77,79] However previous theoretical studies indicate that although in general the bond lengths and force constants for equivalent core and hole state species are closely similar, nonetheless small but significant differences are apparent.[136,137] Detailed theoretical investigations therefore of PES's for core ionized species in the particular case of N_2 and CO would appear to be particularly appropriate at this time. For these simple systems the possibility exists of a detailed non-empirical study incorporating an investigation of the basis set dependence of the computed parameters. This chapter contains a survey of such an investigation together with the results of calculated equilibrium bond lengths and force constants for neutral molecules and hole states, absolute vertical and adiabatic binding energies and electronic reorganizations accompanying core ionizations.

The theoretically computed force constants and equilibrium bond lengths have then been used to calculate Franck-Condon factors and hence band profiles for the core ionized states of CO and N_2.

In the previous chapter we have discussed in detail the dependence of electronic relaxation energies for core ionized species on the detailed electronic structure of the molecular system. In continuation of such

investigations the relaxation accompanying core ionizations for N_2 and CO has been studied by means of density difference contours which lead to a straightforward physical interpretation of the computed changes in bond lengths for the core ionized species.

4.2. Computational Details.

Calculations have been carried out within the Hartree-Fock formalism since we have pointed out in the first two chapters that changes in correlation energy are relatively unimportant in discussing equilibrium bond lengths, force constants and binding energies for core levels of first row elements. Non-empirical LCAO MO SCF calculations have therefore been carried out on PES's for ground and hole states and equivalent core species. The calculations have been performed using the ATMOL system of programs implemented on an IBM 370/195. The basis sets employed were as follows:

1) STO 4-31G[24] and HF 4-31G[25] using best atom exponents;[20]
2) double zeta Slater using best atom exponents;[28]
3) extended Slater basis set which we refer to as triple zeta Slater, using best atom exponents;[31]
4) for hole states STO 4-31G and HF 4-31G with valence exponents appropriate to the equivalent core species which we refer to as optimized basis sets.

The motivation for employing the basis sets described in (4) was supplied by the results in the preceding chapter which show that the partial optimization of exponents yields absolute binding energies in excellent agreement with experiment at a relatively small computational expense thus creating a viable alternative to carrying out extended basis set calculations.

In addition comparable 'optimized' double zeta basis sets were investigated and the relevant observations are discussed in a later section.

4.3. Investigations of Potential Energy Surfaces.

As a preliminary to studying the PES's (in particular equilibrium geometries and harmonic force constants) for the core ionized species, an investigation has been made of both the neutral molecules and equivalent core species. The procedure adopted in each case was to start from the experimental geometries and compute parabolas from a grid corresponding to an extension or compression of 0.1 A.U. A process of successive refinements was then carried out in which the minima were taken as starting points and the intervals were decreased to final values of 0.01 A.U. which corresponded to a minimum of ten calculations. In the particular case of CF^+ the starting geometry appropriate to the minimized CO^+ oxygen hole state (discussed further on) was employed. The calculated bond lengths as a function of basis set are compared with the experimental values in Table 4.1. Considering firstly CO and N_2 it is clear that even at the STO 4.31G level the equilibrium bond lengths are quite accurately reproduced (within $\sim$ 3%). This is also true for NO^+ and by extrapolation for CF^+.

Having computed energy minima for these systems it is clearly of some importance to establish that the shape of the potential energy curve in the vicinity of the minima is also adequately described. In each case the potential surface in the region corresponding to extension or compression by $\sim$ 0.15 A.U. was examined and fitted to a parabola. This involved the computation of a few extra points such that a minimum of 15 points were available for each curve. For this purpose only the STO 4-31G and triple zeta basis sets were investigated.

Table 4.1.

Geometries of N_2, CO, NO^+, CF^+ Corresponding to Minimum Energies (in Atomic Units) and Respective Force Constants (in Millidynes per Angstrom)

Basis	Re_{N_2}	Re_{CO}	Re_{NO^+}	Re_{CF^+}	ΔRe (N_2-NO^+)	ΔRe $(CO-NO^+)$	ΔRe $(CO-CF^+)$	Ke_{N_2}	Ke_{CO}	Ke_{NO^+}	Ke_{CF^+}
HF 4-31G	2.080	2.164	2.024	2.264	0.056	0.139	-0.100	-	-	-	-
STO 4-31G	2.124	2.167	2.050	2.220	0.074	0.116	-0.053	28.10	22.10	-	-
Double Zeta	2.082	2.155	2.058	2.306	0.024	0.098	-0.151	-	-	-	-
Triple Zeta	2.047	2.123	1.983	2.218	0.064	0.140	-0.095	25.10	19.46	28.90	12.71
Experimental	2.074[a]	2.132[a]	2.007[a]	-	0.067	0.125	-	22.96[b]	19.00[b]	24.85[c]	-

[a] reference 118.

[b] G. Herzberg, Spectra of Diatomic Molecules, 2nd Edn. (1950).

[c] Yu.Ya.Kharitonov, Izv. Akad. Nauk. SSR, Otd. Khim. Nauk, 1953 (1962).

The derived force constants are also given in Table 4.1. (Figure 4.1 for example shows the computed potential energy curves for N_2 with the triple zeta basis set and indicates that the harmonic approximation is extremely good in the region of small displacements.) As might be expected the small basis set tends to over-estimate the experimental force constants somewhat (by $\sim$ 25%) whilst the triple zeta basis set gives a more accurate representation. It is clear however that even the small basis set adequately reflects the steeper potential surface of N_2 with respect to CO. (Ratio of force constants calculated 1.27, experimental 1.21.)

Having established that to varying degrees of accuracy as a function of basis set the bond lengths and force constants for these ground state systems may be treated within the Hartree-Fock formalism, we may now proceed to investigate the hole states for N_2 and CO also as a function of basis set. The analysis for the N_{1s}, C_{1s} and O_{1s} localized hole states proceeded along the lines discussed above and the results are shown in Table 4.2.

Considering firstly the results for nitrogen, with the exception of the limited basis set HF 4-31G and STO 4-31G calculations with unoptimized exponents (viz. exponents appropriate to the neutral molecule), it is clear that a significant decrease in bond length is computed in going from the neutral molecule to the hole state. With valence exponents appropriate to the equivalent core species (e.g. O for the nitrogen with the core electron deficit) the limited basis set calculations are in good overall agreement with the triple zeta basis set results. This is also clear from the equivalent cores species (NO^+) itself where experimental data are available for direct comparison. The virtues of using computationally inexpensive basis set (at the 4-31G level) where for the core ionized species partial optimization of exponents is accomplished by taking cognizance of the

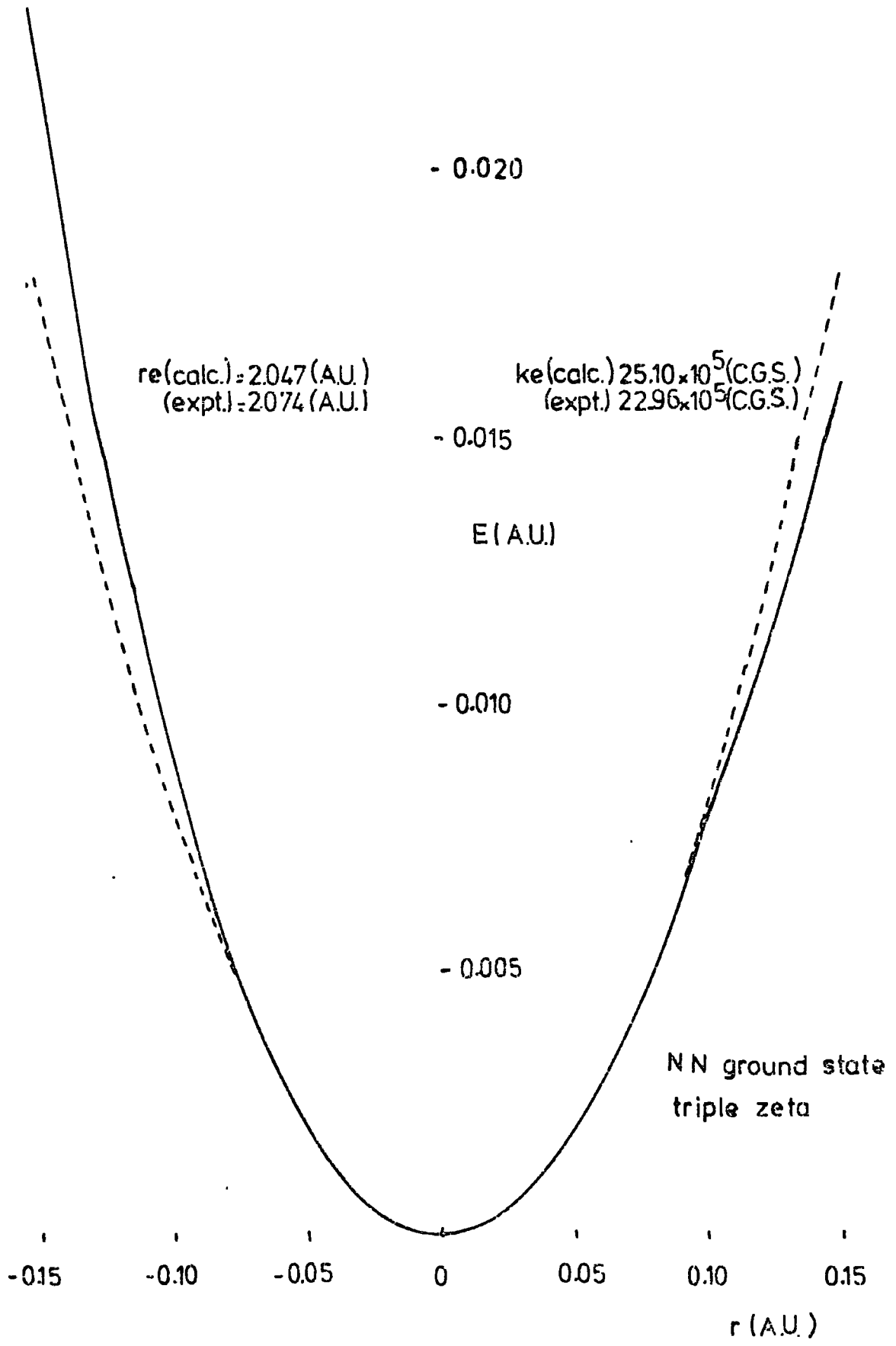

Fig. 4.1.

Potential energy curve for nitrogen molecule. The dashed curve represents the 'harmonic' parabola and was computed from the calculated force constant (Ke).

Table 4.2.

Geometries of $\overset{*}{N}_2$, $\overset{*}{CO}$ and $C\overset{*}{O}$ Corresponding to Minimum Energies (in Atomic Units) and Respective Force Constants (in Millidynes per Angstrom)

Basis	$Re\overset{*}{N}_2$	ΔRe $(N_2-\overset{*}{N}_2)$	$Re\overset{*}{CO}$	ΔRe $(CO-\overset{*}{CO})$	$Re\overset{*}{CO}$	ΔRe $(CO-\overset{*}{CO})$	$Ke\overset{*}{N}_2$	$Ke\overset{*}{CO}$	$Ke\overset{*}{CO}$
HF 4-31G	2.094	-0.014	2.104	0.060	2.316	-0.151	-	-	-
HF 4-31G (Opt.)	2.038	0.043	2.040	0.125	2.281	-0.116	-	-	-
STO 4-31G	2.121	0.004	2.107	0.060	2.266	-0.099	-	-	-
STO 4-31G (Opt.)	2.060	0.064	2.059	0.108	2.237	-0.070	30.70	30.70	15.05
Double Zeta	2.058	0.024	2.052	0.104	2.324	-0.168	-	-	-
Triple Zeta	2.002	0.045	2.010	0.113	2.230	-0.107	29.60	28.90	13.11

equivalent cores concept has been already discussed in relation to absolute binding energies. The work described in this Chapter would strongly suggest that the approach is also successful in describing changes in bond lengths and force constants (see later) accompanying core ionizations. It may be noted that the calculations consistently suggest that the bond length for the hole state is somewhat greater than for the equivalent cores species.

For C_{1s} and O_{1s} hole states of CO an interesting picture emerges in that calculations (independent of basis set) predict a decrease in bond length for the former and an increase for the latter with respect to the neutral molecule. The results for the small basis set calculations with optimized exponents are in very good overall agreement with the triple zeta basis set calculations. In this connection it is interesting to note that in general the 'optimized' small basis set calculations are in better overall agreement with the triple zeta calculations than are those from the double zeta basis set. This can almost certainly be traced to restrictions imposed by allowing only the coefficients to be determined variationally for systems which are strongly perturbed with respect to the ground state species and for which the exponents are essentially optimized.

The calculations again indicate (the sole exception being those for the double zeta basis set pertaining to the C_{1s} hole state) that the computed equilibrium geometries for the hole states are consistently larger than those for the equivalent core species. The comparisons for the small basis set calculations refer in each case to the 'optimized' exponents for the hole state species. This is of some importance in discussing vibrational effects accompanying core ionization and will become apparent in a later section. The discussion thus far should emphasize that limited basis set calculations provide a good description of changes in bond length accompanying

photoionization provided that for the core ionized species valence exponents appropriate to the equivalent core species are employed. If this 'partial optimization' of valence exponents is not invoked then bond length changes in general are typically predicted to be an order of magnitude too small and may also have the wrong sign. This is also clearly evident from recently published data.[138]

In order to make this point clearer we have investigated the relevant core hole states with STO 4-31G basis sets in which the 'best atom valence exponents' for the atom on which the core hole is located, have been varied. To start with we have considered the C_{1s} hole state of CO. Firstly 2p exponents have been varied (while 2s exponents have been fixed at their best atom value[20]) until a minimum for the binding energy was found at $\zeta_{2p} = 2.5$ (see Table 4.3). The same procedure has been repeated in which 2s exponents have been varied while 2p exponents have been fixed at their best atom value.[20] The minimum was found for $\zeta_{2s} = 1.9$ (see Table 4.3). However the use of these 'optimized valence exponents' yields BE = 295.53 eV which is slightly worse than the binding energy obtained with nitrogen valence exponents (see Tables 4.3 and 3.1).

This is not entirely unexpected since in going from an atom to a diatomic molecule the energy surface as a function of orbital exponents is orders of magnitude more complex. Thus whilst for atoms the corresponding surface is effectively partitioned such that exponents for e.g. 2s and 2p functions may be separately optimized, for a molecule changing an exponent of a σ type orbital on one atom can considerably effect the exponent for a π type orbital on the same atom because of the perturbation of the attached atoms. A complete multi-dimensional optimization is impracticable for all but the smallest systems (it would probably have been possible for the

Table 4.3.

Optimization of 2s and 2p Exponents of Carbon in CO at Experimental Geometry with the STO 4-31G Basis Set

Best carbon 2s exponent = 1.6083		Best carbon 2p exponent = 1.5679	
2p exponent	Be (eV)	2s exponent	BE (eV)
1.8	298.00	1.7	300.39
1.9	297.22	1.9	300.24
2.0	296.65	2.1	300.49
2.3	295.88	2.3	300.68
2.5	295.87	2.5	300.74
2.7	296.09	2.7	300.81

2s = 1.6083, 2p = 1.5679[a]	BE = 306.80 eV
2s = 1.9237, 2p = 1.9170[b]	BE = 296.71 eV

[a] Best atom exponents for carbon.

[b] Best atom exponents for nitrogen.

systems studied in this work given sufficient computer time), therefore a procedure for optimization of valence exponents has been invoked in which a plot of the best atom valence exponents[20] for carbon, nitrogen, oxygen and fluorine versus the atomic number allows a straightforward interpolation of the 2s and 2p exponents as a function of 'apparent' atomic number. The values determined in this way are displayed in Table 4.4. The absolute binding energies were then computed as energy differences between ground states and relevant hole states (ΔSCF method). For the former, neutral best atom exponents[20] were used whilst for the latter the 2s and 2p exponents were varied as a function of the 'apparent' atomic number as indicated in Table 4.4. In all cases calculations were performed at experimental geometries. Since the 2s and 2p exponents were both systematically varied whilst the exponents for the core orbitals were unchanged, we would not necessarily expect to obtain minima for the binding energies computed as energy differences. Indeed the results displayed in Fig. 4.2 clearly illustrates this. The important conclusion to be reached from such a study, however, is that for these small basis sets, in each case the calculated absolute binding energies with the valence exponents for the atom on which the core hole is located close to those appropriate to the equivalent cores species and are in close agreement with the experimentally determined values.

For this reason and because of the computational expense the detailed investigation of potential energy curves to obtain force constants was restricted to the 'optimized' STO 4-31G and triple zeta basis sets. The derived potential energy curves and force constants for both neutral molecules, core ionized and equivalent cores species are shown in Figures 4.3a and 4.3b.

Table 4.4.

Interpolated Values of 2s and 2p Best Atom Exponents as a Function of 'Apparent' Atomic Number

Apparent atomic number	2s Exponent	2p Exponent
6.0	1.6083	1.5679
6.2	1.670	1.640
6.4	1.735	1.705
6.6	1.800	1.772
6.8	1.862	1.840
6.9	1.896	1.872
7.0	1.9237	1.9170
7.1	1.960	1.940
7.2	1.992	1.975
7.4	2.058	2.040
7.6	2.120	2.104
7.8	2.185	2.170
7.9	2.216	2.201
8.0	2.2458	2.2266
8.1	2.280	2.270
8.2	2.310	2.300
8.4	2.375	2.365
8.6	2.440	2.430
8.8	2.501	2.496
8.9	2.533	2.527
9.0	2.5638	2.5500
9.1	2.598	2.591

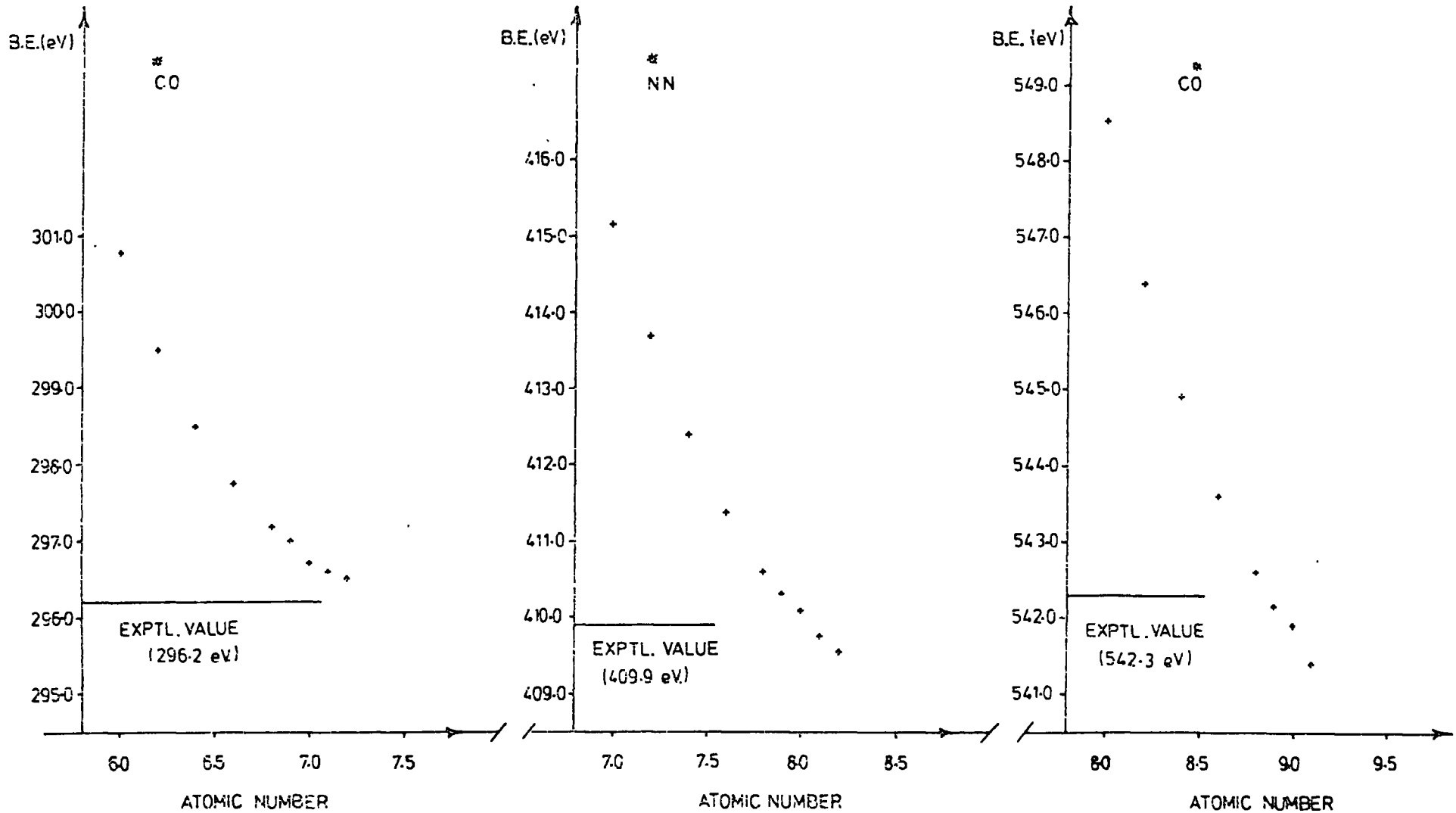

Fig. 4.2.

Plot of calculated (ΔSCF) binding energies for the core levels of CO and N_2 as a function of the valence exponents for the hole state species.

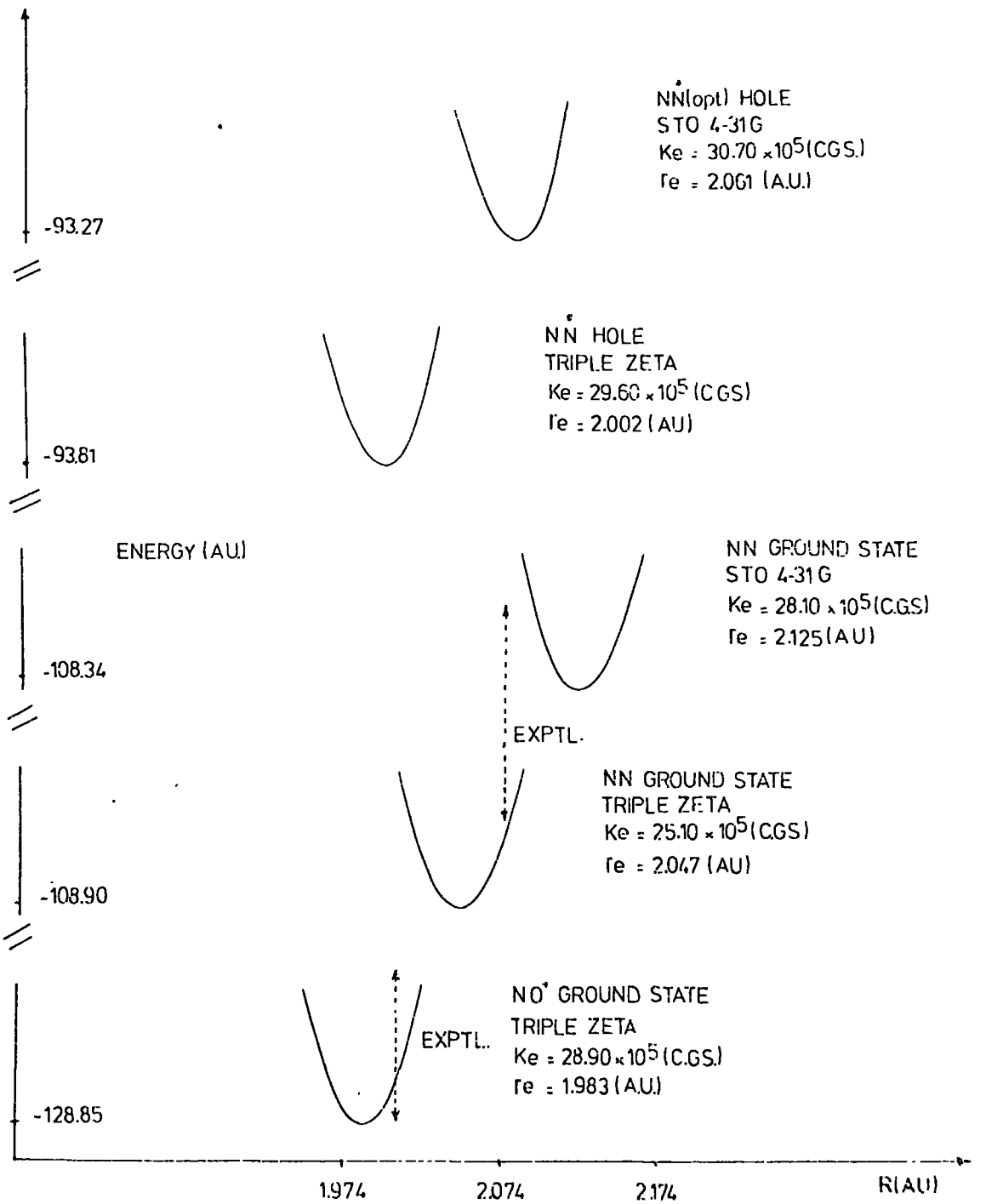

Fig. 4.3a.

Calculated potential energy curves, force constants (Ke) and equilibrium geometries (Re) for N_2^+, NN and NO with triple zeta and 'optimized' 4-31G basis sets.

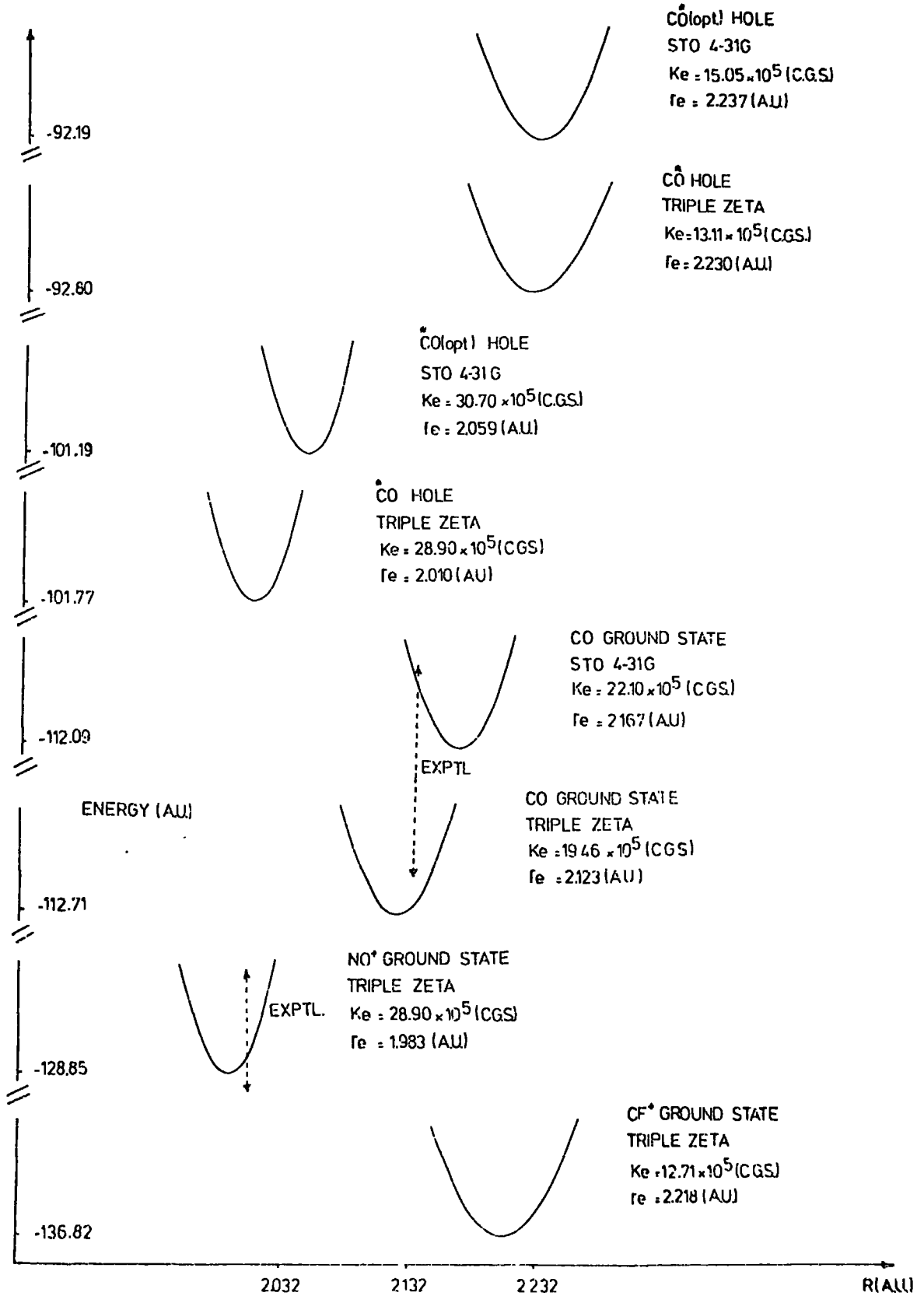

Fig. 4.3b.

Calculated potential energy curves, force constants (Ke) and equilibrium geometries (Re) for CO, CO^*, CO^+, NO^+ and CF^+ with triple zeta and 'optimized' 4-31G basis sets.

Considering firstly Figure 4.3a with the data corresponding to nitrogen, the computed decrease in equilibrium bond length for the core ionized species is seen to be accompanied by a relatively small change in force constant. Comparison of the triple zeta basis set calculations would suggest that the force constants for the hole state and equivalent cores species are essentially the same.

The situation with regard to carbon monoxide however is more complex (Figure 4.3b). For the carbon 1s hole state the decrease in bond length is accompanied by the expected increase in force constant, with potential curves being closely similar to that for the equivalent cores species.

For the O_{1s} hole state the potential energy well is considerably broader indicative of a greatly reduced force constant with respect to the neutral molecule.

These calculations overall would suggest therefore that to a first approximation changes in bond length and force constants in going from a neutral molecule to a given hole state are adequately described by considering the equivalent cores species. Depending therefore on whether there is a decrease or an increase in equilibrium bond length in going from the neutral molecule to a given core hole state the equivalent core model provides either an upper or lower bound respectively to the change in bond lengths and in each case provides a lower bound to the force constant.

4.4. Binding and Relaxation Energies.

(a) Binding Energies.

The wealth of data readily obtainable from the calculations on PES's described in the previous section allows a comprehensive analysis of both vertical and adiabatic core binding energies as a function of basis set and theoretical model. The results are displayed in Tables 4.5 and 4.6, where binding energies have been computed by the ΔSCF method, from Koopmans' theorem and from relaxed Koopmans' values (all these techniques have been discussed in some detail in Chapter II).

Considering firstly the data pertaining to nitrogen, it is clear that the calculated absolute binding energies are in good agreement with the experimental data provided a sufficiently flexible basis set is employed. The relaxed Koopmans' values closely parallel those derived from the hole state calculations as might have been expected. The calculated 'adiabatic' binding energies are virtually identical to the vertical values and this is of some relevance when we come to discuss the vibrational effects accompanying core ionizations.

It is interesting to note that with a medium size basis set (double zeta) the use of valence exponents appropriate to the equivalent core species for the core ionized system fortuitously leads to calculated core binding energies in almost exact agreement with those calculated using best atom exponents appropriate to the neutral atom, with neither being in particularly good agreement with experiment. This may be attributed to the mutual interaction between the two types of variational parameters viz. the coefficients and exponents.

A similar situation obtains for carbon monoxide with the results for the 'optimized' small basis sets being comparable with those for the triple zeta

Table 4.5.

Calculated Core Binding Energies for N_2*

Basis Set	Model†	N_{1s} Binding Energy (eV)†† Vertical (1)	Vertical (2)	Adiabatic
STO 4-31G	K	427.4	427.6	-
	Kr	415.1	415.1	415.1
	Δ	415.1	415.1	415.1
STO 4-31G(Opt.)	K	-	-	-
	Kr	411.8	411.8	411.9
	Δ	410.1	410.2	410.1
HF 4-31G	K	427.4	427.4	-
	Kr	414.4	414.3	414.3
	Δ	414.3	414.3	414.3
HF 4-31G(Opt.)	K	-	-	-
	Kr	410.4	410.5	410.4
	Δ	410.9	410.9	410.9
Double Zeta	K	428.6	428.7	-
	Kr	411.7	411.7	411.7
	Δ	412.6	412.6	412.6
Double Zeta(Opt.)	K	-	-	-
	Kr	411.8	411.8	411.8
	Δ	412.6	412.6	412.6
Triple Zeta	K	427.4	427.2	-
	Kr	410.0	409.9	410.0
	Δ	410.9	410.8	410.8

* Experimental value = 409.9 eV (reference number 77).

† K refers to Koopman's Theorem.
Kr refers to Relaxed Koopmans' Theorem viz. $\frac{1}{2}(\varepsilon + \varepsilon^*)$.
Δ refers to SCF calculations.

†† Vertical (1) and vertical (2) refer to binding energies calculated at the experimental and theoretically optimized equilibrium geometry of the ground state respectively.

Adiabatic refers to binding energies calculated as energy differences for the theoretically optimised ground state and hole state geomctries.

Table 4.6.

Calculated Core Binding Energies for CO**

Basis Set	Model†	C_{1s} Binding Energy (eV)†† Vertical (1)	Vertical (2)	Adiabatic	O_{1s} Binding Energy (eV) Vertical (1)	Vertical (2)	Adiabatic
STO 4-31G	K	309.1	309.2	-	564.5	564.5	-
	Kr	300.8	300.9	300.9	548.6	548.5	548.2
	Δ	300.8	300.9	300.8	548.5	548.4	548.2
STO 4-31G(Opt.)	K	-	-	-	-	-	-
	Kr	298.0	297.8	297.7	544.8	544.7	544.5
	Δ	296.7	296.9	296.6	541.9	541.9	541.8
HF 4-31G	K	310.6	310.8	-	562.0	562.0	-
	Kr	302.1	302.2	302.2	545.3	545.1	544.5
	Δ	302.0	302.0	302.0	544.9	544.8	544.4
HF 4-31G(Opt.)	K	-	-	-	-	-	-
	Kr	298.3	298.4	298.3	540.9	540.7	540.4
	Δ	298.1	298.3	298.0	541.6	541.5	541.1
Double Zeta	K	311.0	311.1	-	563.7	563.7	-
	Kr	298.8	298.9	298.7	542.6	542.5	542.0
	Δ	299.6	299.7	299.5	543.3	543.2	542.9
Double Zeta(Opt.)	K	-	-	-	-	-	-
	Kr	299.0	299.1	299.0	542.6	542.5	541.8
	Δ	299.8	299.9	299.8	542.8	542.7	542.4
Triple Zeta	K	310.0	310.0	-	562.8	562.8	-
	Kr	297.3	297.2	297.0	541.3	541.4	541.0
	Δ	298.1	298.1	297.8	542.0	542.0	541.9

** Experimental values for C_{1s} and O_{1s} holes are 296.2 eV and 542.3 eV respectively.[151]

basis sets. The substantial shortening of the bond length in going to the carbon 1s hole state is reflected in the significant differences that are apparent in the adiabatic and vertical calculated binding energies. It is interesting to note that for the double zeta basis sets the use of the equivalent core valence exponents yields slightly better results for the O_{1s} hole and slightly worse for the C_{1s} hole than employing the neutral best atom exponents. This is not unexpected on the basis of the data previously discussed for the nitrogen core hole.

(b) Relaxation Energies.

The calculated relaxation energies for the N_{1s}, C_{1s} and O_{1s} core levels as a function of basis set are shown in Figure 4.4. In each case the calculations refer to the experimentally determined equilibrium geometries of the neutral molecules. A striking feature of this data is the fact that the 'optimized' small basis set calculations give absolute values for the relaxation energies in good agreement with those calculated with extended basis sets. Although the small 'unoptimized' basis sets characteristically underestimate the total relaxation energy as has been pointed out in the preceding chapter, the trends in relaxation energies are well reproduced by comparison with the extended basis set calculations. Thus the slopes of the relaxation energy vs. change in atomic number are 4.3, 4.2, 4.6, 4.7, 4.6 and 4.6 for HF 4.31G, HF 4.31G (opt.), STO 4.31G, STO 4.31G (opt.), double zeta and triple zeta basis respectively. This reinforces the conclusion reached in the preceding chapter that whilst absolute values of relaxation energies are markedly basis set dependent, differences in relaxation energies are relatively insensitive to the basis set employed.

It is of some interest also to consider changes in relaxation energies as a function of the internuclear distance for the hole states considered

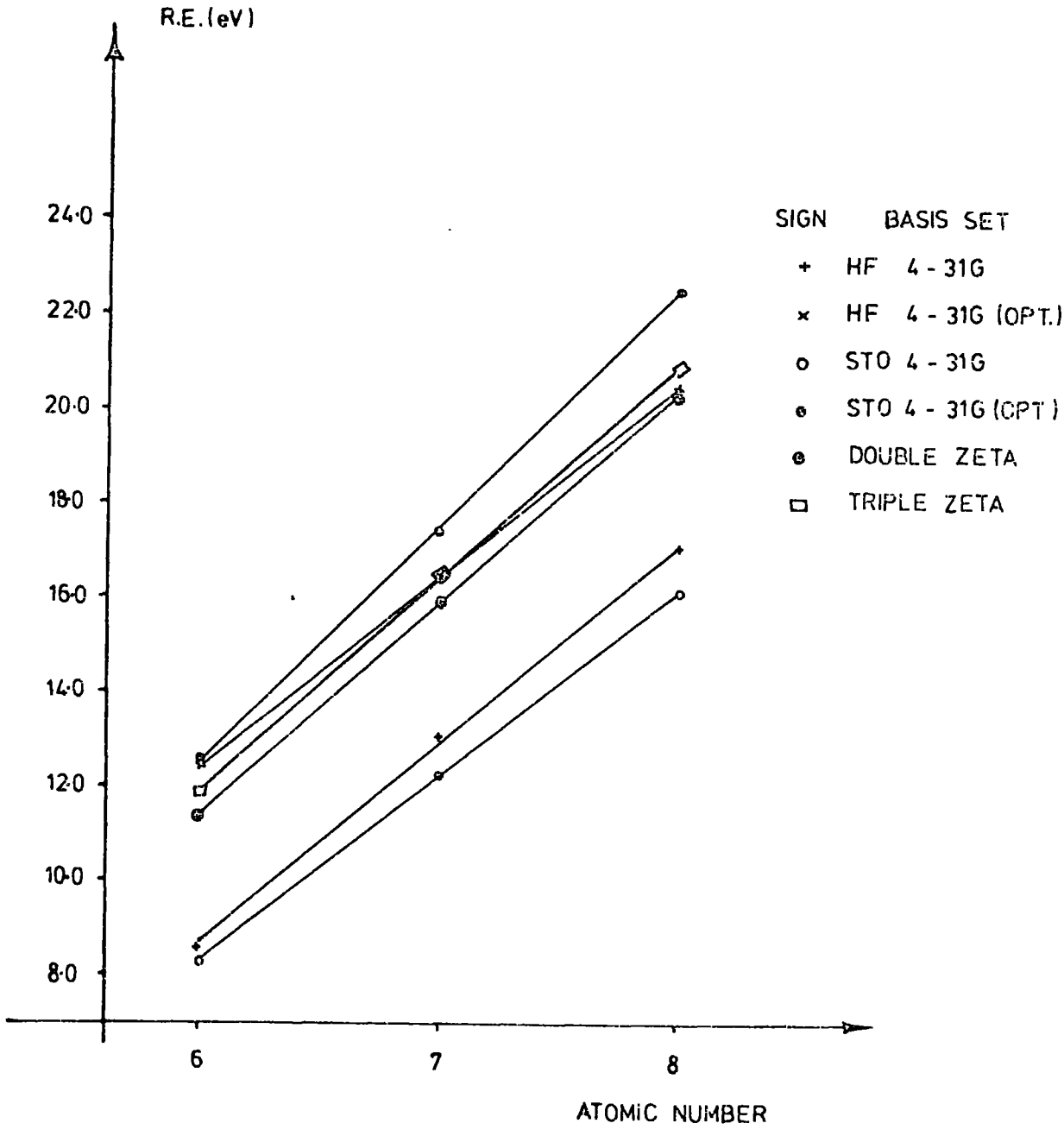

Fig. 4.4.

Plot of calculated relaxation energies as a function of basis set versus the atomic number of the element on which the core hole is localized.

in this work. Detailed investigations of this particular aspect have been carried out with double zeta quality basis sets and the results are displayed in Figure 4.5, where the reference in each case is with respect to the theoretically calculated equilibrium geometries for the neutral molecules. For these closely related systems for the C_{1s}, N_{1s} and O_{1s} holes the changes in relaxation energies are linear functions of the change in bond length with positive slopes (viz. relaxation energy increases with increasing bond length). It is clear however that in each case the changes in relaxation energies represent a small fraction of the total relaxation energies. The order of increasing slope of $C_{1s} < N_{1s} < O_{1s}$ follows the order of increasing total relaxation energies.

(c) Analysis of Electronic Relaxations Accompanying Core Ionizations by Means of Density Contours.

Valence electronic relaxations (reorganizations) accompanying core electron ionizations have been discussed in the preceeding chapter by Mulliken population analysis. Whilst a consideration of population analyses can provide a valuable qualitative picture of the substantial migrations in electron densities which occur on core ionization, the computationally more expensive analyses in terms of detailed density difference contour maps are even more revealing, since they provide a three dimensional picture of the relaxation phenomena. This has recently been demonstrated most effectively by Streitweiser and coworkers,[139] in the particular case of the C_{1s} and O_{1s} hole states of CO. Unfortunately the contours produced make it difficult to appreciate the substantial reorganizations of the electronic charge distribution in the bonding regions which are obviously of some considerable importance in discussing vibrational effects for the core hole states. In the present work density difference contours have been constructed using the ATMOL program package for analysis of molecular wavefunctions, and employing a double zeta basis set.

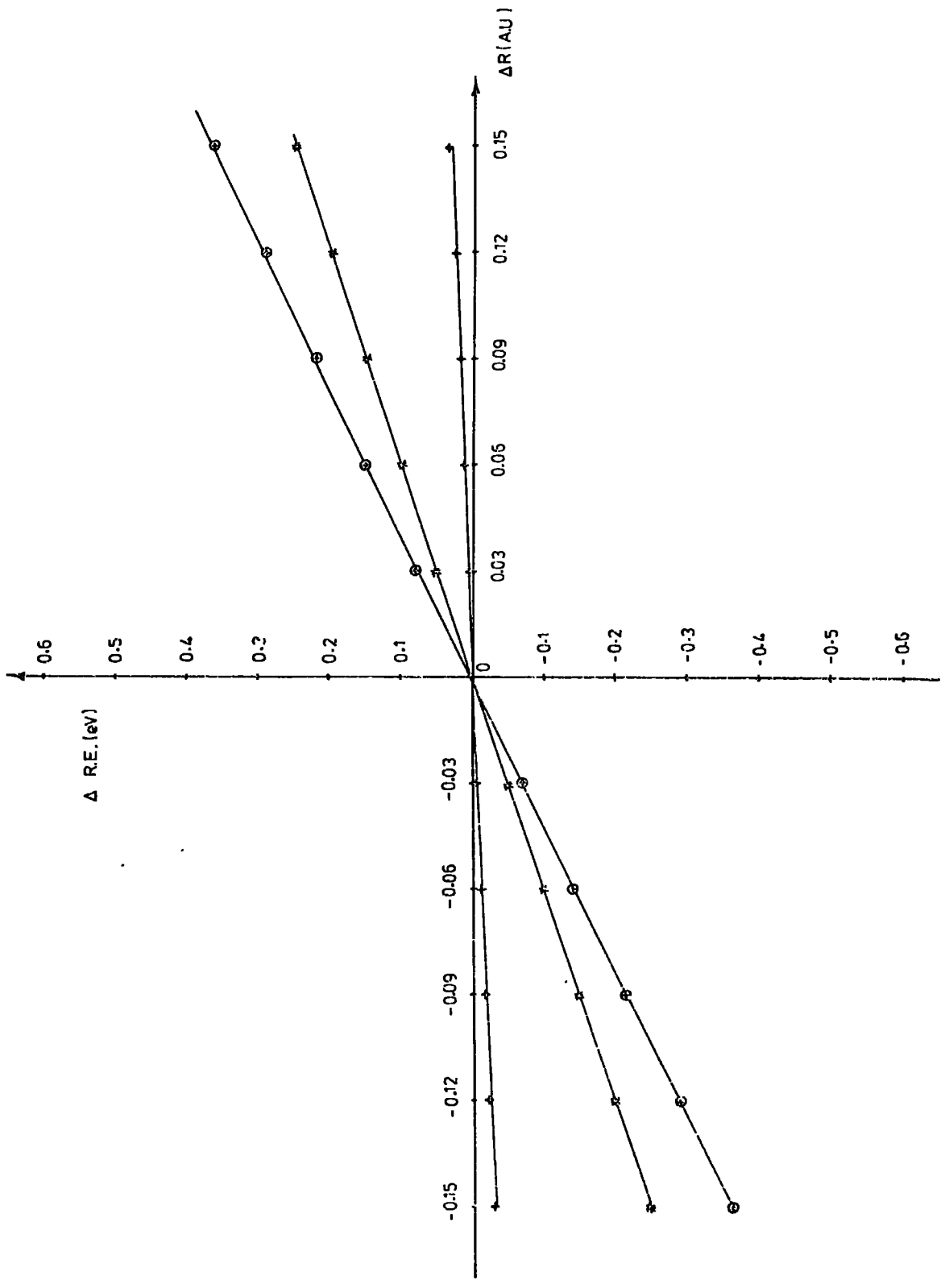

Fig. 4.5.

Plot of differences of relaxation energies for N_2 and CO versus internuclear distance.

⊕ refers to CO^* species.
* refers to N_2^* species.
† refers to CO^* species.

The areas studied were in each case divided into a mesh of 97 x 97 points, and the derived density difference grid was then used to compute the appropriate density difference contours. In computing the density difference contours the same geometries were used for both the ground state and relevant core hole states; these geometries corresponding in each case to those appropriate to the calculated equilibrium geometries of the neutral molecules using a double zeta basis set (2.082 A.U. for N_2 and 2.155 A.U. for CO).

The planes chosen most effectively to illustrate the relaxation phenomena are the molecular (XY) plane covering an area of 10 x 10 A.U. and the plane perpendicular to the molecular axis bisecting the molecule. This plane covered an area of 8 x 8 A.U.

The results for the N_{1s} core hole in N_2 and for the C_{1s} and O_{1s} holes in CO are displayed in Figures 4.6a, 4.6b and 4.6c.* In each case the solid lines correspond to an increase and the dotted contours to a decrease in electron density on going from the neutral molecule to the hole state.

Considering firstly the contours for the molecular planes, the extensive migration of electron density to the vicinity of the atom on which the core hole is located is clearly evident. It is also clear that

---

* Caption for Figures 4.6a, 4.6b and 4.6c.

Electron density difference contours for the hole states of N_2 and CO with respect to the neutral molecules. (The solid contours indicate an increase and the dotted a decrease in density in going from the neutral molecule to the hole state and the markers 'X' indicate the position of the nuclei.) Contours are given in units of (electron/Bohr^3).

A = -0·004
B = -0·008
C = -0·007
D = -0·014
E = +0·007
F = +0·014

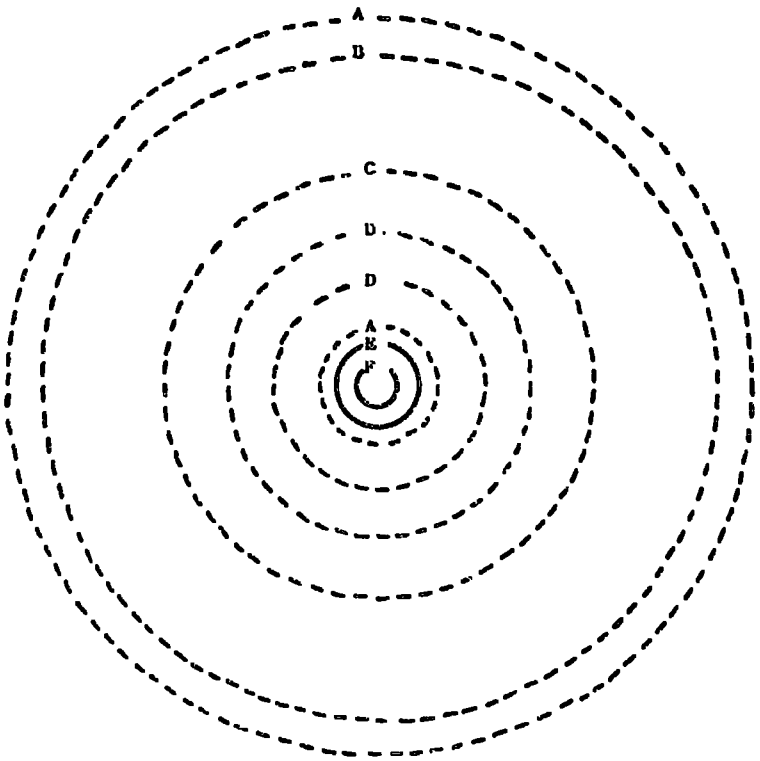

$(N\overset{*}{N})$ - (NN) MOLECULAR PLANE

A = -0·001
B = -0·007
C = -0·014
D = -0·028
E = -0·056
F = -20·0
G = +0·014
H = +0·056
I = +0·113

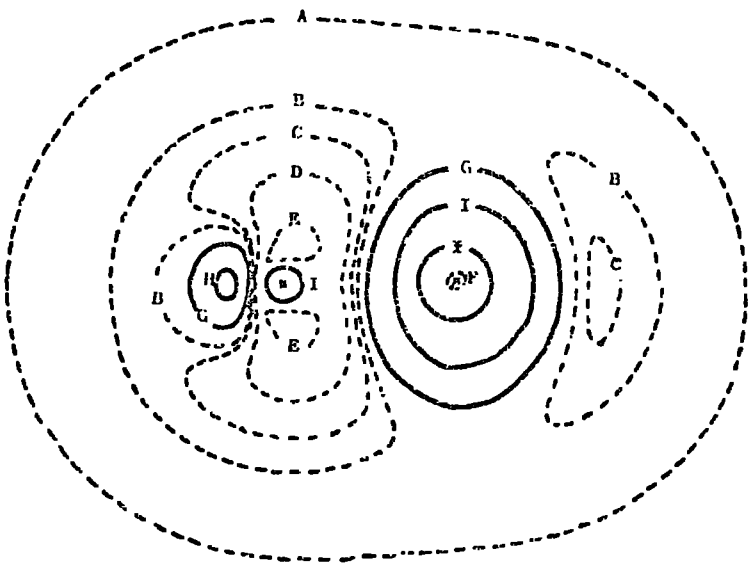

$(N\overset{*}{N})$ - (NN) PLANE ⊥ THROUGH THE CENTRE

Fig. 4.6a.

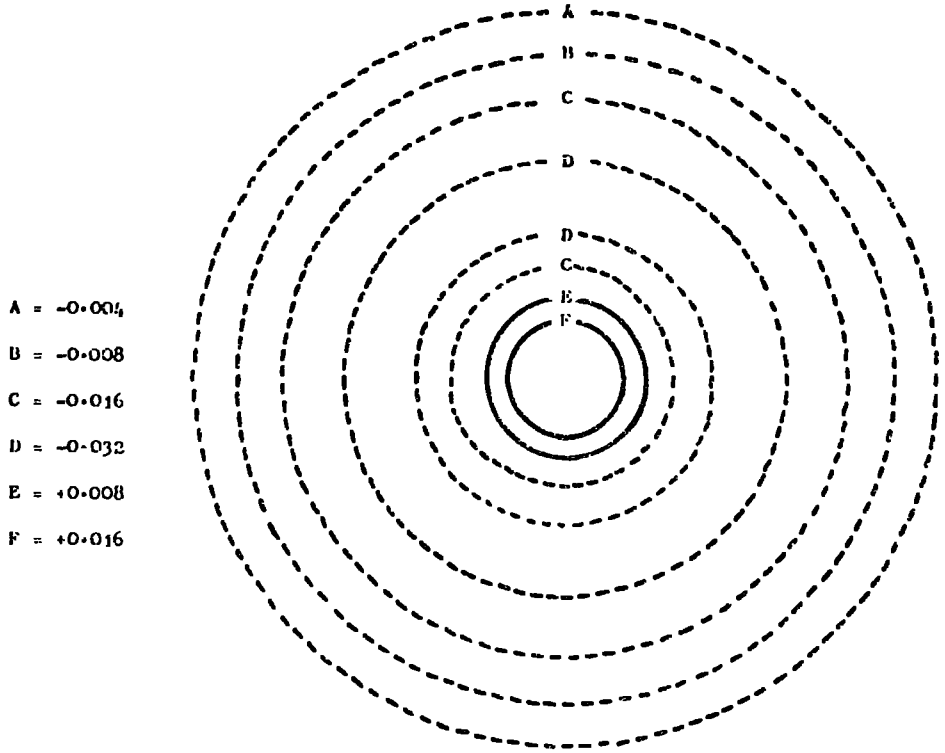

$(\overset{\bullet}{C}\,O)$-(C O) PLANE ⊥ THROUGH THE CENTRE

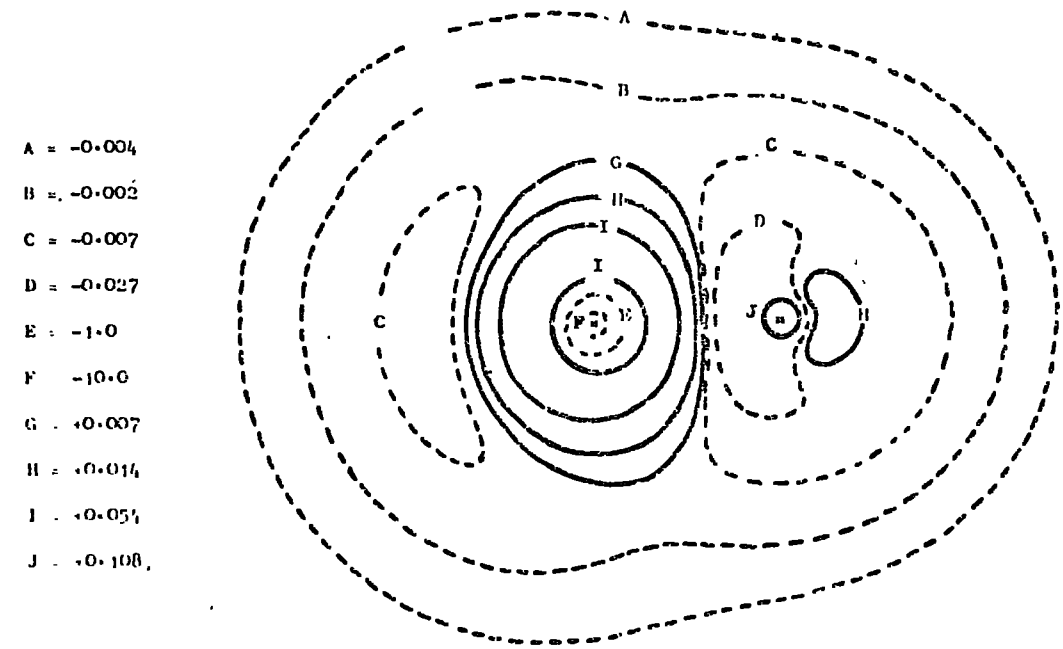

$(\overset{\bullet}{C}\,O)$ - (C O) MOLECULAR PLANE

Fig. 4.6b.

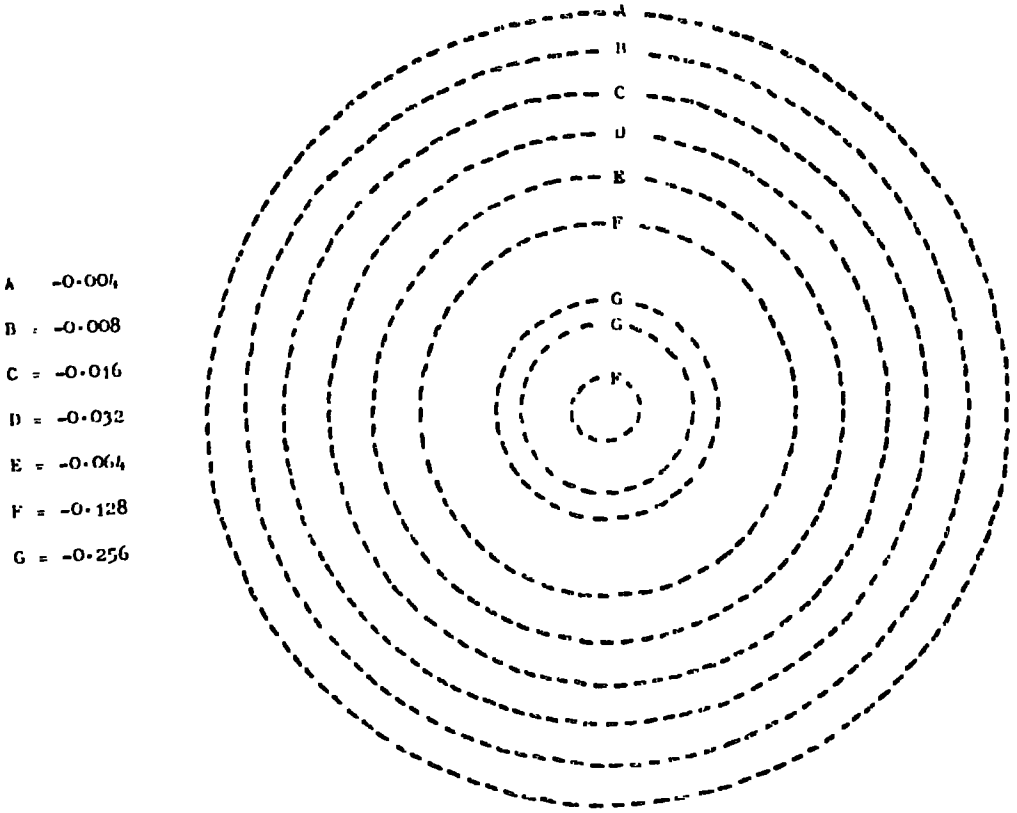

$(C\overset{a}{O})$-(CO) PLANE ⊥ THROUGH THE CENTRE

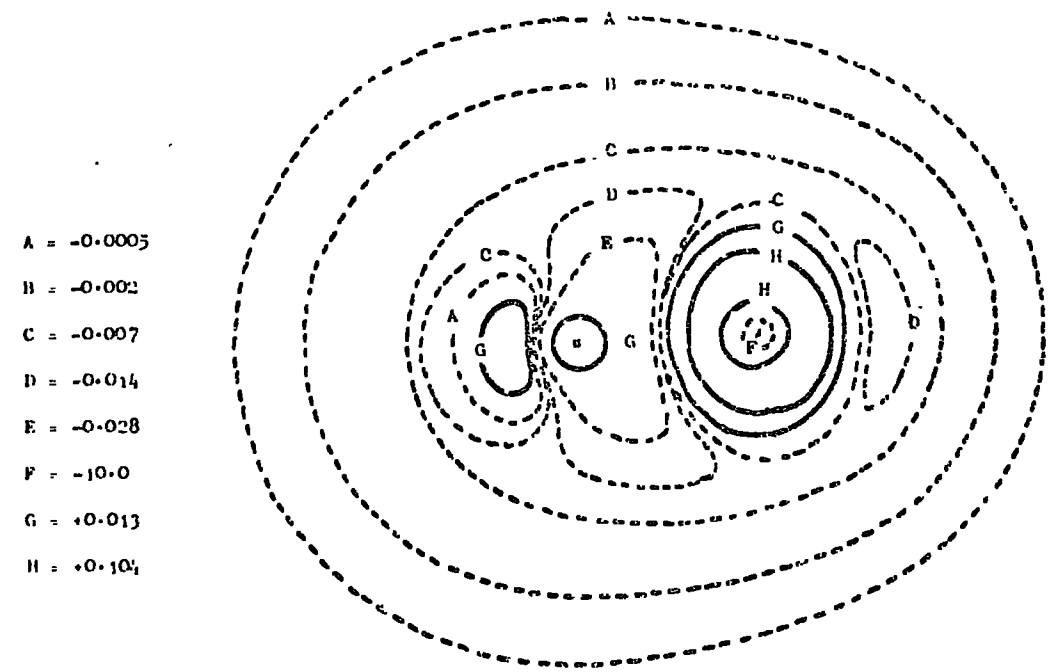

$(C\overset{a}{O})$-(CO) MOLECULAR PLANE

Fig. 4.6c.

there is a very substantial overall spatial contraction of the electron distribution in going from the neutral molecule to the core hole state. That this arises largely from electronic reorganizations of the valence electrons may most readily be inferred by reference to the contours in the immediate vicinity of the nuclei. It is clear that for the atom on which the core hole is located there is a decrease in electron density in this region which contrasts sharply with the large increase in electron density in the region appropriate to the valence electron distribution. Along the internuclear axes the contours corresponding to the molecular plane show that there are substantial changes in electron density with an overall increase in the region close to the nucleus on which the core hole is located and a decrease towards the other atom. The planes perpendicular to and bisecting the molecular axes are particularly revealing in this respect since they show for both the N_{1s} and C_{1s} holes a substantial increase in electron density in the bonding region whilst for the O_{1s} hole there is an overall decrease. These contours therefore provide a simple pictorial rationalization for the driving force behind the decrease in bond length accompanying N_{1s} and C_{1s} core ionization in N_2 and CO respectively and the increase in bond length in going to the O_{1s} core hole state for the latter.

4.5. Vibrational Fine Structure Accompanying Core Ionizations.

(a) Introduction.

It has been shown in Section 4.3 of this chapter that the equilibrium geometries for the core ionized species of N_2 and CO are significantly different from those of the neutral molecules and more particularly the potential energy surfaces (PES's) for the ionized species show substantial changes in force constants.

The development of a high resolution spectrometer incorporating the fine focussing X-ray monochromatization scheme has revealed significant fine structure in the main core photoionization peaks for N_2 and CO which had previously gone undetected.[60,77,79,134,135] An elegant discussion of the interpretation of this fine structure in terms of vibrational excitations accompanying core ionizations has been presented by Siegbahn and co-workers.[60,77,79] As it was previously pointed out, however, it is not entirely clear in the absence of a detailed theoretical examination that force constants and changes in bond length derived for the equivalent core species will be entirely adequate in discussing this data. The detailed analysis presented in Section 4.3 indicates that the potential energy surface for the equivalent cores species form a reasonable basis for the semi-quantitative discussion of the vibrational effects. However two differences were apparent with respect to the hole state species themselves. Firstly as it was previously discussed, depending on whether there is a decrease or an increase in equilibrium bond length in going from the neutral molecule to a given core hole state, the equivalent cores model provides either an upper or lower bound respectively to these changes in bond length. Secondly, the force constants for the equivalent cores species are consistently smaller than those for the corresponding hole states such

that the separation between the vibrational levels is almost certainly underestimated. Thus for the C_{1s} hole state of CO and the N_{1s} hole state of N_2, Siegbahn and co-workers[77] obtained an excellent fit to the observed asymmetric line shapes by computing the relevant Franck Condon factors taking separations between the vibrational energy levels of 0.29 eV and changes in bond lengths inferred from the equivalent cores species (NO^+). The theoretical calculations detailed in the discussion in the previous section, however, suggest vibrational frequencies of 0.33 eV for the C_{1s} and N_{1s} hole states of CO and N_2 respectively. A further point of interest is clearly an examination of the corresponding vibrational effects accompanying core ionization of the O_{1s} level in CO for which there appears to have been no previous detailed theoretical examination, and for which high resolution experimental data have only recently become available.[140] The calculated vibrational frequency for the core ionized species in this case is substantially lower (0.22 eV) than for the other holes.

The discussion to be presented below is within the harmonic approximation and since it will become apparent that vibrational excitations for the ionized states is restricted at normal temperatures to the lowest few levels we may briefly consider the possible importance of anharmonicities for these levels. As a model we may consider the ground state of CO for which experimental data of a high order of accuracy are well documented.[141] For example the change in vibrational separation in going from the $0 \rightarrow 1$ to the $5 \rightarrow 6$ transition amounts to less than 4% (0.26 eV vs. 0.25 eV). Since the interpretation of the unresolved ESCA data essentially involves a detailed lineshape analysis, such small changes in vibrational separations arising from anharmonicity corrections may reasonably be ignored. The effects of any slight anharmonicity would be expected to be even less in respect of the calculated Franck Condon factors,

which were computed using the recurrence relations derived by Ansbacher.[142]

The discussion which follows has focussed on the following points:

(1) The computation of the vibrational envelope for core ionization in N_2 and CO from the theoretically calculated energy separations and Franck-Condon factors, derived from the calculations at the triple zeta level. This enables a detailed comparison to be made with the corresponding analysis by Siegbahn and his co-workers[77] which is based solely on experimental data of ground and relevant equivalent core species, and also allows an extension to be made to a consideration of vibrational effects for the O_{1s} hole state in CO. In this investigation only transitions involving the ground state ($\upsilon'' = 0$) of CO and N_2 need be considered.

(2) Consequent upon the interpretation of the fine structure accompanying core ionization in these systems as arising from vibrational effects, to investigate the likely temperature dependence of the overall bond profiles.

(b) Nitrogen Molecule.

The distinct asymmetry of the direct photoionization peak for the core levels of nitrogen has been interpreted by Siegbahn and co-workers[77] in terms of excitation to the two lowest vibrational levels of the hole state. It is evident from the comparison between the theoretical analysis presented here and the experimental data that higher excitation must be involved. Taking the individual component linewidths obtained from Siegbahn's analysis (FWHM* 0.37 eV) together with the theoretically computed vibrational energy separations, an improved fit may be obtained to the experimental envelope.

---

* FWHM - Full Width at Half Maximum.

The derived Franck-Condon factors for the $\upsilon'' = 0$ to $\upsilon' = 0, 1, 2$ are 80%, 19% and 1% respectively. A more critical test for the calculations however is to take the theoretically derived change in bond length in conjunction with the vibrational separation to compute the relevant Franck-Condon factors. Taking the experimental band profile together with the theoretically calculated energy separations and Franck-Condon factors one obtains almost exact agreement, using as the only variable the FWHM of the individual components. The relevant data are displayed in Figure 4.7, the derived 'best fit' FWHM of 0.39 eV of the individual components being in excellent agreement with that derived from the previous analysis. This solely theoretical analysis differs from that based on the equivalent cores analysis primarily in terms of the somewhat lower overall contributions of the higher vibrational excitations.

(c) Carbon Monoxide.

(i) C_{1s} Levels.

A similar analysis to that presented for nitrogen has been carried out for CO. An improved fit to the experimental data was again obtained when theoretically calculated energy separation (0.33 eV) of individual vibrational components of FWHM derived by Siegbahn[77] (0.48 eV) was taken. This analysis reveals that the large change in bond length is accompanied by the excitation of up to five vibrational quanta and the derived Franck-Condon factors for the $\upsilon'' = 0$ to $\upsilon' = 0, 1, 2, 3, 4$ transitions are 36%, 36%, 20%, 7% and 1% respectively. Again the more critical test of the theory is by direct comparison of a solely theoretically based analysis with the experimental band profile. The quantitative nature of such an analysis is clearly evident from the data displayed in Figure 4.8, the derived FWHM for the individual component of 0.54 eV is again in good

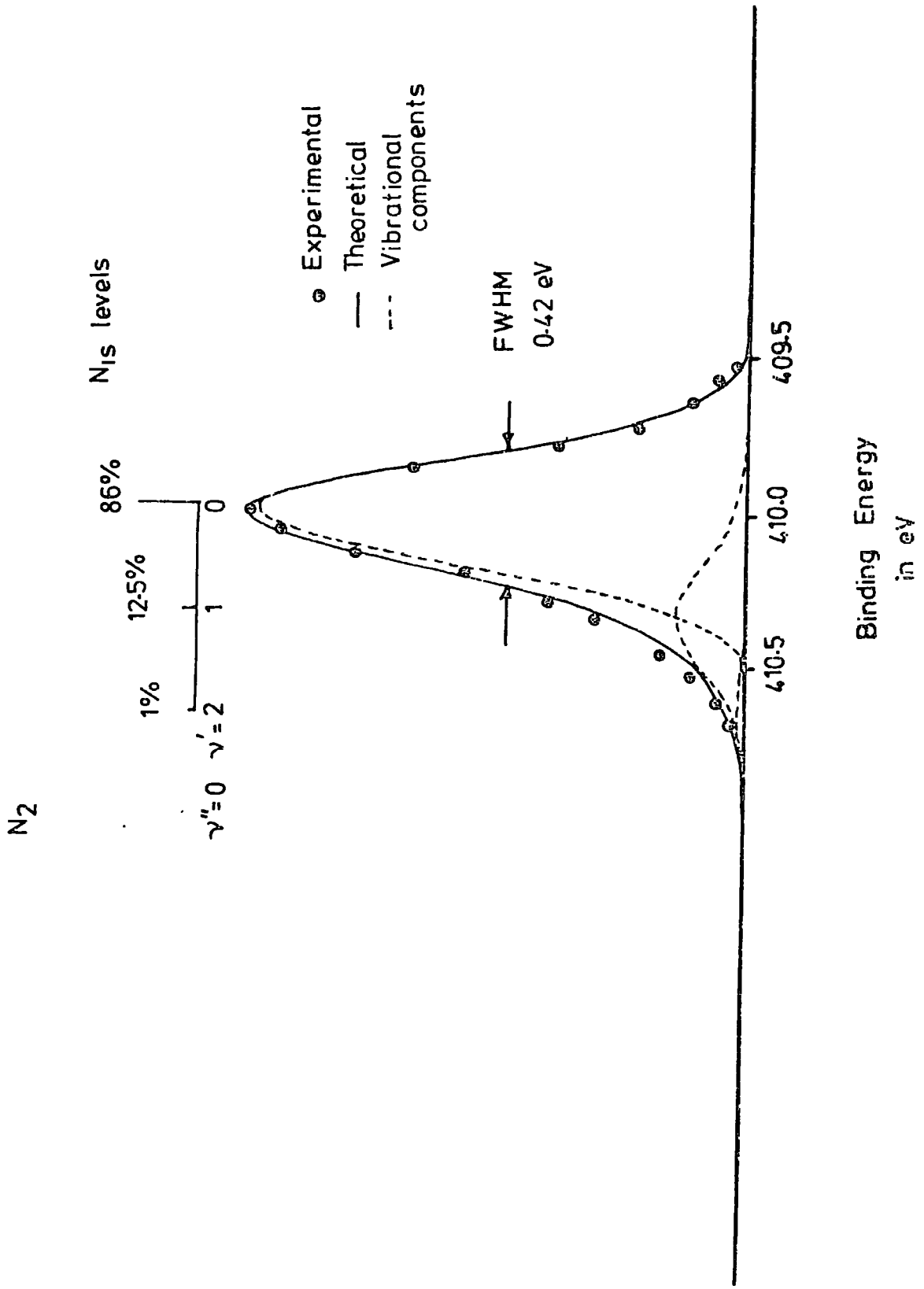

Fig. 4.7.

The N_{1s} spectrum of nitrogen molecule showing three vibrational components of FWHM = 0.39 eV separated by 0.33 eV.

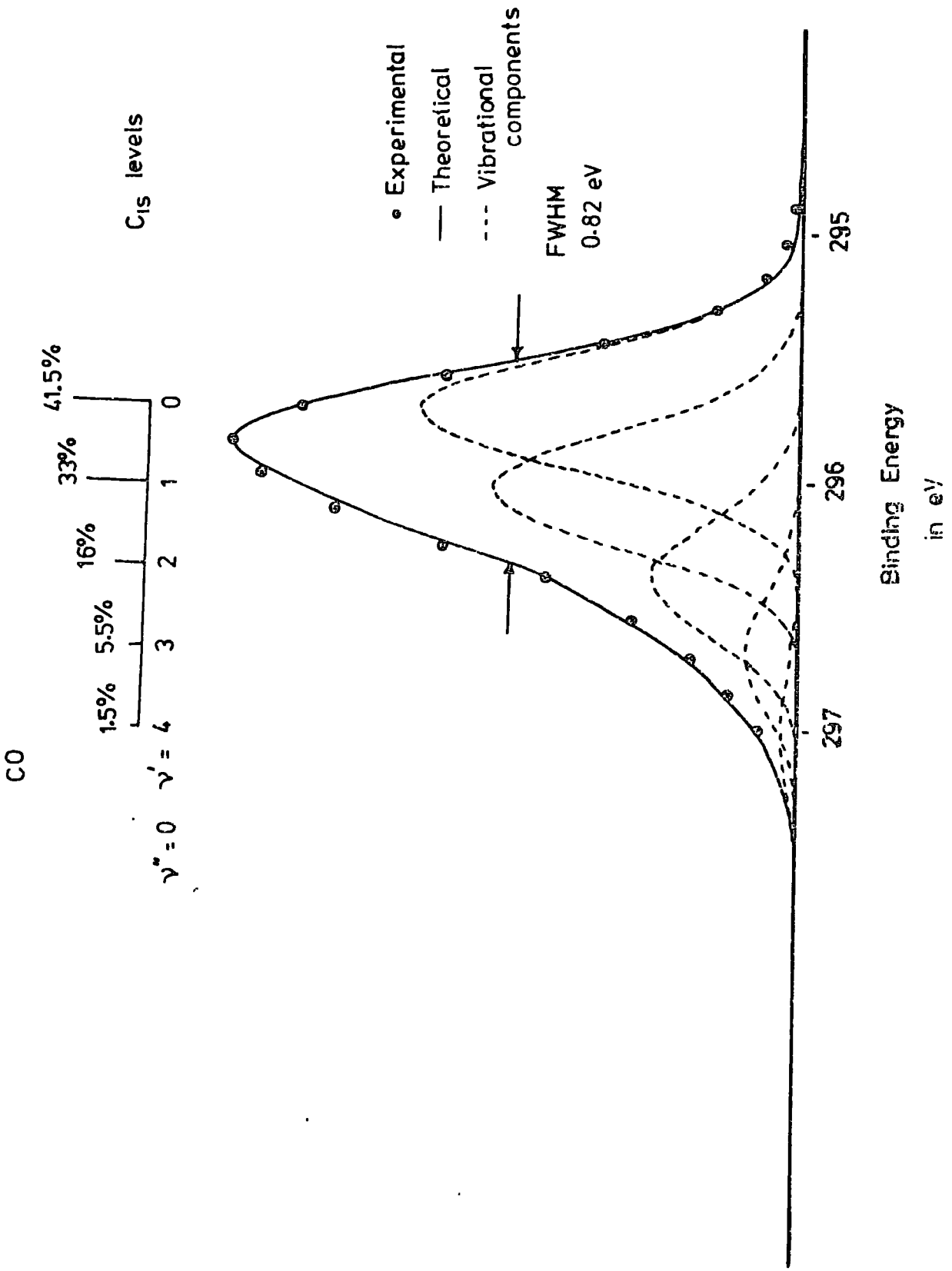

Fig. 4.8.

The C_{1s} spectrum of carbon monoxide showing five vibrational components with FWHM = 0.54 eV separated by 0.33 eV.

agreement with that derived from the equivalent cores analysis. Before an analysis of the vibrational effects accompanying core ionization of the O_{1s} level in carbon monoxide is presented one may briefly consider some previously published high resolution spectra[134] for carbon monoxide since these provide the only experimental criteria currently available in the literature for direct comparison with the theoretical analysis. The published high resolution data pertaining to the C_{1s} levels of carbon monoxide discussed thus far[77] refer to a lower instrumental resolution than that for nitrogen (e.g. FWHM for individual components 0.54 eV versus 0.39 eV from the analysis presented here). However, in an earlier paper[134] in which a detailed description of the high resolution ESCA instrument employing a fine focussed X-ray monochromator was described, core level spectra for carbon monoxide were reported with composite linewidths of 0.65 eV and 0.52 eV for the C_{1s} and O_{1s} levels respectively. Unfortunately the energy scale on which this data is recorded in the literature is such that a detailed examination of the asymmetry of the band envelope is not feasible (energy scale 2.67 mm/eV C_{1s} levels, 3.33 mm/eV O_{1s} levels). If one therefore takes the theoretically derived analysis for the C_{1s} levels described above and systematically varies the component linewidths to fit the published FWHM for the higher resolution spectrum (0.65 eV) one obtains the FWHM for the individual components of 0.32 eV which is in good agreement with that derived from the analysis of the nitrogen spectrum (FWHM = 0.39 eV) and that pertaining to neon (FWHM = 0.39 eV) measured at comparable instrumental resolution.[60,77,134] The theoretically simulated spectra for the C_{1s} levels corresponding to this high resolution are shown in Figure 4.9 where the data have been plotted on energy scales corresponding both to the published data[134] and to that employed in the previous figures. Comparison of the theoretically calculated composite

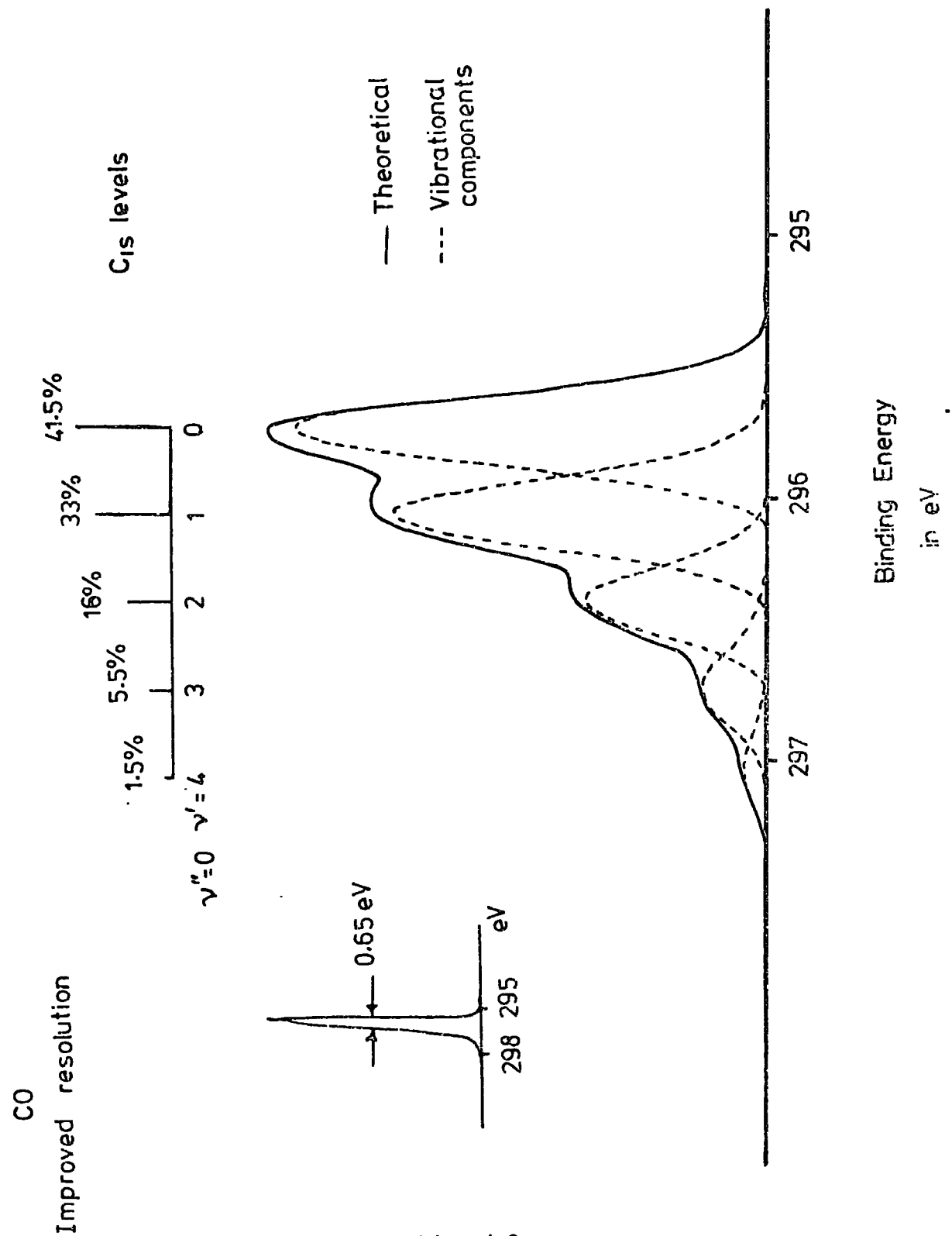

Fig. 4.9.

Theoretically simulated C_{1s} spectra of carbon monoxide on a large and a small energy scale. The individual vibrational components have FWHM = 0.32 eV and are separated by 0.33 eV. Composite linewidth of the peak is 0.65 eV.

band profile and the higher resolution experimental data shows them to be in excellent overall agreement.

(ii) O_{1s} Levels.

As was previously noted, vibrational effects accompanying core ionization of the O_{1s} levels in CO are of particular interest since no detailed analysis has previously been presented. The reason for this may be partly attributed to the lack of experimental data pertaining to the equivalent cores species CF^{+}. An alternative approach to the investigation of vibrational effects accompanying core ionizations has been attempted by Domcke and Cederbaum,[143] who have based their work on a many body formalism using Green's functions.

Whilst their analysis of the C_{1s} vibrational envelope corresponds reasonably closely to that presented here, the fact that the O_{1s} core ionized state has an equilibrium bond length somewhat greater than that of the neutral molecule leads to a divergent situation in the many body approach. It was, therefore, not possible to investigate in detail any vibrational effects, for the O_{1s} hole state, however the authors conclude that 'the O_{1s} electron is strictly non-bonding in the one particle approximation' and state that 'this is in qualitative agreement with the ESCA spectrum of CO which shows no detectable broadening'. The detailed analyses which will be presented below indicate that both of these conclusions are in error and that significant vibrational effects are predicted and may in fact be inferred from the available experimental data.

The theoretical calculations detailed in Section 4.3 show that the force constant for the O_{1s} hole state of CO is substantially smaller than that for the neutral molecule, which accords with the increased bond length

in going to the core ionized species. Taking the force constants and change in bond length derived from the theoretical analysis the energy separations and Franck-Condon factors may readily be computed. In order to simulate the vibrational envelope for the O_{1s} level an estimate of the FWHM for each component is required. The available data in the literature from the high resolution gas phase studies indicate that the composite linewidth associated with the 1s levels of first row atoms is C, $\sim$ 0.32 eV*; N, 0.39 eV*; Ne, 0.39 eV.[60,77,134] It should be emphasized that these linewidths are largely determined by the instrumental contributions (X-ray source, analyzer etc.) since it is known that the natural linewidths are considerably smaller.[60,77,79,134,135] It is clear that the linewidth appropriate to the same instrumental resolution for the O_{1s} level should therefore be $\sim$ 0.39 eV. The highest resolution data for carbon monoxide show that when the composite linewidth for the C_{1s} levels is $\sim$ 0.65 eV that for the O_{1s} levels is $\sim$ 0.52 eV.[134] The significantly broadened peak for the O_{1s} levels may therefore be taken as prima facia experimental evidence for vibrational effects. Taking a FWHM of 0.39 eV for the individual components, the calculated FWHM for the composite spectrum derived from the theoretical analysis is 0.52 eV in complete agreement with the experimental data. Unfortunately the published data is too compressed to clearly show the marked asymmetry of the O_{1s} core level, so that the only experimental parameter available is the total FWHM. Figure 4.10 however, which has been plotted on a comparable scale to that for the expanded C_{1s} spectrum clearly shows the vibrational effects which should be evident in an expanded experimental spectrum of the O_{1s} levels.

---

* These values for the C_{1s} and N_{1s} levels are those derived from the theoretical analysis of the experimental data as described above.

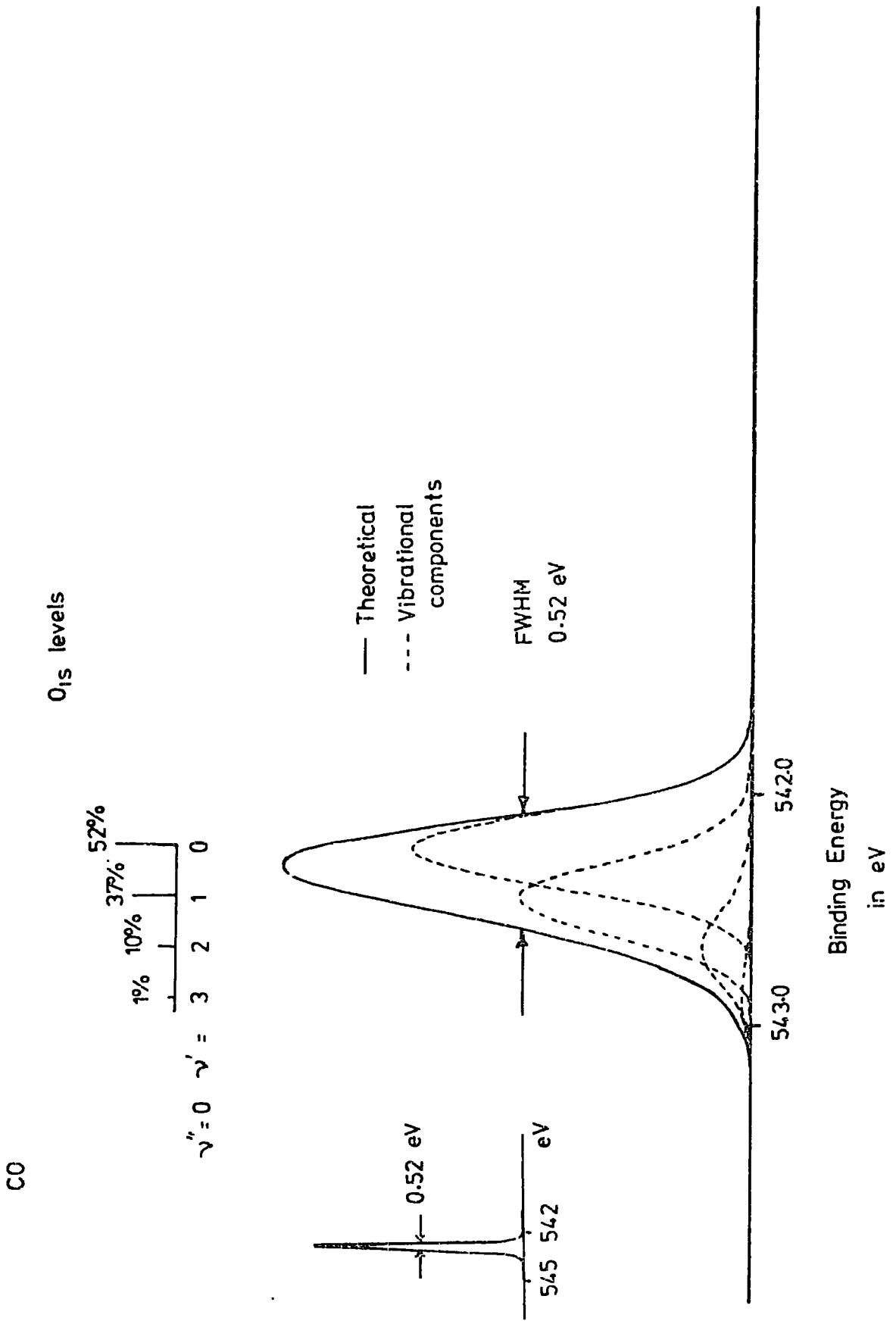

Fig. 4.10.

Theoretically simulated O_{1s} spectra of carbon monoxide on a large and a small energy scale. The four-vibrational components have FWHM = 0.39 eV and are separated by 0.22 eV.

The fact that the O_{1s} spectrum of CO has a smaller FWHM than the C_{1s} spectrum and that the latter is more asymmetric stems mainly from the fact that the individual vibrational components in the O_{1s} spectrum are more closely spaced than for either the carbon hole or for the neutral molecule. For comparison purposes the theoretically simulated O_{1s} level spectrum is also plotted in Figure 4.10 on a comparable scale to that of the published data. Superposition of this spectrum with that previously published, shows the excellent agreement between the two.

The goodness of the analysis of the O_{1s} levels has been fully substantiated by further experimental data[144] kindly provided for us by Professor Kai Siegbahn and Docent Ulrik Gelius. The spectrum of the O_{1s} levels of CO plotted on an expanded scale (Figure 4.11) has been obtained by the Uppsala group[144] employing the fine focus X-ray monochromatization scheme. The asymmetry of the spectrum although less marked than for the C_{1s} levels is clearly apparent and the resolution of the spectrometer giving a composite linewidth of 0.66 eV corresponds to the composite linewidth of 0.82 eV for the C_{1s} levels reproduced in Figure 4.8. Taking theoretically calculated Franck-Condon factors together with calculated vibrational energy separations (0.22 eV) we obtain the best overall fit to the band profile using as the only variable the FWHM of the individual components. This fit is also indicated in Figure 4.11 and is seen to be in excellent overall agreement with the experimental curve (the minor discrepancies at the leading and trailing edges may well arise from the use of purely Gaussian lineshapes since the individual components would be expected to be hybrids arising from the convolution of a Lorentzian line shape contribution due to the inherent width of the core level and a Gaussian from the spectrometer contributions). The derived FWHM for the component peaks is 0.58 eV which is in excellent agreement with that

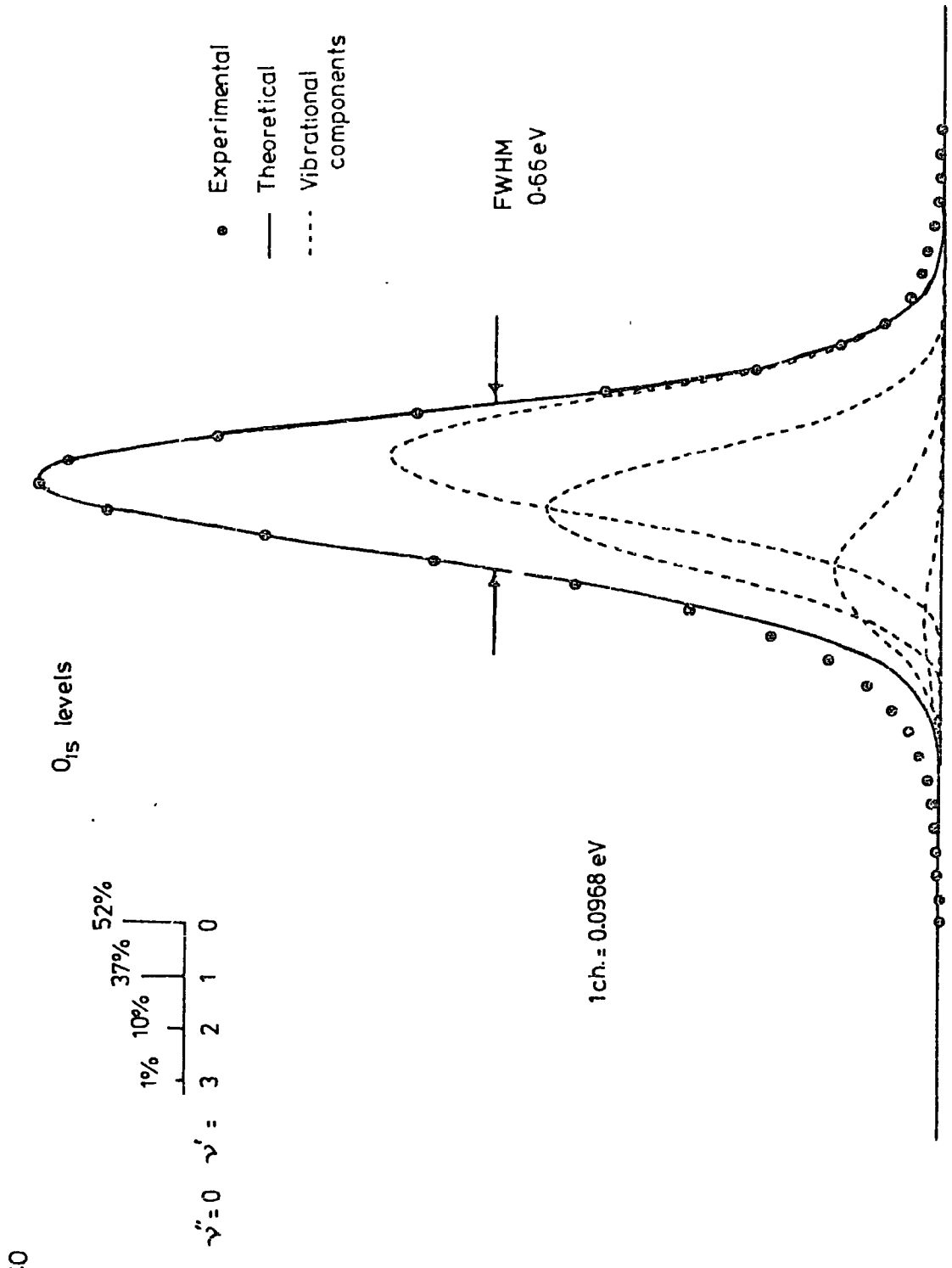

Fig. 4.11.

The O_{1s} spectrum of carbon monoxide showing four vibrational components with FWHM = 0.58 eV separated by 0.22 eV.

calculated from the derived linewidths for the O_{1s} level at higher instrumental resolution (0.39 eV) and for the C_{1s} levels at the same (0.54 eV) and higher instrumental resolution (0.32 eV) based on a first-order analysis of the composite linewidths taking the inherent widths of the levels and the spectrometer contributions in simple quadrature.

(d) Temperature Dependence of Vibrational Fine Structure Profiles.

The interpretation of the band profiles for N_{1s}, C_{1s} and O_{1s} core levels in N_2 and CO as arising from vibrational progressions involving the ground vibrational states of the neutral molecules in each case suggests that a confirmation of this assignment could be made by temperature dependent studies of the band profiles. Unfortunately the vibrational energy spacings for these molecules are such that significant population of other than $\upsilon'' = 0$ level requires considerably elevated temperatures. One needs to restrict oneself therefore to a theoretical analysis which would correspond to realistic experimental conditions, and therefore the charge in band profile for N_2 at 1800K has been considered. The Boltzmann distribution is such that at this temperature the population of the $\upsilon'' = 0$ and $\upsilon'' = 1$ levels are $\sim$ 87% and $\sim$ 13% respectively. The vibrational profile arising from transitions from $\upsilon'' = 0$ to $\upsilon' = 0$, 1, 2 and from $\upsilon'' = 1$ to $\upsilon' = 0$, 1, 2, and 3 using the theoretically calculated energy separations, force constants and change in bond length previously discussed has therefore been considered and the results are displayed in Figure 4.12. The differences with respect to the room temperature spectrum are small but significant and should be detectable with current instrumentation. Thus the FWHM of the high temperature spectrum should be $\sim$ 0.3 eV larger than that at room temperature and the tails at higher and lower binding energies should also be observable.

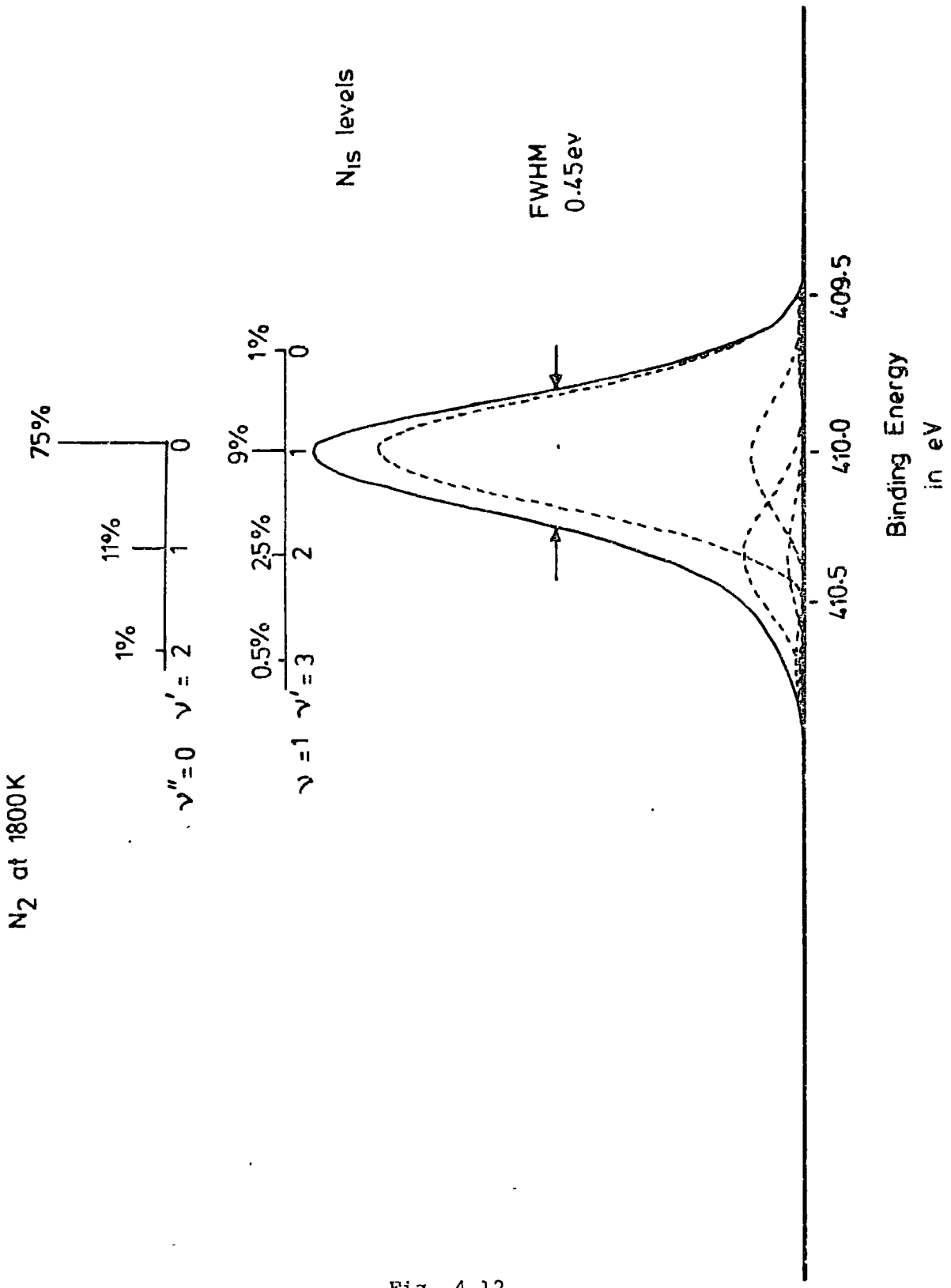

Fig. 4.12.

Theoretically simulated N_{1s} spectrum of nitrogen molecule at 1800 K, showing vibrational excitation from the $\upsilon'' = 0$ and $\upsilon'' = 1$ levels. The individual vibrational components have FWHM = 0.39 eV. The vibrational separations being 0.33 eV.

An alternative experiment to this direct temperature dependent study would be to investigate the high resolution ESCA spectra of molecular beams where vibrational quanta of the ground state species have been selectively excited by means of a tunable laser. There is certainly great scope for both theoreticians and experimentalists in high resolution temperature dependent and molecular beam studies of X-ray photoelectron spectra.

CHAPTER V

THEORETICAL INVESTIGATIONS OF THE VALENCE IONIZED STATES OF N_2 AND CO

Abstract.

Non-empirical LCAO MO SCF calculations at the double zeta level have been carried out on N_2 and CO and their valence ionized states. Changes in ionization potentials, relaxation energies, equilibrium geometries and harmonic force constants have been computed and comparisons drawn with experimental data where available. In appropriate cases it is shown that trends may be rationalized in terms of changes in π bond overlap populations. The computed bond lengths and force constants have been used to calculate ab initio Franck-Condon factors for the valence ionized states and comparison with experimental data reveals overall qualitative agreement.

5.1. Introduction.

In the preceding chapter investigations of core binding energies, potential energy surfaces and vibrational fine structures accompanying core ionizations in CO and N_2 have been described in some detail. This chapter contains an extension of this work to the investigation of the corresponding valence ionized states. Although there have been several previous studies on both the core and valence ionized states of these simple molecules[44,77,143,145-7] a comprehensive study with a common basis set has not previously been attempted, therefore theoretically calculated ionization potentials (binding energies), relaxation energies, vibrational frequencies and equilibrium geometries of the ground and valence ionized states of CO and N_2 are reported here. The computations have been within the Hartree-Fock formalism with basis sets of double zeta quality and where possible comparison has been drawn with experimental data. Changes in equilibrium bond length and force constants have been correlated with π bond overlaps in appropriate cases and the direct computation of Franck-Condon factors provides a stringent test by drawing comparisons between theoretically derived and experimentally determined band profiles.

5.2. Computational Details.

Non-empirical LCAO MO SCF calculations have been carried out within the Hartree-Fock formalism since the arguments discussed in the first two chapters and further substantiated by the results reported in the preceding chapter suggest that changes in correlation energy are relatively unimportant in discussing changes in equilibrium geometries, force constants and ionization potentials of ground and core hole state species. Calculations have been carried out on the ground state and all of the valence hole states using the ATMOL system of programs implemented on an IBM 370/195. Double zeta Slater basis sets with Clementi's best atom exponents[28] have been employed for this purpose as it would have been too expensive to use triple zeta basis for such an extensive investigation and the 'optimized' STO 4-31G basis set successfully used before is only suitable for core hole state species.

5.3. Investigation of Ionization Potentials and Relaxation Energies.

(a) Nitrogen.

The formal electron configuration for the nitrogen molecule may be written:

$$(\sigma_g 1s)^2 \ (\sigma_u 1s)^2 \ (\sigma_g 2s)^2 \ (\sigma_u 2s)^2 \ (\pi_u 2p)^4 \ (\sigma_g 2p)^2.$$

Binding energies have been computed by the ΔSCF technique and comparison with Koopmans' Theorem allows the direct estimation of relaxation energies accompanying ionization. The results are shown in Table 5.1 where comparison is also drawn with results based on the 'relaxed Koopmans' formalism.

The adiabatic binding energies are smaller than their vertical counterparts and the largest difference is for the A $^2\pi_u$ and C $^2\Sigma_g^+$ states, since these include the largest changes in equilibrium bond length with respect to the neutral molecule.

The computed relaxation energies for the valence ionized states are in the order B $^2\Sigma_u^+$ < B $^2\pi_u$ < X $^2\Sigma_g^+$ < C $^2\Sigma_g^+$. It is interesting to note that the overlap between the deep lying valence 2s orbitals on nitrogen is sufficiently large that the valence ionized C $^2\Sigma_g^+$ state corresponds to a delocalized hole which contrasts strongly with the situation for the core hole states discussed in the previous chapter. We shall discuss this point in slightly more detail later on.

The relaxed Koopmans' method discussed in the second chapter was originally derived and used to predict binding energies and their shifts for core hole state species,[86,87,104,108] but it is clear from the present work that the method can also be successfully extended to valence ionized states.

It has already been pointed out in the second chapter that the ΔSCF method does not predict binding energies for valence hole states as

Table 5.1.

Valence Ionization Potentials (in eV) and Relaxation Energies (in eV) for N_2.

Model[a]	$X\ ^2\Sigma_g^+$	$A\ ^2\pi_u$	$B\ ^2\Sigma_u^+$	$C\ ^2\Sigma_g^+$
$(\Delta SCF)_v$	16.64	16.88	21.14	40.91
$\Delta(\Delta SCF)_v$	4.50	4.26	0	-19.77
$(Kr)_v$	16.50	16.83	21.04	40.87
$\Delta(Kr)_v$	4.54	4.21	0	-19.83
K	17.53	17.68	21.80	42.30
$\Delta(K)$	4.27	4.12	0	-20.50
RE	0.89	0.80	0.66	1.39
$(\Delta SCF)_v^{corr}$	18.61	19.05	22.86	-
$\Delta(\Delta SCF)_v^{corr}$	4.25	3.81	0	-
$(\Delta SCF)_{ad}$	16.54	16.31	20.98	38.72
$\Delta(\Delta SCF)_{ad}$	4.44	4.67	0	-17.74
$(Kr)_{ad}$	16.41	16.27	20.87	38.55
$\Delta(Kr)_{ad}$	4.45	4.60	0	-17.68
$\Delta(SCF)_{ad}^{corr}$	18.51	18.48	22.70	-
$\Delta(\Delta SCF)_{ad}^{corr}$	4.19	4.22	0	-
$(IP)_v$	15.57[b]	16.93[b]	18.75[b]	37.3[c]
$\Delta(IP)_v$	3.18	1.82	0	18.55
$(IP)_{ad}$	15.57[b]	16.69[b]	18.75[b]	-
$\Delta(IP)_{ad}$	3.18	2.06	0	-

[a] ΔSCF refers to binding energy calculated by the ΔSCF method,
Kr refers to Relaxed Koopmans' Theorem, viz. $-\frac{1}{2}(\varepsilon + \varepsilon^*)$,
K refers to Koopmans Theorem, viz. $-\varepsilon$,
RE refers to relaxation energy,
IP refers to experimentally measured ionization potentials,
Subscripts v and ad refer to vertical and adiabatic respectively,
Superscript corr refers to electron correlation corrections.

[b] Reference 62.

[c] Reference 59.

accurately as it does for the hole states. Indeed in particular instances it even predicts an incorrect ordering of various valence energy levels. This fact is chiefly attributed to electron correlation (ignored in the ΔSCF technique) which can substantially vary for valence orbitals with different localization characteristics. An attempt has therefore been made to estimate correlation energy differences ΔE_{corr} using the pair population model described in Chapter 1, Section 1.6d. The results from earlier work[52] reported in this laboratory indicates that the $\Delta E_{corr-inter}$ term can be neglected in discussing shifts in ionization potentials thus leaving us with the evaluation of the expression 1.165b and the 'intra-' component of the expression 1.164. The results of these correlation corrections to vertical and adiabatic ionization potentials in the present work are displayed in Table 5.1. Ionization potentials obtained in this way are somewhat larger than the experimental values which most probably arise from deficiencies in the basis sets employed and from the neglect of the $E_{corr-inter}$ term, but far more important is the fact that the shifts in binding energies using this approach are in better agreement with the experimental shifts. Furthermore it is interesting to note that $\Delta E_{corr-intra}$ is larger for the $A\ ^2\pi_u$ state than for the $X\ ^2\Sigma_g^+$ state thus reinforcing the well known fact that correlation energy is responsible for an incorrect ordering of these two states at the Hartree-Fock limit.[44] However the calculations performed in this work do not approach the Hartree-Fock limit and therefore fortuitously predict a correct ordering of these two energy levels for vertical ionization potentials.

(b) Carbon Monoxide.

The formal electron configuration for the carbon monoxide molecule may be written:

$$(O_{1s})^2\ (C_{1s})^2\ (1\sigma)^2\ (2\sigma)^2\ (1\pi)^4\ (3\sigma)^2$$

An analysis along the same lines has been carried out for the valence ionized states of carbon monoxide and the results are shown in Table 5.2. The trends and the gross features of the data for CO are similar to those discussed for N_2.

It is interesting to note that in the particular case of X $^2\Sigma^+$ and A $^2\pi$ the calculations predict the correct ordering, which contrasts with the situation for N_2^+. This arises because the difference in correlation energy changes is insufficient to invert the ordering.

It is noteworthy that the difference between the calculated adiabatic and vertical ionization potentials for the A $^2\pi$ and C $^2\Sigma^+$ states of CO is larger than the corresponding difference for the equivalent A $^2\pi_u$ and C Σ_g^+ states of N_2, and this accords with the experimental data.

Further we may note that the relaxation energies accompanying valence ionizations in CO are uniformly larger than those for N_2 which at first sight might seem somewhat surprising since for the atoms the relaxation energies for valence atomic orbitals increases in the series C < N < O. However the results are readily understandable when due account is taken of the localization characteristics which determine to a large extent the relaxation energy. For the C $^2\Sigma^+$ state of CO for example which corresponds roughly to an O_{2s} lone pair the relaxation energy (2.16 eV) is $\sim$ 50% larger than for the corresponding valence ionized state for nitrogen which we have previously noted is delocalized over the equivalent centres. Snyder[81] has shown (as discussed in Chapter II, Section 1.2.b) that relaxation energy follows roughly a quadratic dependence on charge. Hence on naive arguments the relaxation energy for the delocalized C $^2\Sigma_g^+$ state of N_2^+ should be approximately 0.5 of that for the atom (N^+). The theoretically

Table 5.2.

Valence Ionization Potentials (in eV) and Relaxation Energy (in eV) for CO

Model[a]	$X\ ^2\Sigma^+$	$A\ ^2\Pi$	$B\ ^2\Sigma^+$	$C\ ^2\Sigma^+$
$(\Delta SCF)_v$	14.40	16.22	20.49	40.91
$\Delta(\Delta SCF)_v$	6.09	4.27	0	-20.42
$(Kr)_v$	13.97	15.89	20.63	40.86
$\Delta(Kr)_v$	6.66	4.74	0	-20.23
K	15.68	18.05	22.10	43.07
$\Delta(K)$	6.42	4.05	0	-20.97
RE	1.28	1.83	1.61	2.16
$(\Delta SCF)_v^{corr}$	16.14	18.30	22.23	-
$\Delta(\Delta SCF)_v^{corr}$	6.09	3.93	0	-
$(\Delta SCF)_{ad}$	14.38	15.16	20.46	37.80
$\Delta(\Delta SCF)_{ad}$	6.08	5.3	0	-17.34
$(Kr)_{ad}$	13.94	14.56	20.56	38.12
$\Delta(Kr)_{ad}$	6.6	6.0	0	-
$\Delta(SCF)_{ad}^{corr}$	16.12	17.24	22.0	-
$\Delta(\Delta SCF)_{ad}^{corr}$	6.08	4.96	0	-
$(IP)_v$	14.01[b]	16.91[b]	19.72[b]	38.3[c]
$\Delta(IP)_v$	5.71	2.81	0	-18.58
$(IP)_{ad}$	14.01[b]	16.53[b]	19.72[b]	-
$\Delta(IP)_{ad}$	5.71	3.19	0	-

[a] See Table 5.1.

[b] Reference 62.

[c] Reference 59.

computed results using a modified Hartree-Fock-Slater Method reported by Gelius and Siegbahn[125] (see Table 5.3) show that this is a reasonable approximation, viz. 1.39 eV vs. 3.0 eV.* By contrast the relaxation energy for the C $^2\Sigma^+$ state for CO is proportionately larger with respect to that for the atom (O^+) viz. 2.16 eV vs. 3.6 eV.

For the A $^2\pi$ states a similar situation obtains, the relaxation energy being lower for the symmetrically delocalized π system of N_2. Thus the computed relaxation energy for this state of 0.8 eV may be compared with that for the atom 2.4 eV. For the corresponding state of CO^+ since the LCAO coefficients are largest for the O_{2p} orbitals the relaxation energy might reasonably be expected to fall between the corresponding atomic relaxation energies for O_{2p} and C_{2p} levels. This is in fact the case viz. 1.83 eV versus 1.6 eV and 3.2 eV respectively. Similar arguments may be applied to the X and B states to rationalize the lower relaxation energies for the N_2^+ compared with the CO^+ species.

---

* Comparison of course should strictly be with relaxation energies computed for the valence ionized atoms with the same basis set. Since however we are primarily interested in trends and differences we have used previously published data[125] with more extended basis sets. The error involved in this is likely to be extremely small since the relaxation energies are reasonably well accounted for with the double zeta basis sets.

Table 5.3.

Atomic Relaxation Energies (in eV) for Ionization from Various Subshells Obtained by a Modified Hartree-Fock-Slater Method (taken from reference 125)

Atom	1s	2s	2p
H	0.0		
He	1.5		
Li	3.8	0.0	
Be	7.0	0.7	
B	10.6	1.6	0.7
C	13.7	2.4	1.6
N	16.6	3.0	2.4
O	19.3	3.6	3.2
F	22.0	4.1	3.8

5.4. Investigation of Potential Energy Surfaces.

(a) Description of the Method.

Potential energy surfaces for the ground and for all of the valence hole states of nitrogen and carbon monoxide have been calculated in the manner described in Chapter V. This process has involved computing equilibrium geometries, $(Re)_c$, for these species and constructing potential energy curves around each of the equilibrium positions. These curves have then been used to calculate harmonic force constants, $(We)_c$. Equilibrium geometries and force constants are much less sensitive to electronic correlation, and this has therefore been ignored.

(b) Nitrogen.

The calculated equilibrium geometries $(Re)_c$ and force constants $(We)_c$ for the ground and valence hole state species for the nitrogen molecule together with changes with respect to the neutral molecule are displayed in Table 5.4. For comparison purposes experimental values of these two parameters and the appropriate changes are also displayed in Table 5.4. The overall agreement between the experimental and calculated values of the equilibrium geometries and force constants is very reasonable even if the calculated changes are always slightly too large.

As expected the loss of the strongly bonding π_u 2p electron results in a significant increase in bond length (experimental increase = 7.1%, calculated increase = 9.1%) and a decrease in vibrational frequency (experimental decrease = 24.1%, calculated decrease = 26.7%). The ionization of an electron from the σ_g 2p orbital results in a small increase in bond length (experimental increase = 1.9%, calculated increase = 3.6%) and a corresponding decrease in vibrational frequency (experimental decrease = 10.3%, calculated decrease = 13.3%). Ionization of an electron from the

Table 5.4.

Equilibrium Geometries (in atomic units), Force Constants (in eV) and Bond Overlaps for N_2 and Valence States of N_2^+.[a]

	$X\ ^1\Sigma_g^+$	$X\ ^2\Sigma_g^+$	$A\ ^2\pi_u$	$B\ ^2\Sigma_u^+$	$C\ ^2\Sigma_g^+$
$(Re)_c$	2.082	2.157	2.272	2.001	2.548
$\Delta(Re)_c$	0	-0.075	-0.190	0.081	-0.466
$\Delta(Re)_c$ %	0%	-3.6%	-9.1%	3.9%	-22.4%
$(Re)_{ex}$	2.074[b]	2.113[c]	2.222[c]	2.032[c]	-
$\Delta(Re)_{ex}$	0	-0.039	-0.148	0.042	-
$\Delta(Re)_{ex}$ %	0%	-1.9%	-7.1%	2.0%	-
$\lvert\Delta(R)_s\rvert$	0	0.077	0.219[d]	0.077	0.564
$(We)_c$	0.30	0.26	0.22	0.34	0.17
$\Delta(We)_c$	0	0.04	0.08	-0.04	0.13
$\Delta(We)_c$ %	0%	13.3%	26.7%	-13.3%	43.3%
$(We)_{ex}$	0.29[e]	0.26[f]	0.22[f]	0.30[f]	-
$\Delta(We)_{ex}$	0	0.03	0.07	-0.01	-
$\Delta(We)_{ex}$ %	0%	10.3%	24.1%	-3.4%	-
π overlap	0.998	0.954	0.718	0.960	0.946

[a] Re refers to equilibrium geometry,
We refers to equilibrium (harmonic) force constant,
Subscript c refers to calculated values,
Subscript ex refers to experimental values,
$\lvert\Delta(R)_s\rvert$ refers to change in geometry computed from equation (3).

[b] Reference 118.

[c] Reference 44.

[d] $\lvert\Delta(R)_s\rvert$ = 0.141 when experimental values of ionization potentials and frequencies are used.

[e] Reference 141.

[f] Reference 62.

σ_u 2s orbital results in a decrease in bond length (experimental decrease = 2.0%, calc. decrease = 3.9%) and an increase of the vibrational frequency (experimental increase = 3.4%, calculated increase = 13.3%), whilst for the strongly bonding σ_g 2s orbital whose vibrational structure has not been studied experimentally in any great detail, results according to these calculations in substantial changes in the bond distance (calculated increase = 22.4%) and the vibrational frequency (calculated decrease = 43.3%). However it is quite likely that ionization of this inner valence electron may lead to pre-dissociation, but more experimental evidence and detailed calculations incorporating correlation effects are needed to investigate this hypothesis. The data relating equilibrium geometries and force constants of ground and all singly ionized species (including the localized N_{1s} core hole state species with $(We)_c$ = 0.31 eV and $(Re)_c$ = 2.058 A.U. computed with the double zeta basis set) are graphically displayed in Fig. 5.1. The main feature of this plot is its linearity which is not entirely surprising in view of the preceding discussion.

As was noted the overall trends in computed and experimentally determined changes in vibrational frequencies and equilibrium geometries consequent upon photoionization of various valence electrons accord with expectation based on the bonding, antibonding and non-bonding characteristics of the relevant orbitals. By contrast as shown in this work and by others[77,139,143] the electronic reorganizations accompanying photoionization of core electrons give rise to substantial changes in potential energy surfaces despite the fact that they may be considered formally as non-bonding. These changes are the results of electronic reorganization (relaxation) effects of valence electrons accompanying core electron ionizations, which are much larger than the electronic reorganization

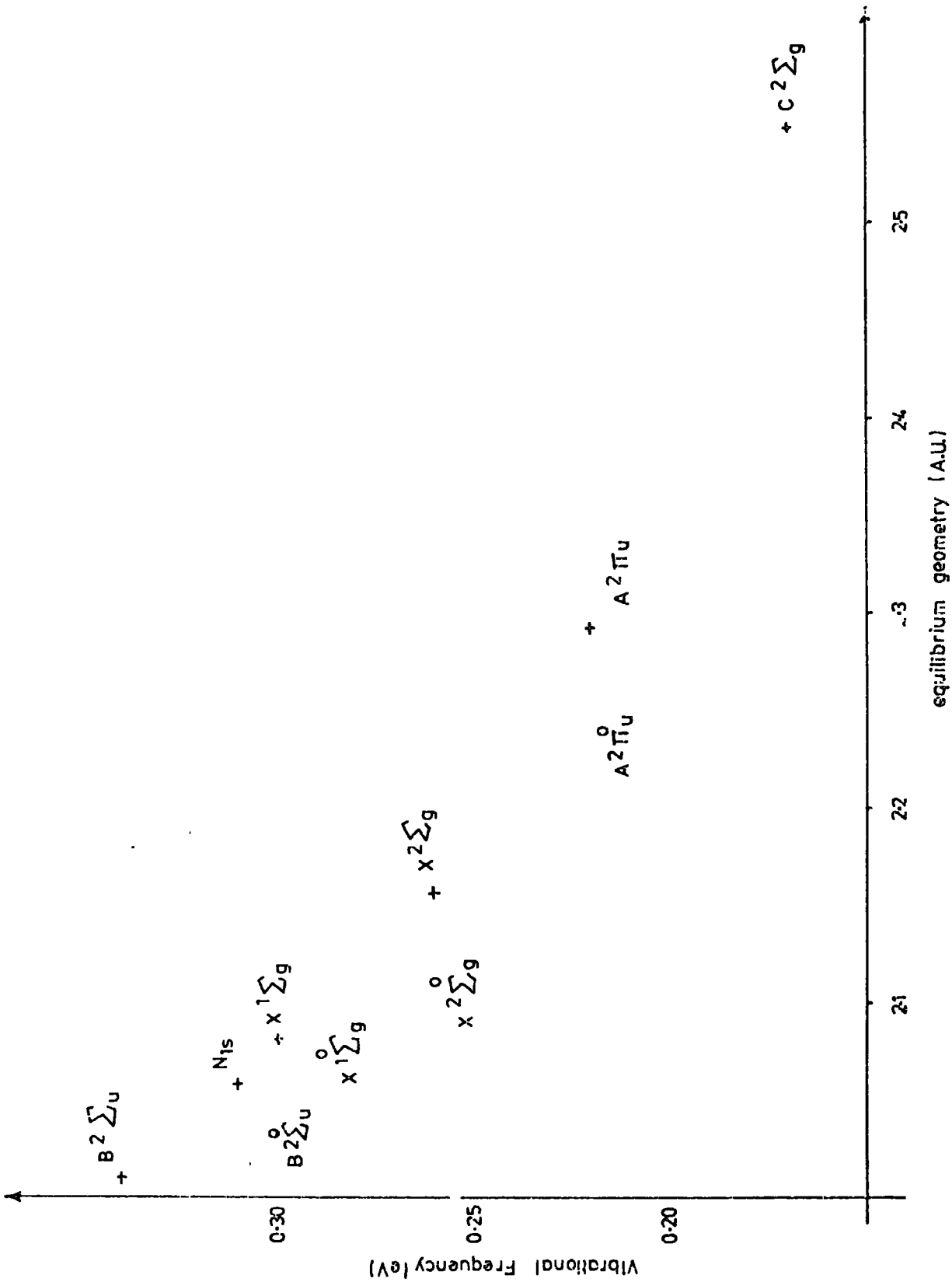

Fig. 5.1.

Plot of vibrational frequencies versus equilibrium geometries for N_2 and all hole states of N_2^+.

o refers to experimental data.

+ refers to theoretically computed data.

effects consequent upon valence electron ionizations, since for core electrons there is a greater change in potential at the nucleus.

Table 5.4 also contains values of $|\Delta(R)_s|$ which are the computed changes in equilibrium bond lengths inferred from the semi-classical formula developed by Price.[148]

$$\Delta(R)_s^2 = 0.543\ (I_v - I_a)\mu^{-1}\omega^{-2} \qquad \ldots\ (5.1)$$

where μ is reduced mass in atomic units,

ω is vibrational frequency of the ionized molecule in kcm^{-1},

I_v and I_a are vertical and adiabatic ionization potentials respectively in eV and $|\Delta(R_s)|$ is the change in equilibrium geometry in Angstroms.

It can be seen that the changes in equilibrium bond lengths calculated using (5.1) are not much improved over the corresponding changes computed from the ab initio calculations. This can be partly attributed to the fact that the values of both the vibrational frequencies, $(We)_c$, and the ionization potentials (determined by the ΔSCF method) used in (5.1) depend on the computed potential energy surfaces of the hole state species and thus indirectly on the values of $(Re)_c$. The $A\ ^2\pi_u$ state is the only ionized state for which there is an experimentally observed difference between the adiabatic and vertical ionization potentials. Using these values together with the experimentally determined vibrational frequency, $(We)_{ex}$, yields $|\Delta(R)_s| = 0.141$ A.U. which is in an excellent agreement with the directly determined experimental value $\Delta(Re)_{ex} = 0.148$ A.U.

It is noteworthy that the calculated differences in vertical and adiabatic ionization potentials show an almost linear correlation with the computed change in bond length on going from the neutral molecule to the ionized state as might have been anticipated.

Table 5.4 also contains values of the π bond overlaps (from the Mulliken population analysis) for the ground and valence hole state species of N_2 pertaining to the equilibrium geometry of the neutral molecule. The loss of the π electron obviously results in a decrease of π electron density giving rise to a small value of the π bond overlap for the $A\ ^2\pi_u$ species. Interestingly enough the π bond overlap also decreases for the core ionized species (π bond overlap with double zeta basis set = 0.816). This can be rationalized on the basis that the localized N_{1s} core hole state of N_2^+ can, (according to the equivalent cores approximation), formally be written as NO^+. In this molecule, there is a certain energy mismatch between the p atomic orbitals on N and O^+ which take part in the π bonding which results in a decrease of the π bond overlap. The π bond overlap for the other ionized states is not much different from that for the ground state molecule, since ionization is in each case from symmetrically delocalized σ orbitals. The relevance of the values of π bond overlaps for heteronuclear molecules in the context of vibrational fine structure becomes more apparent in the case of CO.

(c) Carbon Monoxide.

Table 5.5 exhibits the calculated values of force constants and equilibrium geometries for the ground and valence hole states of carbon monoxide. Agreement with experimental data is again very reasonable except for the results pertaining to the $B\ ^2\Sigma^+$ state. This state arises from ionization of the 2σ electron which can be described as belonging to the lone pair on oxygen. On the basis of the equivalent core concept an analogy may be drawn with CF^+. The large degree of polarity inferred from this analogy suggests that double zeta basis set is insufficiently flexible to describe accurately small changes in the relevant potential energy surface of this system.

Table 5.5.

Equilibrium Geometries (in atomic units), Force Constants (in eV) and Bond Overlap for CO and Valence States of CO^+.[a]

	$X\ ^1\Sigma^+$	$X\ ^2\Sigma^+$	$A\ ^2\Pi$	$B\ ^2\Sigma^+$	$C\ ^2\Sigma^+$
$(Re)_c$	2.155	2.129	2.486	2.116	2.945
$\Delta(Re)_c$	0	0.026	-0.331	0.039	-0.790
$\Delta(Re)_c$ %	0%	1.2%	-15.4%	1.8%	-36.7%
$(Re)_{ex}$	2.132[b]	2.107[c]	2.349[c]	2.208[c]	-
$\Delta(Re)_{ex}$	0	0.025	-0.217	-0.076	-
$\Delta(Re)_{ex}$ %	0%	1.2%	-10.2%	-3.6%	-
$\lvert\Delta(R)_s\rvert$	0	0.032	0.397[d]	0.038	1.299
$(We)_c$	0.28	0.29	0.17	0.28	0.09
$\Delta(We)_c$	0	-0.01	0.11	0	0.19
$\Delta(We)_c$ %	0%	-3.6%	39.3%	0%	67.9%
$(We)_{ex}$	0.27[e]	0.27[f]	0.20[f]	0.21[f]	-
$\Delta(We)_{ex}$	0	0	0.07	0.06	-
$\Delta(We)_{ex}$ %	0%	0%	25.9%	22.2%	-
π overlap	0.770	0.800	0.426	0.644	0.622
σ overlap	0.031	0.413	-0.171	0.165	-
Total overlap	0.801	1.213	0.255	0.809	-

[a] See table 5.4.

[b] Reference 118.

[c] Reference 145.

[d] $\lvert\Delta(R)_s\rvert$ = 0.204 when experimental values of ionization potentials and frequencies are used.

[e] Reference 141.

[f] Reference 62.

The loss of an electron from the strongly bonding 1π orbital or from the 1σ orbital for which there is a substantial electronic reorganization results in both cases in substantial decreases in force constants and concomitant increases in equilibrium bond lengths. In considering the vibrational fine structure for these ionized states however the possibility of pre-dissociation cannot be discounted.

For ionization of the 3σ orbital which is computed to be essentially non-bonding there is virtually no change in vibrational frequency with respect to the ground state molecule. However the bond length is slightly decreased (experimental decrease = 1.2%, calculated decrease = 1.2%). It is of interest in rationalizing these results to compare the values of π bond overlaps (Table 5.5) computed for the neutral molecule and the ionized species pertaining to the equilibrium geometry of the neutral molecule (2.155 A.U.). The loss of an electron from the 3σ orbital which can be approximately described as the lone pair orbital on carbon can be viewed as decreasing the effective energy mismatch of the orbitals on the constituent atoms (viz. the carbon is approximated by N^+). One manifestation of this therefore in a simplistic view is that the π bond overlaps (which dominate the bonding interaction between carbon and oxygen) should increase on going to the ionized species and this in turn suggests that the equilibrium bond length should decrease.

For the 2σ orbital which roughly corresponds to a lone pair on oxygen, the situation is the reverse of that for the 3σ orbital since the effective energy mismatch between orbitals on carbon and oxygen becomes larger. As a consequence the π bond overlap decreases which on naive arguments provides a rationalization for the increase in bond length and decrease in force constant for the ionized species. We have already pointed out that a basis set of double zeta quality is not sufficiently flexible (in the

absence of detailed optimizations of exponents) to even qualitatively describe the changes in geometry and force constants for this particular state. This contrasts as we have shown with predictions based on simple considerations of π bond overlaps.

In the previous chapter detailed attention has been drawn to the changes in equilibrium geometries and force constants accompanying core ionization in CO with a variety of basis sets. It is interesting in this connection to draw a comparison between the computed changes in π bond overlaps for the core ionized species with that for the valence ionized species described above, with a common basis set (double zeta). Since the previous work on core hole states did not include an investigation of changes in force constants and bond lengths at the double zeta level, for the sake of completeness these have been included in this work and are displayed in Table 5.6. The main qualitative features of these results

Table 5.6.

Equilibrium Geometries (in atomic units), Force constants (in eV) and Bond Overlaps for CO and Core Hole States of CO^+.

	$X\ ^1\Sigma^+$	C_{1s}	O_{1s}
$(Re)_c$	2.155	2.052	2.324
$\Delta(Re)_c$	0	0.103	-0.169
$\Delta(Re)_c$ %	0%	4.7%	-7.8%
We	0.28	0.33	0.19
$\Delta(We)_c$	0	-0.05	0.09
$\Delta(We)_c$ %	0%	-17.8%	32.1%
π overlap	0.770	0.776	0.386

are the same as those described in the preceding chapter with larger basis sets but differ in qualitative detail especially for the O_{1s} core ionized

species. The π bond overlaps again reflect the overall computed changes in equilibrium geometries and force constants thus paralleling the results for the valence ionized states discussed above. It should be noted that this simplistic analysis is only viable for these simple systems because the total bond overlap populations are dominated by the π contributions.

The data relating equilibrium geometries and force constants of ground and all hole state species are displayed in Fig. 5.2. The almost linear display of the points (excepting the point pertaining to the $B\ ^2\Sigma^+$ state) is again worth noting.

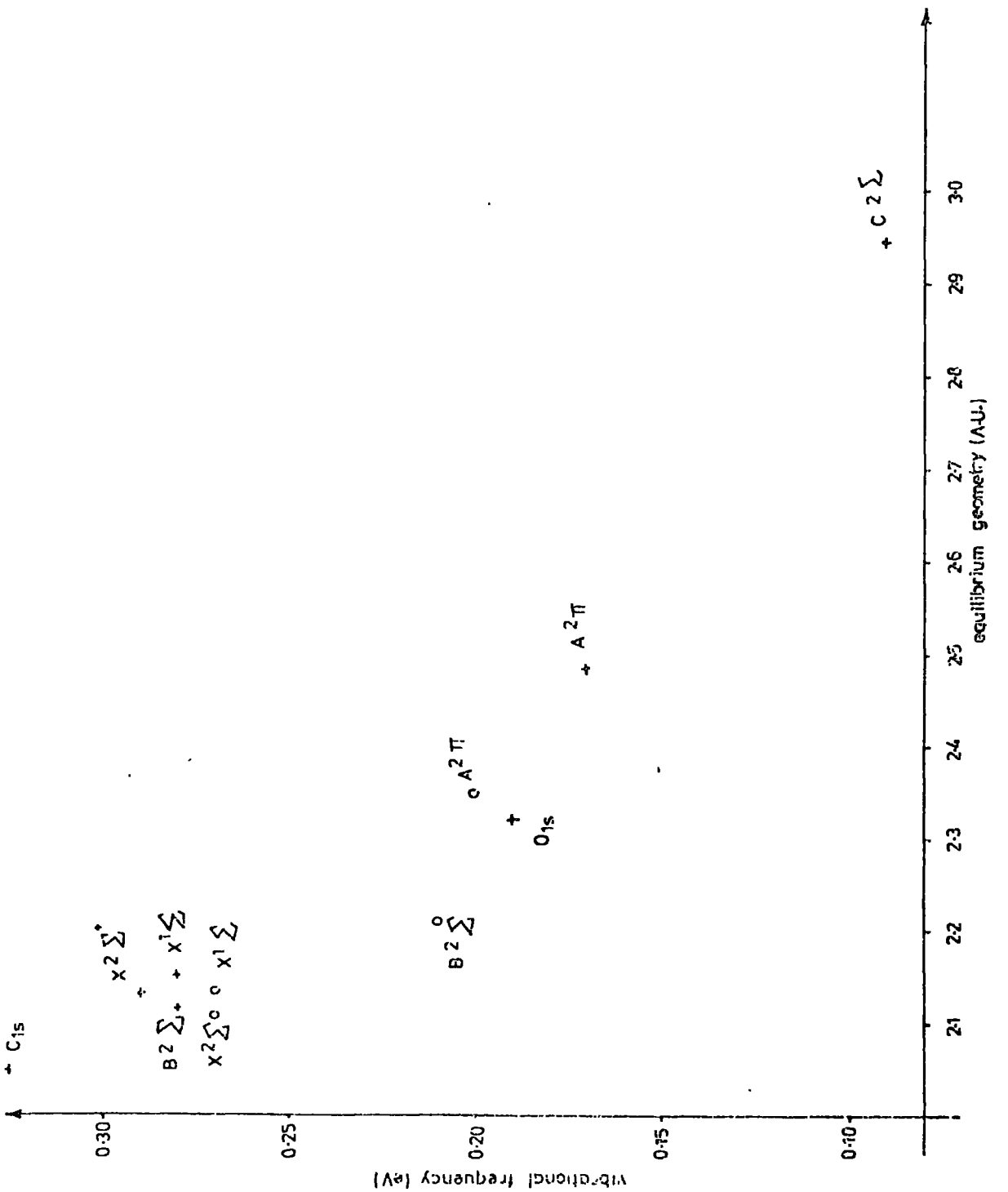

Fig. 5.2.

Plot of vibrational frequencies versus equilibrium geometries for CO and all hole states of CO^+.

o refers to experimental data.
+ refers to theoretically computed data.

5.5. Investigation of Vibrational Fine Structure.

(a) Description of the Method.

In this section we consider in detail the calculated vibrational fine structure accompanying valence ionization in N_2 and CO in an analogous manner to that described for the core hole states in Chapter IV. The approach involves the direct calculation of Franck-Condon factors from the computed changes in equilibrium bond lengths and force constants in the harmonic approximation using Ansbacher's recursion relationships.[142]

(b) Nitrogen.

Franck-Condon factors are much more sensitive functions of equilibrium geometries than of force constants since the former appear in the relevant expressions[142] as differences whereas the latter mainly involve ratios which are somewhat less sensitive functions of the basis set. These sensitivities are directly reflected in computed values of the Franck-Condon factors for the valence hole states of nitrogen which are displayed in Table 5.7.

Considering firstly the $X\ ^2\Sigma_g^+$ and $B\ ^2\Sigma_u^+$ states whose experimental equilibrium geometries differ by only 2% with respect to the neutral molecule; the Franck-Condon factors computed using the experimental data are in good agreement with the observed intensities indicating that anharmonicity corrections are relatively unimportant since the transitions involve sections of the potential energy surfaces of the ground and the hole state species which are well described by quadratic potentials. However the Franck-Condon factors computed with theoretically calculated geometries and force constants are rather poor. This discrepancy may be attributed to the fact that although the theoretical calculations predict correctly trends in shifts in equilibrium geometries, $\Delta(Re)_c$, the absolute values of the changes which directly influence Franck-Condon factors are almost twice as large as the experimentally observed changes.

Table 5.7.

Franck-Condon Factors for Valence States of N_2 and CO

State	N_2 $(FCF)^a_{th}$	N_2 $(FCF)^b_{ex}$	Experimental[c] intensity	State	CO $(FCF)^a_{th}$	CO $(FCF)^b_{ex}$	Experimental[c] intensity
$X\ ^2\Sigma_g^+$ v = 0	68.3	90.2	93.2	$X\ ^2\Sigma^+$	94.4	96.4	96.7
1	27.7	9.5	6.5		5.6	3.6	3.3
2	4.0	0.3	0.3				
$A\ ^2\pi_u$ v = 0	11.5	27.6	25.8	$A\ ^2\pi$	0.7	8.6	8.2
1	28.8	39.9	29.6		4.4	24.4	17.2
2	29.5	22.7	22.6		11.9	28.9	20.7
3	18.5	7.7	12.9		19.3	21.3	17.9
4	8.1	1.8	5.7		21.8	10.8	14.0
5	2.7	0.3	2.1		18.4	4.2	10.4
6	0.2		0.7		12.3	1.3	5.0
7			0.5		6.6	0.4	3.1
8			0.1		3.0	0.1	1.7
9					1.1		1.1
10					0.4		0.5
$B\ ^2\Sigma_u^+$ v = 0	61.7	88.9	90.4	$B\ ^2\Sigma^+$	90.4	72.8	70.0
1	28.9	10.4	8.9		9.2	25.3	24.5
2	7.9	0.7	0.7		0.4	2.8	5.4
3	1.5						

a $(FCF)_{th}$ refers to Franck-Condon factors calculated using Ansbacher formulae[142] with theoretically obtained data.

b $(FCF)_{ex}$ refers to Franck-Condon factors calculated using Ansbacher formulae with experimentally obtained data.

c Reference 149.

For the π ionized state for which the computed changes in force constant and equilibrium geometry are substantial, the computed Franck-Condon factors based on the experimentally determined values are in reasonable overall agreement with the experimental data, however since up to 8 vibrational quanta are excited the effects of neglect of anharmonicity now becomes more apparent. The solely theoretically based results apart from the intensity of the (0,0) transition are in reasonable overall agreement with the experimental data.

(c) Carbon Monoxide.

The main features of vibrational fine structure accompanying valence ionization in CO follow from the discussion given for N_2. The results are again displayed in Table 5.7.

It is interesting to note whilst that for the $X\ ^2\Sigma^+$ state of CO theoretically calculated Franck-Condon factors agree well with those experimentally determined which is not the case for N_2. The calculations also correctly predicted the more extended vibrational progression for the $A\ ^2\pi$ state of CO^+ compared with N_2^+. It is clear therefore that ab initio calculations of the Franck-Condon factors for the valence ionized states requires basis sets considerably better than double zeta Slater in quality if a quantitative description is required.

CHAPTER VI

SOME THEORETICAL INVESTIGATIONS OF THE CORE AND THE VALENCE IONIZED STATES IN CO_2.

Abstract.

Ab initio calculations within the Hartree-Fock formalism have been carried out on CO_2 to investigate the vibrational band profile of its high resolution ESCA spectrum. This method has involved calculations of the equilibrium geometries and the harmonic force constants, for the symmetric and the antisymmetric vibrational modes, of the ground and the core hole state species. Comparisons have been drawn with similar investigations on CO presented in Chapter IV. It is shown that the excitation of the anti-symmetric vibrational mode is responsible for the high value of the FWHM pertaining to the O_{1s} peak. Binding and relaxation energies have been computed for the core and all the valence electrons and the values of the relaxation energies for the latter have been compared with their localization characteristics. A possibility of a localized nature of the inner valence electrons is investigated.

6.1. Introduction.

A detailed study of ionization phenomena in simple diatomic molecules has been presented in the two previous chapters. The discussion has mainly focussed on ab initio Hartree-Fock investigations of binding and relaxation energies, equilibrium geometries and harmonic force constants of the ground and hole state species and vibrational band profiles of photoelectron spectra of these systems. The validity of these ab initio studies has been supported by the available experimental data and this has prompted an extension of this technique to the investigations of the triatomic CO_2 molecule whose high resolution ESCA spectrum[150] exhibits an interesting feature in that the O_{1s} band is much broader than the C_{1s} peak which is in the opposite sense to that observed in the spectrum of carbon monoxide[77] recorded at a comparable resolution and investigated theoretically in Chapter IV.

Equilibrium geometries and harmonic force constants for both symmetric and antisymmetric vibrational modes have therefore been calculated for the ground and the core hole state species which have then been used to compute Franck-Condon factors and hence band profiles of the core ionized states of CO_2.

Such an extensive study offers at the same time the possibility of investigating binding and relaxation energies accompanying photoionizations of both core and valence electrons.

6.2. Computational Details.

Non-empirical LCAO MO SCF calculations have been carried out within the Hartree-Fock formalism since we have shown on the work described in the two previous chapters that changes in correlation energy are relatively unimportant in discussing changes in equilibrium geometries, force constants and ionization potentials of ground and hole state species. Calculations have been carried out on the ground, the core and all the valence hole states of CO_2 using the ATMOL system of programs implemented on an IBM 370/195.

The basis sets employed for the calculations on the C_{1s} and the O_{1s} levels were:-

(i) STO 4-31G[24] using best atom exponents;[20]

(ii) for hole states 'optimized' STO 4-31G using best atom exponents;[20]

(iii) double zeta Slater using best atom exponents.[28]

The calculations on valence levels were performed with basis set (iii) since basis sets (i) and in particular basis set (ii) are in general more suitable for calculations on core levels.

6.3. Investigation of Binding and Relaxation Energies.

(a) Core Levels.

The localized O_{1s} and the C_{1s} core binding energies have been computed with various basis sets by Koopmans', relaxed Koopmans' and the ΔSCF methods already described in the previous chapters, and the results of these calculations are tabulated in Table 6.1, where the C_{1s} and the O_{1s} core binding energies for carbon monoxide have been displayed for comparison purposes. The trends in binding energies for both the C_{1s} and the O_{1s} levels calculated with various models for the differing basis sets are similar for both molecules. This feature is reflected in the values of the chemical shifts ΔC_{1s} and ΔO_{1s} between CO and CO_2 (also displayed in Table 6.1) which remain fairly constant at all levels of calculations and agree reasonably well with the experimental shifts of 1.4 eV and -1.5 eV respectively.[152] This is also true for shifts in relaxation energies displayed in Table 6.1. The difference between the adiabatic and the vertical binding energies for the C_{1s} levels of CO_2 is almost zero whereas for the O_{1s} levels this difference is predicted to be 0.43 eV (see footnote e, Table 6.1). This strongly contrasts with the situation in CO reported in Chapter IV and is of considerable importance when we come to discuss vibrational effects accompanying core ionizations.

(b) Valence Levels.

The formal valence electron configuration for CO_2 may be written:

$$(\sigma_g^{a})^2\ (\sigma_u^{a})^2\ (\sigma_g^{b})^2\ (\sigma_u^{b})^2\ (\pi_u)^2\ (\pi_g)^2$$

The values of ionization potentials (binding energies) with their shifts and relaxation energies for outer and inner valence hole states calculated at different levels of approximation are displayed in Table 6.2 and 6.3 respectively.

Table 6.1.

Calculated Core Binding (in eV) and Relaxation Energies (in eV) for CO_2[a] and CO[a]

Basis Set	Model[b]	CO_2 C_{1s} Vertical[c]	CO_2 C_{1s} Adiabatic[d]	CO_2 O_{1s} Vertical[c]	CO C_{1s} Vertical[c]	CO O_{1s} Vertical[c]	ΔC_{1s} Vertical[c]	ΔO_{1s} Vertical[c]
STO 4-31G	K	311.6	-	563.7	309.2	564.5	2.4	-0.8
	Kr	302.3	302.3	547.2	300.8	548.5	1.4	-1.3
	ΔSCF	302.5	302.5	547.1	300.8	548.4	1.7	-1.3
	RE	9.1	-	16.6	8.4	16.1	0.7	0.5
STO 4-31G (Opt.)	K	-	-	-	-	-	-	-
	Kr	299.4	299.4	543.4	297.8	544.7	1.6	-1.3
	ΔSCF	298.7	298.6	540.5	296.9	541.9	1.8	-1.4
	RE	12.9	-	23.1	12.3	22.6	0.6	0.5
Double Zeta	K	314.3	-	563.2	311.1	563.7	3.2	-0.5
	Kr	301.0	301.0	541.7	298.9	542.5	2.1	-0.8
	ΔSCF	302.1	302.1	542.4[e]	299.7	543.2	2.4	-0.8
	RE	12.2	-	20.8	11.4	20.5	0.8	0.3

[a] Experimental values for C_{1s} and O_{1s} holes are 297.6 eV and 540.8 eV respectively (reference 152).
Experimental values for C_{1s} and O_{1s} holes in CO are 296.2 and 542.3 eV respectively (reference 151), hence experimental shifts are ΔC_{1s} = 1.4 eV and ΔO_{1s} = -1.5 eV.

[b] K refers to Koopmans' Theorem, viz. $-\varepsilon$.
Kr refers to Relaxed Koopmans' Theorem, viz. $-\frac{1}{2}(\varepsilon + \varepsilon^*)$.
ΔSCF refers to ΔSCF calculations.
RE refers to Relaxation Energy, viz. K - ΔSCF.

[c] Vertical refers to binding energies calculated at theoretically optimized equilibrium geometry of the ground state.

[d] Adiabatic refers to binding energies calculated as energy differences for the theoretically optimized ground state and hole state geometries.

[e] Adiabatic binding energy at this level of approximation = 542.1 eV.

Table 6.2.

Ionization Potentials (in eV) and Relaxation Energies (in eV) for Outer Valence Hole States of CO_2.[a]

Model[b]	$X\ ^2\Pi_g$	$A\ ^2\Pi_u$	$B\ ^2\Sigma_u^+$	$C\ ^2\Sigma_g^+$
K	15.2	20.3	20.1	22.1
Δ(K)	6.9	1.8	2.0	0
Kr	14.4	19.7	19.2	21.3
Δ(Kr)	6.9	1.6	2.1	0
ΔSCF	14.4	19.7	19.2	21.3
Δ(ΔSCF)	6.9	1.6	2.1	0
RE	0.8	0.5	0.9	0.7
$(\Delta SCF)_{corr}$	16.6	21.7	21.3	23.3
$\Delta(\Delta SCF)_{corr}$	6.7	1.6	2.0	0
IP	13.8	17.3	18.1	19.4
Δ(IP)	5.6	2.1	1.3	0

[a] Calculations performed at the theoretically optimized equilibrium geometry of the neutral molecule.

[b] See Table 5.1

$(\Delta SCF)_{corr}$ refers to $\Delta SCF + \Delta E_{corr-intra}$

IP refers to the experimentally determined values (reference 62).

Table 6.3.

Ionization Potentials (in eV) and Relaxation Energies (in eV) for the Inner Valence Hole States of CO_2.[a]

Model[b]	D $^2\Sigma_u^+$	D $^2\Sigma^+$	E $^2\Sigma_g^+$	E $^2\Sigma^+$
K	41.6	41.6	43.1	43.1
Kr	40.7	39.1	42.2	39.8
ΔSCF	40.7	39.6	42.2	39.6
RE	0.9	2.1	0.8	3.5

[a] Calculations performed at the theoretically optimized equilibrium geometry of the neutral molecule.

[b] See Table 5.1.

Considering firstly the outer valence levels, the data in Table 6.2 indicate that there is no difference between the ΔSCF and relaxed Koopmans' values both slightly overestimating the binding energies in comparison with the experimental data.[62] Further the ordering of the $B\ ^2\Sigma_u^+$ and the $A\ ^2\pi_u$ levels is inverted compared with experimental data which has also been observed by Horsley and Fink[155] in their extended basis set calculations. A similar reverse of ordering of two closely spaced Σ and π levels has been observed for the two highest energy levels ($X\ ^2\Sigma_g^+$ and $A\ ^2\pi_u$) in N_2 and discussed in some detail in Chapter V where this phenomenon has been rationalized on the basis of the neglect of changes in correlation energy in going from the ground to the ionized state. An attempt has therefore been made to estimate ΔE_{corr} using the pair population method described in Chapter I, section 1.6.d. and Chapter V, section 5.3. and the modified ΔSCF values are shown in Table 6.2. Comparison with the experimental data[62] suggests that the ionization potentials corrected for ΔE_{corr} terms are grossly overestimated but their shifts are improved. A similar observation in the case of N_2 was noticed and discussed in some detail in Chapter V. It was noted in the preceding chapter that relaxation energies of valence electrons depend largely on their localization characteristics. Using the same arguments as in Chapter V we can go some way in explaining why the relaxation energy for the π_u electron is larger than for the π_g electron, the former being delocalized over 3 centres whereas the latter is delocalized only over the two oxygen atoms. Similar arguments can be extended to explain the values of the relaxation energies for the $B\ ^2\Sigma_u^+$ and $C\ ^2\Sigma_g^+$ states where however the situation is slightly more complicated due to the complex delocalization characteristics of the molecular orbitals consisting of 2s and 2p atomic orbitals on the carbon and the two oxygens.

The results pertaining to σ_g^a and σ_u^a inner valence electrons are shown in Table 6.3. The most interesting feature of these data is the possibility of a localized nature of the two ionized states because the overlap integral between the 2s atomic orbitals on the oxygen atoms which mainly compromise the two molecular orbitals is quite small. The data suggest that the degenerate localized states are lower in energy by more than 1 eV than the corresponding delocalized states which are split by 1.5 eV. These results suggest that the ionized states of the σ_g^a and σ_u^b electrons correspond to localized holes. It is interesting to note that these states are sufficiently localized to be core like in nature and one manifestation of this is that the shift in binding energy with respect to the corresponding O_{2s} level in CO is quite similar to that for the O_{1s} core ionized species. ($\Delta\ O_{2s}$ = 0.8 eV, $\Delta\ O_{1s}$ = 1.3 eV as calculated with double zeta basis set). It is also interesting to note that the corresponding shifts calculated for the delocalized O_{2s} hole are 0.2 eV and -1.3 eV for the ungerade and gerade respectively. This localized nature of the O_{2s} hole state is of considerable importance when we come to discuss vibrational effects accompanying ionizations because the antisymmetric stretch can become vibrationally excited only if the symmetry of the system changes on photoionization. The relaxation energies again closely follow the localization pattern of the molecular orbitals and fit into Snyder's[81] model discussed earlier on in Chapters II and V. The relaxation energy (0.8 eV) for the delocalized E $^2\Sigma_g^+$ state which extends over the 3 centres is more than 3 times smaller than the relaxation energy (3.5 eV) of the corresponding localized E $^2\Sigma$ state which is made up mainly from the 2s atomic orbital belonging to one of the oxygens (with atomic RE = 3.6 eV*). The ungerade molecular orbital has

* Atomic relaxation energies are tabulated in Table 5.3.

contributions only from the 2s oxygen atomic orbitals, therefore the relaxation energy of the delocalized D $^2\Sigma_u^+$ state (0.9 eV) is about half that for the corresponding localized D $^2\Sigma^+$ state (2.1 eV) which is again made up mainly of a 2s atomic orbital of one of the oxygen atoms.

6.4. Investigations of Potential Energy Surfaces.

Investigations of PES's in this work have involved computation of equilibrium geometries and force constants of the neutral molecule, and of the C_{1s} and O_{1s} core hole state species. The extra three degrees of freedom of CO_2 over the diatomic systems studied in the previous chapters have made the analysis of the PES's more complicated because in addition to the symmetric mode one must also consider antisymmetric and bending modes (the importance of the latter as far as vibrational analysis is concerned will be dealt with in a later section).

The neutral molecule and the C_{1s} hole state species possess $D_{\infty h}$ symmetry, therefore their vibrations can be described by symmetric and antisymmetric normal modes which can be depicted by quadratic potential energy functions[153] which are comparable to those for diatomic molecules. Therefore equilibrium geometries and harmonic force constants for symmetric and antisymmetric modes have been computed for the neutral molecule and the C_{1s} hole state in the manner described in Chapter IV. The situation is more complicated for the O_{1s} species because the localized nature of the O_{1s} hole states effectively destroys the $D_{\infty h}$ symmetry exhibited by the ground state molecule. A detailed analysis of the multidimensional PES of $\overset{*}{CO}_2$ ion is needed to calculate accurately its equilibrium geometry and force constants. This however requires a greatly increased amount of computing time and therefore to a first approximation a simplified procedure was adopted which has proved to give very good results needed for the vibrational analysis discussed in detail in the next section. The calculations on $\overset{*}{CO}_2$ with the double zeta basis set have shown that a simultaneous and equal compressions and extensions of both carbon oxygen bonds produce a quadratic PES (which has been used to compute the force constant for the 'symmetric' stretch of $\overset{*}{CO}_2$) with

the minimum corresponding to the equilibrium geometry of the neutral molecule. This result seems to suggest that the vibrational excitation of what we refer to as the 'symmetric mode' of $\overset{*}{CO}_2$ is very small indeed, because the Franck-Condon factors governing the extent of such excitations depend largely on the difference in the equilibrium geometries of the ground and the excited species, which has been discussed in some detail in the context of diatomic species in the previous chapter. The equilibrium geometry and the antisymmetric force constant of $\overset{*}{CO}_2$ were therefore estimated from a quadratic curve constructed by a compression of one carbon oxygen bond and a simultaneous and equal extension of the other keeping the distance between the two oxygens constant and equal to that computed in the neutral molecule. The results of such investigations are given in Tables 6.4 and 6.5 where corresponding data for the neutral and the core ionized states of carbon monoxide are displayed for comparison purposes.

Considering firstly the data in Table 6.4, it is clear that the C_{1s} hole state of CO_2 has a slightly shorter equilibrium carbon-oxygen bond length than the neutral molecule. A similar observation is noted when we compare the equilibrium geometries of CO and $\overset{*}{CO}$ where however the changes ΔRe are less basis set dependent but larger in magnitude. On the other hand the carbon-oxygen$^*_{1s}$ bond is substantially longer in the O_{1s} species of CO_2 than in the ground state molecule, the magnitude of the change being comparable to that between CO and $\overset{*}{CO}$ species and much smaller than the change of the carbon-oxygen bond length between CO_2 and $\overset{*}{CO}_2$. This observation will become again significant when we discuss vibrational fine structure accompanying core ionizations.

The computed force constants for the symmetric and the antisymmetric modes of the ground state, and of the C_{1s} and O_{1s} hole state are displayed in Table 6.5. The data seem to suggest that there are no substantial

Table 6.4.

Geometries (in atomic units) of CO_2, CO and their Core Hole State Species Corresponding to Minimum Energies

Basis	Geometries of carbon-oxygen bonds in CO_2, $\overset{*}{C}O_2$ and $OC\overset{*}{O}$						Geometries of carbon-oxygen bonds in CO, $\overset{*}{C}O$ and $C\overset{*}{O}$		
	ReCO	$Re\overset{*}{C}O$	$ReCO^{*1}$[a]	$ReCO^{2}$[a]	$\Delta Re_{(CO-\overset{*}{C}O)}$	$\Delta Re_{(CO-\overset{*}{C}O^{1})}$	ReCO	$\Delta Re_{(CO-\overset{*}{C}O)}$	$\Delta Re_{(CO-C\overset{*}{O})}$
STO 4-31G	2.211	2.200	-	-	0.011	-	2.167	0.060	-0.099
STO 4-31G (Opt.)	-	2.160	-	-	0.051	-	-	0.108	-0.070
Double zeta	2.226	2.199	2.346	2.106	0.027	-0.120	2.155	0.104	-0.168
Experimental[b]	2.192	-	-	-	-	-	2.132	-	-

[a] $ReCO^{1}$ refers to $C-\overset{*}{O}$ bond in $OC\overset{*}{O}$.
$ReCO^{2}$ refers to C-O bond in $OC\overset{*}{O}$.

[b] Reference 118.

Table 6.5.

Force Constants (in milidynes per angstrom) for CO_2, CO and their Core Hole State Species

Basis	$K_s^a CO_2$	$K_a^a CO_2$	$K_s^* CO_2$	$K_a^* CO_2$	$K_s^* CO_2$	$K_a^* CO_2$	KCO	$\overset{*}{K}CO$	$\overset{*}{K}CO$
STO 4-31G	18.6	16.1	20.5	16.4	-	-	22.1	-	-
STO 4-31G (Opt.)	-	-	23.0	17.9	-	-	-	30.7	15.1
Double Zeta	16.5	13.4	17.3	11.6	11.3	16.9	20.7	28.4	9.8
Experimental	16.8[b]	14.2[b]	-	-	-	-	19.0[c]	-	-

[a] K_s and K_a refer to the force constants for the symmetric and the antisymmetric mode respectively.

[b] reference 154.

[c] reference 141.

differences for both the symmetric and the antisymmetric force constants between the neutral and the C_{1s} ionized species. The force constant for the symmetric stretch is predicted with all three basis sets to be slightly larger for the C_{1s} hole state species than for the neutral molecule. This result seems to fit with an earlier observation discussed above namely that the carbon-oxygen bond in $\overset{*}{C}O_2$ is only slightly shorter than in CO_2. The calculations on the antisymmetric force constant seem to be less consistent. The small basis sets predict a slight increase whereas the double zeta basis set calculations suggest a small decrease on going from the ground to the C_{1s} hole state. The estimates of the force constants for the O_{1s} core hole state species where we have to a first approximation ignored the interaction between the two modes again suggest that these are subtle differences in the force constants on going from the neutral to the ionized molecule.

The comparable situation in the case of carbon monoxide is different, as substantial differences in force constants (regardless of the basis set) between the neutral molecule and the C_{1s} and O_{1s} species are predicted. This has already been discussed in Chapter IV.

6.5. Vibrational Fine STructure Accompanying Core Electron Ionizations.

(a) Introduction.

It was shown in the two previous chapters that the method we have employed for studying PES's of diatomic molecules yields results (in particular equilibrium geometries and force constants) which can be successfully used to interpret and predict high resolution ESCA and UPS spectra of these simple systems. We have therefore decided to use this method to interpret Siegbahn's[150] high resolution ESCA spectrum of CO_2 which shows a remarkable difference between the two band shapes with FWHM of the C_{1s} and O_{1s} peaks equal to 0.64 eV and 1.32 eV respectively. This is a rather different situation from that previously discussed in Chapter IV where we noted the reverse trend in the ESCA spectrum of CO at approximately comparable resolution with respective values of FWHM equal to 0.82 eV and 0.65 eV.

A theoretical analysis along similar lines discussed in Chapter IV was therefore carried out on both the C_{1s} and O_{1s} levels of CO_2 with the computed values of the equilibrium geometries and the force constants at the double zeta level. The Franck-Condon factors were calculated for both vibrational modes using the Ansbacher[142] recurrence relationships with appropriate corrections for force constants and reduced masses.[153]

(b) C_{1s} Levels.

The simulation of the C_{1s} spectrum of CO_2 has presented no real problem because the $D_{\infty h}$ symmetry of the system is conserved on photo-ionization and therefore one needs to consider only vibrational excitation of the symmetric modes ($\upsilon'_{S,O,O}$). The separation of the individual vibrational components of this progression is governed by the force constants of the symmetric mode of $\overset{*}{CO}_2$ (17.3 md/Å) which corresponds to the vibrational frequency of 0.17 eV. The simulation of the C_{1s}

band was accomplished using this value (0.17 eV) for the separation of vibrational components together with the computed Franck-Condon factors for the transitions between the symmetric modes of CO_2 and $\overset{*}{CO}_2$. The FWHM of the individual components was taken to be 0.54 eV which is the same value derived in Chapter IV from the ESCA spectrum of $\overset{*}{CO}$ recorded at a comparable resolution. The computed spectrum of $\overset{*}{CO}_2$ together with the relevant Franck-Condon factors are displayed in Figure 6.1. The FWHM compares favourably with that measured by Siegbahn[150] (0.64 eV). This good overall agreement supports the view that one does not need, to a first approximation, to take into account the bending vibrations for the construction of the band envelope of photoelectron spectra of CO_2, because the PES for this mode is little perturbed on an electron ionization. This is well documented in the UPS spectra[62] of CO_2 whose well resolved vibrational progressions show virtually no vibrational excitation of the bending mode.

(c) O_{1s} Levels.

The construction of the band envelope for the high resolution ESCA spectrum of the O_{1s} levels in CO_2 is rather more elaborate because one needs to consider vibrational excitations of both the symmetric and the antisymmetric modes. (The results pertaining to the C_{1s} spectrum discussed above suggest that the bending vibrations can again be ignored to a first approximation). However we have pointed out in the previous section (6.4) that the vibrational excitation of the symmetric mode of $\overset{*}{CO}_2$ is negligible and therefore the band profile of the O_{1s} peak is mainly governed by the vibrational progression (0,0,$\upsilon a'$) of the antisymmetric mode which greatly simplifies the vibrational analysis. The force constant of this mode for $\overset{*}{CO}_2$ is computed to be 16.9 md/Å which corresponds to a vibrational frequency of 0.32 eV. Taking the FWHM of the individual vibrational

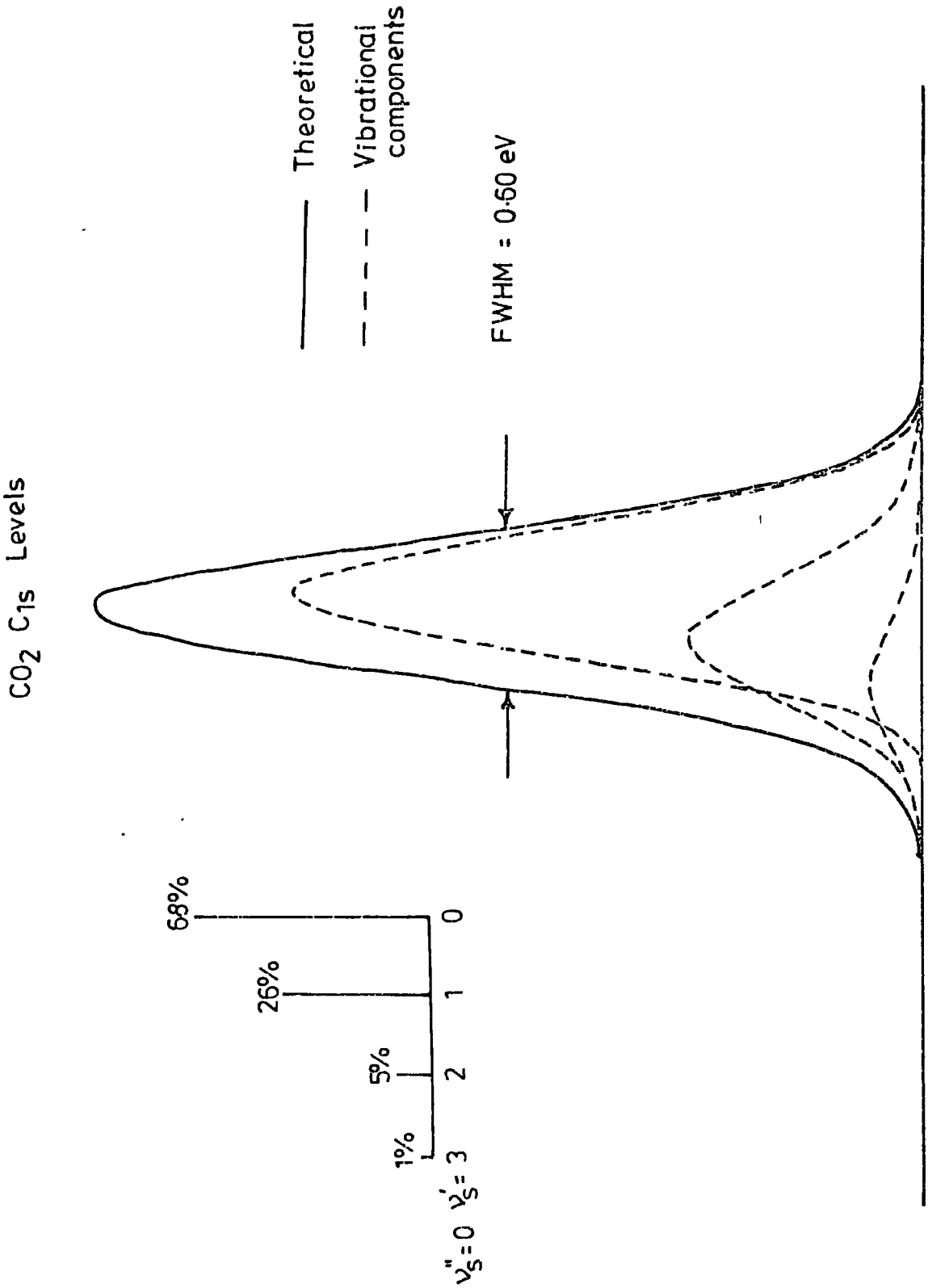

Fig. 6.1.

Theoretically simulated C_{1s} spectrum of CO_2. The four vibrational components have FWHM = 0.54 eV and are separated by 0.17 eV.

components with their separations of 0.32 eV to be 0.58 eV (which is the value derived in Chapter IV from the spectrum of CO^* recorded at a comparable resolution) together with the calculated Franck-Condon factors for the transitions between the antisymmetric modes of CO_2 and CO_2^* yields a broad band envelope with a FWHM = 0.94 eV which is shown in Figure 6.2. The agreement with the experimental spectrum which exhibits a FWHM = 1.32 eV is not as good as in the case of the C_{1s} spectrum since the model used in interpreting it is cruder. Nonetheless the results obviously go some way in explaining the reason for the overall shape and larger FWHM for the band profile of CO_2^*.

(d) Inner Valence Levels.

It was pointed out in section 6.3 that ionization of the σ_g^a and σ_u^a inner valence electrons leaves the ion in a localized state. Experimental verification of this requires a high resolution photoelectron spectrum. However the experimental difficulties are such that at the present time only relatively low resolution spectra are available in this energy region. From the work presented above we would expect the localized states to exhibit substantial vibrational broadening due to the excitation of the antisymmetric modes (and also possibly the symmetric mode although this seems less likely on the basis of the analysis presented above for the corresponding core ionized systems). On the basis of the calculations described in this work it seems likely that the interpretation of any high resolution spectra of the O_{2s} region of CO_2 will be in terms of vibrational progressions involving the antisymmetric stretching mode for the localized hole states. This contrasts with the interpretation which would previously have been presented on the basis of the excitation of only symmetric modes for the ungerade and gerade symmetrically delocalized states. Broadening in this case would have been interpreted as arising from the split in energy between the two states together with the superimposed

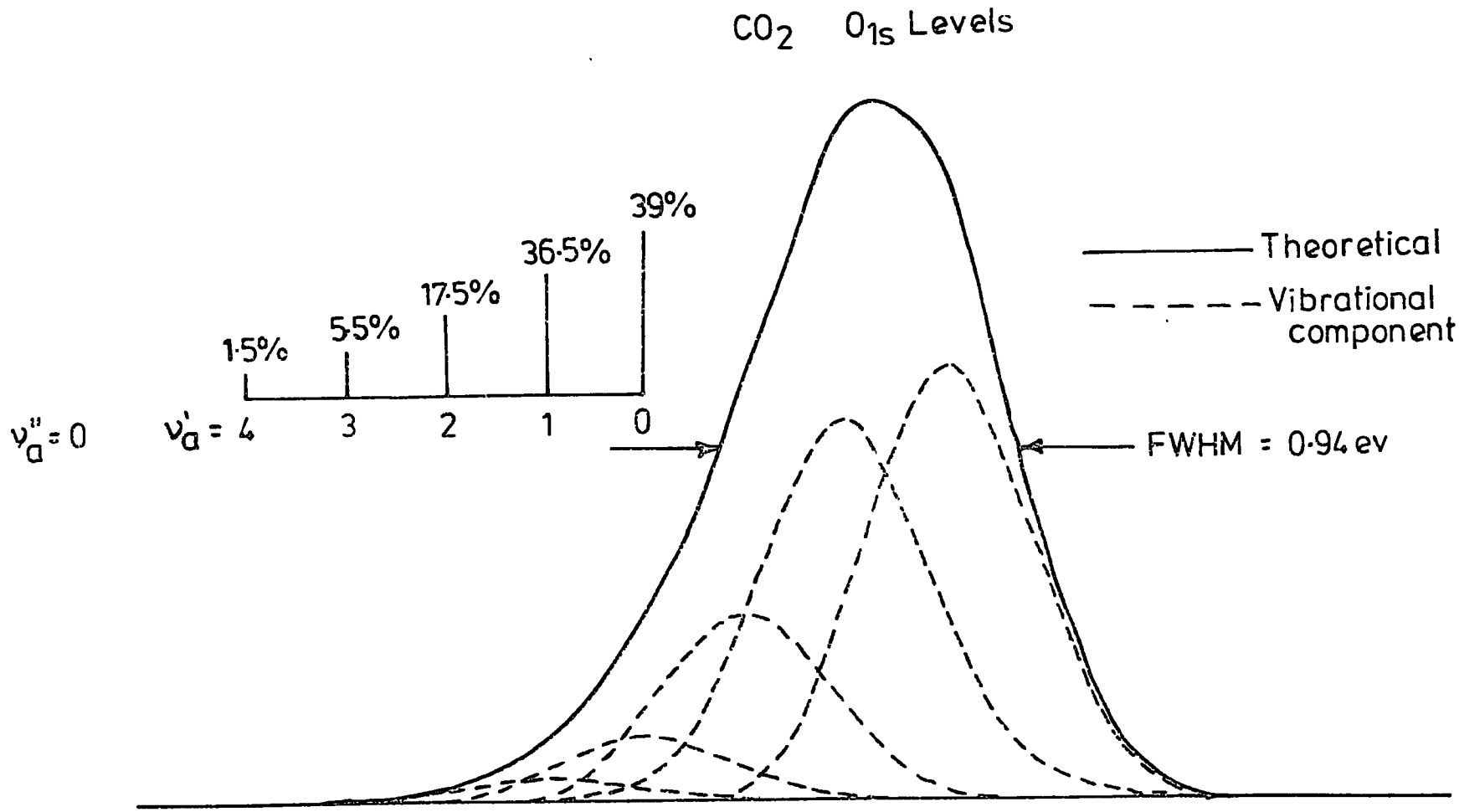

Fig. 6.2.

Theoretically simulated O_{1s} spectrum of CO_2. The five vibrational components have FWHM = 0.58 eV and are separated by 0.32 eV.

vibrational fine structure. Since the vibrational frequencies are likely to be substantially different for the symmetry and antisymmetric modes (viz. for the neutral molecule $\upsilon_{sym} = 1330$ cm.$^{-1}$, $\upsilon_{asym} = 2349$ cm.$^{-1}$) the investigation of vibrational fine structure should readily reveal the validity of the prediction of localized hole states for the O_{2s} levels of CO_2.

APPENDIX 1

ORBITAL EXPONENTS FOR VARIOUS SLATER BASIS SETS

Slater Minimal Basis Set Exponents.[20]

	H	C	N	O	F	Cl	Br
1s	1.2	5.6727	6.6651	7.6579	8.6501	16.5239	34.2471
2s		1.6083	1.9237	2.2458	2.5638	5.7152	12.8217
2p		1.5679	1.9170	2.2266	2.5500	6.4966	15.5282
3s						2.3561	6.7395
3p						2.0387	6.5236
4s							2.6382
3d							6.5197
4p							2.2570

Slater Double Zeta Basis Set.[28]

	H	C	N	O	F	Cl
1s	0.9716	5.2309	6.1186	7.0623	7.9179	12.0587
1s'	1.2321	7.9690	8.9384	10.1085	10.0110	17.6501
2s		1.1678	1.3933	1.6271	1.9467	4.9261
2s'		1.8203	2.2216	2.6216	3.0960	6.9833
3s		-	-	-	-	2.0091
3s'		-	-	-	-	3.3416
2p		1.2557	1.5059	1.6537	1.8454	5.3574
2p'		2.7263	3.2674	3.6813	4.1710	9.5670
3p						1.6092
3p'						2.8587

Slater Extended Basis Set.[31]

	C	N	O
1s	9.055	10.586	12.418
1s	5.025	6.037	6.995
3s	6.081	7.334	8.681
2s	2.141	2.539	2.922
2s	1.354	1.588	1.818
2p	6.827	7.677	8.450
2p	2.779	3.270	3.744
2p	1.625	1.890	2.121
2p	1.054	1.222	1.318

APPENDIX 2

GROUND STATE ENERGIES OF MOLECULES CALCULATED AT EQUILIBRIUM GEOMETRIES

STO 4-31G[a]

Formula	Energy (A.U.)	Formula	Energy (A.U.)
CH_4	-40.0076	$(CH_3)CH{=}O$	-152.0985
CH_3OH	-114.4004	$H_2C{=}CHF$	-176.0707
C_2H_4	- 77.6552	$F_2C{=}CH_2$	-274.4807
$H_2C{=}O$	-113.2291	C_2H_5F	-177.2756
$H_2C{=}NH$	- 93.5412	$C_2H_4F_2$	-275.7019
HCN	- 92.3876	$C_2H_3F_3$	-374.1266
$H_2N{-}COH$	-168.0049	$FC{\equiv}CH$	-149.2173
NH_3	- 55.8903	$FC{\equiv}CF$	-273.1839
CO	-112.0932	CH_3F	-138.4178
H_2O	- 75.5488	CH_2O_2	-187.6806
C_2H_2	- 76.4343	NH_2OH	-130.2461
$F_2C{=}O$	-310.0826	$CH_3C{\equiv}N$	-131.2560
CH_3NH_2	- 94.7332	FCN	-190.7609
C_2H_6	- 78.8562	H_2O_2	-149.8807
$HFC{=}O$	-211.6671	FOH	-173.8648
NH_2NH_2	-110.5895	HF	- 99.5725
NH_2F	-154.2365	F_2	-197.7995
HCl[b]	-458.1401	Cl_2[b]	-915.0774
HBr[b]	-2560.7733	Br_2[b]	-5120.3646

[a] Fluorine atoms have been investigated with HF 4-31G basis.

[b] The basis set includes polarization functions of d type on the halogens and p type on the hydrogen (see Chapter III).

Double Zeta

Formula	Energy (A.U.)	Formula	Energy (A.U.)
HF	-100.0237	F_2	-198.7273
HCl	-460.0240	Cl_2	-918.9239
CO	-112.6762[a]	N_2	-108.8637[a]
CF^+	-136.7758[a]	NO^+	-128.7592[a]
CO_2	-187.5109[a]		

Triple Zeta[a]

CO	-112.7098	N_2	-108.9006
CF^+	-136.8210	NO^+	-128.8504

STO 4-31G[a]

CO	-112.0941	N_2	-108.3419
CF^+	-136.0360	NO^+	-128.1889
CO_2	-186.5364		

HF 4-31G[a]

CO	-112.1746	N_2	-108.3944
CO^+	-136.1457	NO^+	-128.2188

[a] Energies refer to theoretically optimized equilibrium geometries given in the text.

REFERENCES

1. M. Born and J. Oppenheimer, Ann. Physik, 84, 457 (1927).

2. Longuet-Higgins, Advances in Spectroscopy, 2, 429 (Interscience 1962).

3. J.C. Slater, Phys. Rev., 34, 1293 (1929).

4. P.O. Löwdin, Phys. Rev., 97, 1474 (1955).

5. P.O. Löwdin, Phys. Rev., 97, 1490 (1955).

6. R. McWeeny and B. Sutcliffe, Methods of Molecular Quantum Mechanics, A.P., New York (1969).

7. R. McWeeny, Rev. Mod. Phys., 32, 335 (1960).

8. J.P. Dahl, H. Johansen, D.R. Truax and T. Ziegler, Chem. Phys. Letters, 6, 64 (1970).

9. V. Fock, Z. Physik, 61, 126 (1930).

10. D.R. Hartree, Proc. Cambridge Phil. Soc., 24, 89 (1928).

11. P.A.M. Dirac, Proc. Cambridge Phil. Soc., 26, 376 (1930); 27, 240 (1931).

12. T.A. Koopmans, Physica, 1, 104 (1933).

13. C.C.J. Roothaan, Rev. Mod. Phys., 32, 179 (1960).

14. R.K. Nesbet, Proc. R. Soc., A320, 312, 322 (1955).

15. D.B. Cook, Ab Initio Valence Calculations in Chemistry, Butterworths (1974).

16. R.S. Mulliken, J. Chem. Phys., 23, 1833, 1841, 2338, 2343 (1955).

17. J.C. Slater, Phys. Rev., 36, 57 (1930).

18. S.F. Boys, Proc. Roy. Soc. (London), A200, 542 (1950).

19. See e.g. I. Shavitt, Method in Computational Physics, 2, 1 (1963).

20. E. Clementi and D.L. Raimondi, J. Chem. Phys., 38, 2686 (1963).

21. E. Clementi, D.L. Raimondi and W.P. Reinhardt, J. Chem. Phys., 47, 1300 (1967).

22. J.M. Foster and S.F. Boys, Rev. Mod. Phys., 32, 303 (1960).

23. W.J. Hehre, R.F. Stewart and J.A. Pople, J. Chem. Phys., 51, 2657 (1969).

24. R.F. Stewart, J. Chem. Phys., 52, 431 (1970).

25. R.F. Stewart, J. Chem. Phys., 50, 2485 (1969).

26. E. Clementi, IBM J. Res. Develop. Suppl., 9, 2 (1965).

27. R. Ditchfield, W.J. Hehre, J.A. Pople, J. Chem. Phys., 54, 724 (1971).

28. E. Clementi, J. Chem. Phys., 40, 1944 (1964).

29. E. Clementi, R. Matcha and A. Veillard, J. Chem. Phys., 47, 1865 (1967).

30. S. Huzinaga, C. Arnau, J. Chem. Phys., 53, 451 (1970).

31. A.D. McLean and M. Yoshimine, Supplement to 'Computation of Molecular Properties and Structures', IBM J. Res. Develop. (November 1967).

32. S. Huzinaga, J. Chem. Phys., 42, 1293 (1965).

33. S. Huzinaga and Y. Sakai, J. Chem. Phys., 50, 1371 (1969).

34. A. Veillard, Theoret. Chim. Acta., 12, 405 (1968).

35. J.L. Whitten, J. Chem. Phys., 44, 359 (1966).

36. E. Clementi and D.R. Davis, J. Comput. Phys., 2, 223 (1967).

37. T.H. Dunning, J. Chem. Phys., 53, 2823 (1970).

38. R.K. Nesbet, J. Chem. Phys., 40, 3619 (1964).

39. A.D. McLean and M. Yoshimine, Tables of Linear Molecule Wave Functions, a supplement to IBM J. Res. Develop., 12, 206 (1968).

40. G. Burns, J. Chem. Phys., 41, 1521 (1964).

41. Summaries of these methods can be found in various textbooks on theoretical (organic) chemistry, e.g. W.G. Richards and J.A. Horsley, Ab Initio Molecular Orbital Calculations for Chemists, O.U.P. (1970).

42. CNDO, INDO, NDDO are discussed in: J.A. Pople and D. Beveridge, Approximate Molecular Orbital Theory, McGraw Hill, N.Y. (1970). EHMO is discussed in e.g. R. Hoffmann, J. Chem. Phys., 39, 1397 (1963).

43. P.O. Löwdin, Advan. Chem. Phys., 2, 207 (1959).

44. P.E. Cade, K.D. Sales and A.C. Wahl, J. Chem. Phys., 44, 1973 (1966).

45. D.T. Clark, Ann. Reports (B) of the Chemical Society, page 40 (1972).

46. W.J. Hehre, R. Ditchfield, L. Radom and J.A. Pople, J. Amer. Chem. Soc., 92, 4796 (1970).

47. E.A. Hylleraas, Z. Physik., 48, 469 (1928).

48. E.A. Hylleraas, Z. Physik., 54, 347 (1929).

49. L.C. Snyder and H. Basch, J. Amer. Chem. Soc., 91, 2189 (1969).

50. R.K. Nesbet, Phys. Rev., 56, 155 (1967).

51. D.T. Clark and D.M.J. Lilley, Tetrahedron, 29, 845 (1973).

52. D.T. Clark and I.W. Scanlan, J. Chem. Soc. Faraday Trans. II, 70, 1222 (1974).

53. C. Hollister and O. Sinanoglu, J. Amer. Chem. Soc., 88, 13 (1966).

54. C.C.J. Roothaan, Rev. Mod. Phys., 23, 69 (1951).

55. P.O. Löwdin, Rev. Mod. Phys., 35, 496 (1963).

56. H.F. Schaefer III, The Electronic Structure of Atoms and Molecules, Addison Wesley (1972).

57. W.A. Goddard III, T.H. Dunning Jr., W.J. Hunt and P.T. Hay, Accts. Chem. Res., 6, 368 (1973).

58. K. Siegbahn, C. Nordling, A. Fahlman, R. Nordberg, K. Hamrin, J. Hedman, G. Johansson, T. Bergmark, S.-E. Karlsson, I. Lindgren and B.J. Lindberg, ESCA - ATomic, Molecular and Solid State Structure by Means of Electron Spectroscopy, Nova Acta Regiae Soc. Sci. Upsaliensis Ser. IV, Vol. 20 (1967).

59. K. Siegbahn, C. Nordling, G. Johansson, J. Hedman, P.F. Heden, K. Hamrin, U. Gelius, T. Bergmark, L.O. Werme, R. Manne and Y. Baer, ESCA Applied to Free Molecules, North Holland, Amsterdam (1969).

60. K. Siegbahn, Conference Proceedings, Namur 1974, J. Electron Spectry, 5, 3 (1974).

61. P. Auger, J. Phys. Radium, 6, 205 (1925).

62. D.W. Turner, C. Baker, A.D. Baker and C.R. Brundle, Molecular Photoelectron Spectroscopy, Wiley-Interscience (1970).

63. W.C. Price, A.W. Potts and D.G. Streets, Electron Spectroscopy Conference Proceedings, Asilomar, Calif., U.S.A.), D.A. Shirley (Editor), North-Holland Publ. Co., p.187 (1972).

64. M.O. Krause, T.A. Carlson and R.D. Dismukes, Phys. Rev., 170, 37 (1968).

65. A. Veillard and E. Clementi, J. Chem. Phys., 49, 2415 (1969).

66. E. Clementi and H. Popkie, J. Am. Chem. Soc., 94, 4057 (1972).

67. P. Bagus, Phys. Rev., 139, A619 (1965).

68. B.T. Pickup and O. Goscinski, Molec. Phys., 26, 1013 (1973).

69. R. Manne and T. Åberg, Chem. Phys. Letters, 7, 282 (1970).

70. T. Åberg, Phys. Rev., 156, 35 (1967).

71. H.W. Meldener and J.D. Perez, Phys. Rev. A, 4, 1388 (1971).

72. J. Franck, Trans. Faraday Soc., 21, 536 (1926).

73. E.U. Condon, Phys. Rev., 28, 1182 (1926).

74. E.U. Condon, Phys. Rev., 32, 858 (1928).

75. E. McGuire, Phys. Review, 185, 1 (1969).

76. G. Herzberg, Molecular Spectra and Molecular Structure, Vol. III, Princeton, New Jersey, Van Nostrand (1966).

77. U. Gelius, S. Svensson, H. Siegbahn, E. Basilier, Å. Faxälv and K. Siegbahn, Chem. Phys. Letters, 28, 1 (1974).

78. D.T. Clark, D.B. Adams, J. Electron Spectry, 7, 401 (1975).

79. U. Gelius, Conference Proceedings, Namur, 1974, J. Electron Spectry., 5, 985 (1974).

80. P.S. Bagus and H.F. Schaefer, J. Chem. Phys., 56, 224 (1972).

81. L.C. Snyder, J. Chem. Phys., 55, 95 (1971).

82. J.N. Murrell and B.J. Ralston, J. Chem. Soc. Faraday Trans. II, 68, 1393 (1972).

83. L.J. Aarons, M.F. Guest and I.H. Hillier, J. Chem. Soc. Faraday Trans. II, 11, 1866 (1972).

84. H. Siegbahn, Technical Notes, UUIP-891, Uppsala University Institute of Physics (1975).

85. D.W. Davis, J.M. Hollander, D.A. Shirley and T.D. Thomas, J. Chem. Phys., 52, 3295 (1970).

86. D. Liberman, Bull. Amer. Phys. Soc., 9, 731 (1964).

87. L. Hedin and A. Johansson, J. Phys. B2, 2, 1336 (1969).

88. W.L. Jolly and D.N. Hendrickson, J. Am. Chem. Soc., 92, 1863 (1970).

89. W.L. Jolly and D.N. Hendrickson, Acct. Chem. Res., 3, 193 (1970).

90. W.J. Jolly, Electron Spectroscopy (Conference Proceedings, Asilomar, Calif., U.S.A.), D.A. Shirley (Editor), North-Holland Publ. Co., p.629 (1972).

91. D.T. Clark and D.B. Adams, J. Chem. Soc. Faraday Trans. II, 68, 1819 (1972).

92. D.T. Clark and D.B. Adams, Theor. Chim. Acta, 31, 171 (1973).

93. D.C. Frost et al., Chem. Phys. Letters, 13, 391 (1972).

94. R. McWeeny and A.A. Velenik, Mol. Phys., 24, 1421 (1972).

95. O. Goscinski, B.T. Pickup and G. Purvis, Chem. Phys. Letters, 22, 167 (1973).

96. O. Goscinski, G. Howat and T. Åberg, J. Phys. B: Atom Molec. Phys., 8, 11 (1975).

97. O. Goscinski, M. Hehenberger, B. Roos and P. Siegbahn, Chem. Phys. Letters, 33, 427 (1975).

98. U. Gelius, Physica Scripta, 9, 133 (1974).

99. D.T. Clark, R.D. Chambers and D.B. Adams, J. Chem. Soc. Perkin I, 674 (1975).

100. D.T. Clark and D.M.J. Lilley, Chem. Phys. Letters, 9, 234 (1971).

101. D.T. Clark, D. Kilcast and W.K.R. Musgrave, Chem. Comm., 516 (1971).

102. D.T. Clark, D. Kilcast, D.B. Adams and W.K.R. Musgrave, J. Electron Spectry., 6, 117 (1975).

103. M.E. Swartz, Chem. Phys. Letters, 6, 631 (1970).

104. D.W. Davis and D.A. Shirley, J. Electron Spectry., 3, 137 (1974).

105. H. Basch, Chem. Phys. Letters, 5, 337 (1970).

106. G. Howat and O. Goscinski, Chem. Phys. Letters, 30, 87 (1975).

107. H. Siegbahn, R. Medeiros and O. Goscinski, J. Electron Spectry., 8, 149 (1976).

108. D.W. Davis and D.A. Shirley, Chem. Phys. Letters, 15, 185 (1972).

109. J.C. Slater, Adv. Quantum Chem., 6, 1 (1972).

110. K.H. Johnson, Adv. Quantum Chem., 7, 143 (1973).

111. J.W. Connolly, H. Siegbahn, U. Gelius, C. Nordling, J. Chem. Phys., 58, 4265 (1973).

112. J. Linderberg and Y. Öhrn, Propagators in Quantum Chemistry, Academic Press, London (1973).

113. L.S. Cederbaum, Theoret. Chim. Acta, 31, 239 (1973).

114. L.S. Cederbaum, J. Phys. B8, 290 (1975).

115. L.S. Cederbaum, W. von Niessen and W.P. Kraemer, J. Chem. Phys., in press (1976).

116. G.D. Purvis and Y. Öhrn, J. Chem. Phys., 60, 4063 (1974).

117. G.D. Purvis and Y. Öhrn, J. Chem. Phys., 62, 2045 (1975).

118. Tables of Internuclear Distances and Configurations in Molecules and Ions. Ed. L.E. Sutton, Chem. Soc. Special Publications, No. 11 (1958) and No. 18 (1965).

119. D.B. Adams and D.T. Clark, Theoret. Chim. Acta, 31, 171 (1973).

120. D.T. Clark, W.J. Feast, D. Kilcast, W.K.R. Musgrave, J. Poly. Sci. Al, 11, 389 (1973).

121. D.T. Clark, D. Kilcast, D.B. Adams, W.K.R. Musgrave, J. Electron Spectry., 1, 227 (1972).

122. D.W. Davis, D.A. Shirley, T.D. Thomas, J. Chem. Phys., 56, 671 (1972).

123. Unpublished data, cf. reference 59.

124. M.F. Guest, I.H. Hillier, V.R. Saunders and M.H. Wood, Proc. Roy. Soc. (London) A333, 201 (1973).

125. U. Gelius and K. Siegbahn, Disc. Faraday Soc. Chem. Soc., 54, 257 (1972).

126. L.C. Snyder, J. Chem. Phys., 55, 95 (1971).

127. W.B. Perry and W.L. Jolly, Chem. Phys. Letters, 23, 529 (1973).

128. D.M.J. Lilley, Ph.D. thesis, University of Durham (1973).

129. D.M.J. Lilley and D.T. Clark, in preparation.

130. J.A. Pople, Theoret. Chim. Acta, 28, 213 (1973).

131. K. Siegbahn, private communication.

132. U. Gelius, G. Johansson, H. Siegbahn, C.J. Allan, D.A. Allison, J. Allison and K. Siegbahn, J. Electron. Spectry., 1, 285 (1972/73).

133. Y.S. Khodeyev, H. Siegbahn, K. Hamrin and K. Siegbahn, Chem. Phys. Letters, 19, 16 (1973).

134. U. Gelius, E. Basilier, S. Swensson, T. Bergmark and K. Siegbahn, J. Electron Spectry., 2, 405 (1974).

135. H. Fellner-Feldegg, U. Gelius, B. Wamberg, A.G. Nilsson, E. Basilier and K. Siegbahn, Conference Proceedings, Namur 1974: J. Electron. Spectry., 5, 64 (1974).

136. I.W. Scanlan, Ph.D. Thesis, University of Durham (1974).

137. D.T. Clark, I.W. Scanlan and J. Müller, Theoret. chim. Acta, 35, 341 (1974).

138. A.D. Buckingham, N.C. Handy and R.J. Whitehead, J. Chem. Soc. Faraday Trans. II, 1, 95 (1975).

139. J. Cambray, J. Gasteigner, A. Streitwieser (Jr.) and P. Bagus, J. Am. Chem. Soc., 96, 5978 (1974).

140. K. Siegbahn and U. Gelius, private communication.

141. G. Herzberg, Molecular Spectra and Molecular Structure, Vol. 2, New York, Van Nostrand (1950).

142. F. Ansbacher, J. Naturforsch, 14a, 889 (1959).

143. W. Domcke and L.S. Cederbaum, Chem. Phys. Letters, 31, 582 (1975).

144. K. Siegbahn and U. Gelius, personal communication.

145. D.P. Chong, F.G. Hering and D. McWilliams, J. Electron. Spectry., 7, 429 (1975).

146. L.S. Cederbaum and W. Domcke, J. Chem. Phys., 60, 2878 (1974).

147. T. Ho Lee and J.W. Rabalais, J. Chem. Phys., 61, 2747 (1974).

148. W.C. Price, lecture notes from the Royal Institute of Chemistry, Summer School in Photoelectron Spectroscopy, Swansea (1972).

149. T.L. Gardener and J.A.R. Samson, J. Chem. Phys., 60, 3711 (1974).

150. K. Siegbahn, private communication.

151. T.D. Thomas, J. Chem. Phys., 53, 1744 (1970).

152. D.W. Davis, J.M. Hollander, D.A. Shirley and T.D. Thomas, J. Chem. Phys., 52, 3295 (1970).

153. J.C.D. Brand and J.C. Speakman, Molecular Structure, Edward Arnold (Publishers) Ltd., London (1960).

154. E.B. Wilson, J.C. Decius and P.C. Cross, Molecular Vibrations, McGraw-Hill (1955).

155. J.A. Horsley and W.H. Fink, J. Phys. B, 2, 1261 (1969).